University of Minnesota
St. Anthony Falls Hydraulic Laboratory

Project Report No. 284

MODEL STUDY OF THE MINNESOTA RIVER NEAR WILMARTH POWER PLANT, MINNESOTA

by

Gary Parker,

Marcelo Garcia,

Helgi Johannesson,

and

Kazunori Okabe

Prepared for

NORTHERN STATES POWER COMPANY
Minneapolis, Minnesota

December 1988
Minneapolis, Minnesota

TABLE OF CONTENTS

ACKNOWLEDGEMENTS

Heinz Stefan provided considerable help to the project in its initial stages and read this report. The figures were drafted by Aaron Gimbel. Jack Vandenburg, Dave Roberts, and other shop staff aided in the design and construction of the model. Karl Wikstrom provided photographic advice. Pat Swanson edited the report. Masato Sekine provided help with the data analysis. Christopher Cavett provided help with the model operation.

LIST OF FIGURES

I. INTRODUCTION

The Wilmarth Power Plant, owned and operated by Northern States Power Company, is located on the east bank of the Minnesota River, just downstream of the City of Mankato (Figure 1). The plant receives its cooling water from an intake on the river (Figure 2).

The plant has been in operation for over 35 years. In 1981, a tendency for sand to accumulate in the intake screenhouse was observed. The plant superintendent in 1983, J. M. Pappenfus, commented as follows in a memorandum; "We are suspicious that the river has recently changed" [1]*. Since then, dredging has been required to prevent further siltation at the intake.

In the summer of 1986, H. Johannesson and G. Parker of St. Anthony Falls Hydraulic Laboratory, conducted a brief study of the problem. They concluded that it is associated with a reversal in the sense of a river bend at the intake [2]. At the time of construction of the plant, the intake was located at the downstream end of the outside (east side) of a bend. Since then, the sense of the bend has reversed, resulting in the formation of a large point bar just upstream of the intake (Figures 2 and 3). This bar is the cause of the sedimentation.

Johannesson and Parker also noted that the west bank just opposite the intake had been severely degraded due to the excavation of material from the adjacent floodplain for construction purposes (Figure 3). This would allow for further migration of the river to the west, i.e. away from the intake. In order to alleviate the problem, they proposed the construction of a riprapped levee to stabilize the west bank, and the use of impermeable dikes to restore the bend to its previous, favorable configuration.

In the fall of 1986, another study of the problem was conducted at St. Anthony Falls Hydraulic Laboratory, at the request of Northern States Power Company [3]. Bank protection, spur dikes, skimmer walls, and intake relocation were studied as possible alternatives for alleviating siltation at the intake. It was pointed out therein that prudent selection of one of these alternatives would properly require a movable bed model of the reach in question.

Planning for the model study was begun in earnest in the summer of 1987. Both a global model of a reach of river several thousand feet long, and a local model focusing on the immediate vicinity of the intake, were considered. The former choice is more appropriate for the consideration of such large–scale measures as levees and dikes, whereas the latter is suited for

---

*Numbers in brackets indicate references on page 26.

a study of a skimmer wall. In light of the large size of the bar upstream of the intake, a local solution was not considered likely to result in a permanent amelioration of the sedimentation. As a result, it was decided to pursue the global model study.

The model study was commenced on December 16, 1987. This report provides a summary of results obtained in the course of the study.

II. THE SETTING

The Minnesota River downstream of Mankato flows in sandy alluvium, in a box–like valley about 3,000 ft (900 m) in width. Within the study reach, the valley itself is oriented nearly along a north–south axis (Figure 4).

Throughout most of its length, the Minnesota River displays a proclivity for free meandering within its floodplain. In particular, Johannesson and Parker [4] studied a strongly sinuous reach (Figure 4) just downstream of the study reach, and documented meandering tendencies over the course of 42 years. Rates of channel shift were found to be on the order of several meters per year. Immediately upstream of the study reach, however, the river flows through the City of Mankato. Within Mankato, the river is riprapped, so as to preclude overbank flow as well as channel migration.

In the study reach, the river varies from straight to only mildly sinuous (Figure 4) The fact that the east bank of the river tends to hug the valley wall here has probably helped to stabilize the channel configuration over the last 40 years. Several areas of the floodplain have been excavated for sand and gravel fill along the study reach. The most important of these is immediately opposite the screenhouse; it is apparent as a pond in Figures 2 and 3. Much of the bottom of this pond is 11 ft (3.4 m) or more below the general level of the floodplain. The excavation apparently took place sometime between the years 1971 and 1980. At present, the river is eroding westward into the excavation, along which the river bank is very low.

Also of interest is the large spur dike, running perpendicular to the river on the west side of the floodplain immediately opposite the intake in Figure 3. This dike was built by the same landowner as the one owning the adjacent excavation, perhaps to prevent the river from avulsing into it and neighboring cropland. A view of the dike, as well as the excavation, is provided in Figure 5. A top elevation of 773.5 ft (235.8 m) effectively prevented overtopping even during severe floods, so that the entire floodplain flow was diverted back into the channel at a point just opposite the screenhouse.

The U.S. Army Corps of Engineers recently determined that the effect of the spur dike was to raise flood stages to unacceptable levels. As a result, it was removed in 1987. The debris from the removal was stored on the floodplain, so as to form the mound denoted in Figure 2.

The river has been gaged in Mankato since 1903, at a site approximately 14,000 ft (4300 m) upstream of the intake. Based on these records, the following flood frequencies were determined:

Discharge (cfs)	Recurrence Interval (years)
14,400	2
28,300	5
39,000	10
53,500	25
64,800	50
76,300	100
94,100	largest on record

The flow duration curve at Mankato is plotted in Figure 6. In Figure 7, river water surface elevation as measured at the screenhouse is plotted versus discharge. Records are available for flows up to 40,000 cfs (1130 cumecs)

Water surface elevation at bankfull flow is near 762.5 ft (232.4 m) above MSL. Bankfull discharge was estimated from this elevation and the river slope as measured from a topographical map, in conjunction with flow records at Mankato. The following parameters thus pertain to bankfull conditions.

Parameter	Value
Discharge	$Q = 20{,}000$ cfs
Water surface slope	$I = 0.00019$
Channel width	$B = 345$ ft
Mean depth	$H = 15$ ft
Mean flow velocity	$U = 3.9$ ft/s

The bed of the river consists mostly of clean sand. Although sediment samples were not taken from the river bed at the site, it was visually confirmed that sediment on exposed bars is similar to material found at the Mankato gaging site, and near the town of Le Sueur. This latter material generally has a median size D_{50} near 0.5 mm [5]. Several size distributions taken at Mankato are shown in Fig. 8.

III. MODEL DESIGN

As shown in Figure 4, the area selected for the model study is 6,400 ft (1950 m) in length, and 3,200 ft (971 m) in width. The intake is located about midway from the upstream end of the model.

River scale models are based on the principle of Froude similarity. That is, where g denotes gravitational acceleration, the following criterion must be satisfied;

$$\left[\frac{V}{\sqrt{g H}} \right]_m = \left[\frac{V}{\sqrt{g H}} \right]_p$$

where m denotes model and p denotes prototype.

A horizontal scale ratio λ_h of 1:160 allows for fitting the model within a basin with minimum dimensions 40 ft x 20 ft (12.2 m x 6.1 m). The model basin is schematized in Figure 9. Space has been allowed for a head box and sediment trap as well as the area of the Minnesota River and floodplain to be modelled.

If the model were to be undistorted, the vertical scale ratio would be identical to the horizontal one. The water surface slope in the model would then be identical to that in the prototype, and the difference in elevation of the water surface between the upstream and downstream ends of the model would be near 2 mm. This value is too low to set accurately. Accordingly, the model was distorted, as is customary in the case of models of sand-bed rivers.

A vertical scale ratio λ_v of 1:40 was thus selected. This implies a distortion factor of 4. That is, the model slope is quadrupled compared to the prototype, and can thus be set accurately in the course of experimentation. It should be noted that lateral slopes are similarly distorted.

The following scale relations result from the above assumptions; where x denotes horizontal distance,

$$(x)_m = \lambda_h \, (x)_p = \frac{1}{160} \, (x)_p$$

$$(H)_m = \lambda_v \, (H)_p = \frac{1}{40} \, (H)_p$$

$$(S)_m = \frac{\lambda_v}{\lambda_h} (S)_p = 4 (S)_p$$

$$(V)_m = \lambda_v^{1/2} (V)_p = \frac{1}{\sqrt{40}} (V)_p$$

$$(Q)_m = \lambda_h \lambda_v^{3/2} (Q)_p = \frac{1}{160(40)^{3/2}} (Q)_p$$

These scale relations allow for sizing of the model, and the design of the piping and water discharge system. The surface of the floodplain and the river banks were then molded in concrete, using templates constructed from a detailed topographic map of the field site.

Henceforth in this report, all parameters determined in the model are reported in prototype units, unless specifically stated otherwise.

Direct geometric scaling of the 0.5 mm bed sediment in the prototype according to the above principles would result in a model sediment of several microns in diameter. Such material would likely display cohesion, and would not allow for the accurate reproduction of erosion and deposition patterns in the model. On the other hand, if sand of prototype size were used in the model, it would barely move at the reduced scale. The appropriate resolution of this problem is to employ a light–weight sediment. In the present study, crushed walnut shells with a specific gravity near 1.4 have been employed. The median diameter was selected so as to satisfy the following model criterion;

$$\left[\frac{u_*}{v_s} \right]_m = \left[\frac{u_*}{v_s} \right]_p$$

Here v_s denotes the fall velocity of the median size of the sediment, and u_* denotes the shear velocity, given by the relation

$$u_* = \sqrt{gHS}$$

The model sediment size estimated by this method is near 0.5 mm. Crushed walnut shells with median sizes of 0.3 mm and 0.7 mm are available commercially. As a result of favorable experience with the coarser size [5], it was selected for the present study. A typical size distribution is shown in Figure 8. It can be seen therein that the model sediment is more uniform in size distribution than that of the prototype. The walnut shells are fed into the model at the upstream end by means of a screw–type feeder.

The model setup allows for accurate measurement of water discharge and sediment feed rates. Water surface and bed elevations are measured with a point gage. Velocity measurements are taken with a magnetic flow meter with a 10 mm probe; the signals are processed with a microcomputer.

IV. OVERVIEW OF THE STUDY

The model study was conducted in six parts: basin preparation, field data collection, and model design; model construction; calibration; tests on west bank reconstruction; tests on measures for removing the bar upstream of the screenhouse, and preparation of the final report. These are outlined in Figure 10, along with the approximate time period each phase occupied.

The design of the model has been discussed in section III. Section V is devoted to the calibration of the model. Calibration runs were performed at discharges of 4,000, 10,000, 20,000, and 40,000 cfs. As noted earlier, a discharge of 20,000 cfs corresponds to bankfull flow. It was found that the bar located just upstream of the intake in the field could be accurately reproduced in the model. Bed elevations in the model tended to be slightly higher than in the field, but the overall correspondence in pattern proved to be quite satisfactory. The overwidened channel upstream of the intake showed a general tendency to fill during above–bankfull flows, and scour during below–bankfull flows. At a flow of 40,000 cfs, a tendency for channel avulsion into the excavation zone shown in Figure 3 was manifested.

The possibility of channel avulsion arises from two causes. As can be seen in Figures 2, 3, and 5, the excavation discussed in section II has resulted in considerable damage to the west bank of the river just upstream of the intake. This, combined with the removal of the floodplain spur dike visible in Figure 5, leaves an open path of low elevation for flood flow on the west side of the floodplain. In Section VI, a summary of experiments on the reconstruction of the west bank is presented. The final design is based on the twin goals of protecting against avulsion, while at the same time not increasing water surface elevations measurably during floods. As a result, the proposed levee is only slightly higher than the surrounding floodplain.

Section VII is devoted to measures for removing the large bar upstream of the intake, and restoring flow and bed topography at the intake to the favorable conditions that prevailed when the plant was constructed. Three classes of countermeasures were considered; sudden channel constrictions, fields of impermeable in–channel rock–fill spur dikes, and fields of permeable in–channel pile dikes. All of these are intended to narrow the overwidened channel upstream of the intake. The resulting higher velocities should scour out the bar. In addition, appropriate flow deflection can ensure that the deepest part of the channel lies on the side of the intake.

A total of eight alternatives were tested in detail; the first two consist of channel constrictions, and the last eight consist of various configurations of impermeable in–channel spur dikes. The recommended alternative consists of a field of three impermeable dikes. Permeable dikes were not tested in light of the good performance obtained from impermeable dikes, and the relatively higher cost expected to construct permeable dikes.

A diagnostic study of the cause of the formation of the bar upstream of the intake was performed in parallel to the model study [6]. The diagnostic study indicates that the cause of the bar is not the excavation opposite to it, as was originally thought. Rather, as can be seen in Figure 3, the bar has been migrating downstream at an average rate near 47 ft/year (14 m/year), at least since 1938. It is only recently that the bar has migrated sufficiently close to the intake to cause sedimentation problems. A numerical calculation presented in the diagnostic study indicates that the bar can be essentially removed by restoring channel alignment near the intake to that prevailing in 1961. These results were used in setting the placement of the channel constrictions and dikes discussed in section VII.

V. MODEL CALIBRATION

Direct measurements of the rate of transport of bed sediment in large streams such as the Minnesota River are rarely available. As a result, there is no direct way to determine the feed rate of sediment required at the upstream end of the model river, in order to reproduce field conditions. For each discharge, the appropriate feed rate must thus be found by trial and error.

This calibration is carried out as follows. The selected water discharge is commenced in the model. The height of the tailgate at the downstream end of the model is then adjusted so as to obtain the water surface elevation at the screenhouse measured in the field, and given in Figure 7. If the sediment feed rate is too low, the equilibrium water surface slope obtained after a sufficiently long time interval will be lower than the estimated field value (0.00019). If the sediment feed rate is too high, the slope will likewise be too steep. Testing of successive combinations of tailgate elevations and feed rates allows for the determination of the correct settings.

Calibration was carried out for the following selected flows:

Discharge (cfs)	Percent of Time Exceeded	Description
4,000	20.5	low flood
10,000	5.9	medium flood
20,000	1.2	bankfull
40,000	0.2	high flood

These flows were chosen for specific reasons. The lowest flow of 4,000 cfs (110 cumecs) is still well above the median and mean flows at Mankato of 1,230 cfs (35 cumecs) and 2,800 cfs (80 cumecs), respectively. It is far larger than the discharge taken at the intake by the power plant (26–52 cfs, or 0.73–1.45 cumecs). It was estimated to be near the lowest discharge at which the river could be expected to be reasonably active, and thus capable of creating its own bed morphology via erosion and deposition. The choice of bankfull flow is obvious, and the intermediate flood flow of 10,000 cfs (280 cumecs) allows for coverage of the range of active, but below bankfull flows. The choice of 40,000 cfs (1130 cumecs) is dictated by the fact that this is the largest flow for which a screenhouse water elevation can be estimated from Figure 6. It is slightly higher than a 10 year flood.

As noted above, calibration was carried out by running each of the above flows until equilibrium conditions could be verified over many hours of model time (days of field time). This procedure, while necessitated in order to determine the correct sediment feed rate, may reproduce long–term bed topographies only rarely or never realized in the field at the highest discharge of 40,000 cfs (1130 cumecs). This is because so high a flow is not likely to continue for such an extended period of time in the field before the hydrograph drops. Data for this flow must be interpreted with this in mind.

The water surface elevations attained in the model at calibrated conditions are indicated in Figure 7 for the four flows. The agreement with the field data is excellent. In Figure 11, calibrated (model) sediment feed rates in grams/min are plotted against (prototype) discharge. At a low flood flow, the feed rate is essentially zero. For flows in excess of bankfull, the transport capacity of sediment is seen to grow rather slowly, as the flow spreads overbank.

In Figure 12, mean bed elevation at a cross–section is plotted as a function of downvalley distance for all four calibration runs as well as the field measurements. The locations of the cross–sections are denoted on Figure 2. The field measurements were taken during the period spanning late December of 1987 to early January of 1988; discharge was on the order of 700 cfs (20 cumecs) during this time.

Cross–sections 11 to 14 in Figure 12 constitute a zone of river expansion, where the river is wider than average. As one would expect, this zone is seen to fill as flood discharge increases, and to scour as flow declines. On the other hand, cross–sections 20–22 are located at a constriction; here the reverse is observed. Bed elevations in the model tend to be somewhat higher than those observed in the field, but at the lower flows, the discrepancy is modest everywhere except at the constriction.

Plots of river bottom bathymetry are presented in Figure 13. It is apparent that the bar upstream of the intake house can be reproduced very well in the model. At 4,000 cfs (110 cumecs), much of the bar was found to be exposed in the model. The bathymetric map for the field does not indicate which areas of the bar were exposed, but it is known that a portion of the bar is above water for much of the year. The top of the bar is, in fact, partially vegetated at present. The exposed bar is shown in the model and the field in Figures 14a and 14b.

Figure 15 provides bathymetric information in a form that is more quantitatively useful. Bed elevation contours are plotted relative to the mean bed height between cross–sections 8 to 28, an area that includes all of the bar as well as the river adjacent to the intake. The mean bed heights above MSL are given below

Case	Mean Bed Height (ft)
4,000	747.5
10,000	748.5
20,000	747.0
40,000	750.0
field	745.0

Mean bed elevations are seen to be somewhat high in the model, but the difference is less at the flows at and below bankfull conditions. A comparison of the bed topography at 10,000 cfs (280 cumecs) with the field topography reveals a notable similarity in bar shape, indicating that the model is performing well.

The calibration runs also provided an opportunity to observe patterns of flow over the floodplain at the high flood flow. As this run was continued for a considerable length of time, substantial amounts of sediment were deposited on the floodplain, as shown in Figure 16. Both the pattern of sediment deposition and the streaklines of the surface flow indicated a tendency for flow to leave the channel along the west bank opposite the bar, flow through the excavation and over the floodplain across the previous location of the spur dike (see Figures 3 and 5), and re–enter the channel downstream. This path of flow, demarcated in Figure 17, suggests the route of a possible avulsion in the future. The low west bank clearly leads to a loss of channel capacity just upstream of the intake. Whether this might actually happen in the field depends upon, among other things, the duration of the period of overbank flow.

During the calibration run at 40,000 cfs (1130 cumecs), it was found that an excessive amount of water was flowing over the floodplain. In reality, much of the floodplain is heavily vegetated, leading to much higher roughness than that of the bare concrete of the model. Accordingly, wire mesh was placed in areas of dense vegetation to approximate the added roughness in the model, as is apparent in Figure 16. After adjustment by trial and error, these were replaced with standard roughness strips, as illustrated later. It was found that along cross–section 16 (Figure 2), 55% of the flow remained in the channel, and 45% flowed along the floodplain to the west of the channel.

VI. EXPERIMENTS ON WEST BANK RECONSTRUCTION

Johannesson and Parker [2] suggested that the construction of a levee along the degraded west bank opposite the bar could help stabilize the river. It could also help prevent an avulsion of the channel into the excavation, which would leave the intake without water. It would not, however, eliminate or ameliorate the sedimentation problem associated with the bar. The suggested levee is illustrated in Figure 18. It was to be built no higher than floodplain elevation in order to prevent a raising of the water surface level during severe floods, something to which the U.S. Army Corps of Engineers could be expected to object. Based on the rather sketchy information available at the time, this elevation was estimated to be near 761.5 ft (232.1 m). The dike was to be about 1200 ft (370 m) long. The downstream end was to be tied onto the floodplain spur dike shown in Figure 5, which was still in existence at the time.

Subsequently, a more detailed topographic map has indicated that much of the floodplain not subjected to excavation is at or above an elevation of 764 ft (232.9 m). Accordingly, this elevation was selected for the purpose of testing schemes for west bank reconstruction.

Two options were selected for testing. These are shown in Figure 18. In the case of Option 1, the levee is built as close as possible to the existing bank. This would require the installation of riprap from the top to the bottom of the bank, in order to protect the toe from failure. A crane would probably be required for the purpose of installation under water. In addition, a filter layer or geotextile would also be recommended. This option would have the advantage of preventing any further migration of the channel to the west and away from the intake.

In the case of option 2, the levee is set back some 30 ft (9 m) from the existing bank line. A sufficient supply of riprap would be stockpiled in the offset; it would be self–launched as the river attempted to erode into the levee. This method would likely be less costly than Option 1. It would, however, allow for some channel shift. The fact that it would be difficult to provide for the added safety of a filter layer or geotextile down the bank slope constitutes a disadvantage worth mentioning.

In order to conduct the tests, the levee was molded from a putty–like sealant material. The upstream end of the levee was tied into a natural levee with an elevation near 764 ft (232.9 m). This natural levee should be replaced with a riprapped levee. The model river was then allowed to come into equilibrium at bankfull conditions. At this time, bed elevations were surveyed. The discharge was then increased until the levee was overtopped. This occurred at a discharge near 26,000 cfs (730 cumecs) in both cases. The discharge was then raised to 40,000 cfs (1130 cumecs), and measurements

of surface velocity in the channel and on the floodplain were taken before the bed had much time to respond to the flood flow. This was done to approximate a flood hydrograph in the field.

An issue of importance concerns the mode of overtopping of the levee. Since it is not far above bankfull elevation, it can be expected to be overtopped approximately once every four or five years on the average. A large water surface differential between the river and floodplain sides of the levee would lead to spillway–like conditions, with the possibility of ravelling of the riprap. Although this possibility should be taken into account when designing the dike, it was found in the model study that floodplain flow from upstream kept the elevation differential to a minimum at the time of overtopping.

In neither case was the levee found to have much effect on river bed elevations at bankfull flow. The measured elevations with and without the levee of either option proved to be so similar that they hardly bear presentation in this report.

Surface water velocity measurements, taken at 10 mm below the water surface, in the river and adjacent floodplain in the vicinity of the bar are presented in Figure 19 for both options. The figure reveals that a substantial floodplain flow is still present in the vicinity of the excavation. Although the patterns of measured velocity vectors are very similar, Option 1 appears to be slightly more successful at keeping flow more confined to the channel. Surface flow velocities near the west bank are nowhere in excess of 7.6 ft/s (2.3 m/s), providing a basis for the design of riprap.

In the case of both options, the tendency for deposition of sediment on the floodplain is substantially reduced. This is apparent in Figure 20. It should be borne in mind, however, that the deposition apparent in Figure 16 is the result of a much longer duration of overbank flow than that of Figure 20.

In the case of Option 2, surface water velocities in the channel, immediately adjacent to the west bank, were measured at incipient overtopping conditions (26,000 cfs, or 740 cumecs). The measurements were taken at 10 mm below the water surface. They are shown in Figure 21.

At this point it is appropriate to discuss a result of the diagnostic study [6]. A numerical model was used therein to predict the bed topography that would result if the river were returned to the configuration that prevailed before the bar became apparent in the vicinity of the intake. Calculations indicate that if a complete restoration were realized, the present large bar would be replaced by a smaller bar at point B in Figure 18. The predicted bar is illustrated in Figure 7c of the diagnostic study [6]; it would put pressure on the opposite bank. As a result, any west bank reconstruction should continue at least as far upstream as section 9 in Figure 18. Recommendations in section VIII take this observation into account, and include the possible levee cross sections illustrated in Figures 22 and 23. .

VII. EXPERIMENTS ON BAR REMOVAL AND CHANNEL RESTORATION

The experiments on bar removal and channel restoration were commenced only after the results from the diagnostic study [6] were available. The diagnostic study indicated that two aspects of channel configuration need to be corrected if good flow conditions adjacent to the intake are to be restored.

The first of these concerns the sense of the bend. In 1961, the intake was located on the outside of a gentle bend, where velocities tend to be higher and flows deeper (Figure 3). By 1987, the sense of that bend had reversed as the bar migrated into its present position. The bar has thus generated its own depositional zone, and is poised to bury the intake in a few years. This problem can be corrected by restoring the sense of the bend.

The second concern is that of excess channel width. It can be seen in Figure 2 that just upstream of the intake, the bankfull width of the river is nearly twice the value prevailing farther upstream or downstream. The excess width creates an environment that is on the whole depositional and further elevates the bar.

Any restorative measure must address both of these concerns. In addition, the measure must not destabilize the levee shown in Figure 18, must in fact realize improved conditions at the intake, and must be cost–effective.

Detailed experiments were conducted on eight alternatives Alternatives 1 and 2 consist of rock pad constrictions, and alternatives 3 ~ 8 consist of one or more impermeable in–channel spur dikes in various configurations. These are summarized below. Where two alternatives have the same number of spur dikes, the implication is that the configuration is different.

Alternative	Configuration
1	small pad
2	large pad
3	1 dike
4	2 dikes
5	3 dikes
6	3 dikes
7	2 dikes
8	3 dikes

Complete data sets are available for alternatives 6, 7, and 8, from which the final recommendation was selected. The experiments for the five earlier alternatives were exploratory in nature; the data sets for these are not entirely complete. A complete data set consists of the following items taken at all four flows of 4,000, 10,000, 20,000, and 40,000 cfs: videotapes of flow and bed configuration; photographs of flow and bed configuration; downstream water surface profiles; and measurements of bed elevations along sections 8 to 18, as shown in Figure 2. The available data sets are summarized in Table 1:

Each of the various alternatives is discussed in some detail below.

ALTERNATIVE 1. This option was intended to provide a simple and inexpensive means of rectifying the problem at the intake. It consists of a rock pad built out from the (proposed) levee on the west bank into the flow. It is positioned opposite, but just upstream of, the intake. The rock pad provides a local constriction, accelerating the flow and encouraging scour just before sediment derived from the bar passes in front of the intake.

The rock pad was built from pea gravel with a model diameter of 4 ~ 9.5 mm. This size loosely corresponds to an effective diameter of 2 ft (0.6 m) in the prototype. Detailed tests were performed at 10,000 cfs. Visual observations were made at 20,000 cfs. Tests were not performed at 4000 and 40,000 cfs.

The bed configuration and pattern of streamlines can be seen in Figures 24a and 24b, respectively. An effective concentration of flow streamlines is realized at the intake. Only the tip of the bar visible in Figure 14a is removed, however. The abrupt protrusion of the pad encourages deep local scour around its base. Associated with the local scour is an angled vortex that tends to suspend sediment eroded from the bar, and deliver it past the intake.

In Figure 25a, the channel cross–section at section 14.5 for Alternative 1 with Q equal to 10,000 cfs is compared with the cross–section measured in the calibration run at section 14, and at the same discharge (A key to the locations of the numbered sections can be found in Figure 2.). Section 14.5 just passes through the outer tip of the pad. The constricting effect of the pad is readily apparent, in terms of an overall lowering of bed elevation by some 8 ft (2.4 m). In the scour hole along the pad, as much as 13 ft (4 m) of lowering is evident.

The effect of the constriction does not extend very far upstream. By section 13, the bed profile at 10,000 cfs with the pad in place differs only slightly from that for the calibration run at the same discharge. It is seen in Figure 25b, however, that deep scour is realized along the west bank at the leading edge of the pad (section 13.5). This deep scour could have the effect of destabilizing the (proposed) west bank levee. It is caused by the abrupt constriction induced by the pad.

TABLE 1

Alternative	Q (cfs)	Videos	Photos	Water Surface Elevs.	Bed Elevs.
1	4,000				
	10,000	√	√		√
	20,000	√	√		
	40,000				
2	4,000	√	√		
	10,000	√	√		√
	20,000	√	√		
	40,000	√	√		
3	4,000	√	√		√
	10,000	√	√		√
	20,000	√	√		
	40,000		√		
4	4,000	√	√	√	√
	10,000	√	√		
	20,000	√	√	√	√
	40,000		√	√	
5	4,000				
	10,000	√	√		
	20,000				
	40,000				
6	4,000	√	√	√	√
	10,000	√	√	√	√
	20,000	√	√	√	√
	40,000	√	√	√	√
7	4,000	√	√	√	√
	10,000	√	√	√	√
	20,000	√	√	√	√
	40,000	√	√	√	√
8	4,000	√	√	√	√
	10,000	√	√	√	√
	20,000	√	√	√	√
	40,000	√	√	√	√

It is seen from Figure 2 that the intake section falls between section 15 and 16. In Figure 25c, the intake section for Alternative 1 is compared with that for the calibration run, again at 10,000 cfs. Whereas the bed was deeper on the west side and shallower on the east (intake) side in the calibration run, the opposite is true for Alternative 1. It follows that an improvement of conditions has been realized there.

Flow streamlines are shown for a flow of 20,000 cfs in Figure 26. The pad is fully submerged at this flow. The tendency for suspension of sediment along the leading edge of the scour hole at the base of the pad is, however, intensified.

ALTERNATIVE 2. In this option, the rock pad constriction of Alternative 1 has been enlarged. The bed topography and pattern of streamlines at a flow of 10,000 cfs can be seen in Figures 27a and 27b, respectively. The scour hole along the upstream side of the pad is even more pronounced, and copious deposition occurs in the lee of the pad. A pronounced lee separation zone can be seen behind the pad in Figure 27b. Sediment suspension was observed to be intense.

It can be seen in Figure 28a that the scour along the base of the (proposed) west bank levee is as much as 12 ft (3.7 m), or 4 ft (1.2 m) deeper than in the case of Alternative 1. Intake depth, however, is only marginally larger than that of Alternative 1, as can be seen in Figure 28b.

Tests were also performed at 4,000, 20,000, and 40,000 cfs for this option. In Figure 29 the tendency for a flow of 4,000 cfs to truncate the downstream end of the bar is evident. Flow streamlines at 20,000 and 40,000 cfs are shown in Figures 30 and 31, respectively. An overall tendency for sediment to accumulate in the overwidened region, and for the bar to rebuild itself, is not measurably mitigated by the rock pad.

ALTERNATIVE 3. This option represents the first of a series using model impermeable in–channel spur dikes. The field prototype would be constructed from rock fill with side slopes at the angle of repose. In the model, however, distortion does not allow a similar construction. As a result, each impermeable dike was constructed from sheet metal, with vertical sidewalls.

The following specifications were used for the dikes employed in Alternatives 3 ~ 8. Model dike thickness was set at 1 in (2.54 cm), corresponding to a field value of 13 ft (4 m). The base of each dike was protected with appropriate quantities of model riprap with a size distribution identical to that used for the rock pads of Alternatives 1 and 2. In all cases, the top elevation of the dike was set at 759 ft, i.e. 3.5 ft lower than the adopted bankfull elevation, and 5 ft lower than the top of the west bank levee. This value insures that each dike is fully submerged at flows of bankfull or larger, and helps minimize the effect of the dike on flood stages.

Alternative 3 consists of a single impermeable dike built out from the west bank. The associated bed topography and flow streamlines at a flow of 10,000 cfs can be seen in Figures 32a and 32b, respectively. The effect of the spur dike is seen to be very similar to that of the pad of Alternative 2.

Deep scour was again manifested along the upstream side of the dike, raising the possibility of destabilization of the west bank levee. Sediment suspension along the scour hole was likewise intense at discharges of 10,000 cfs and larger. At a discharge of 10,000 cfs, the intake section tends to be deep on both sides of the channnel, with a central ridge, as seen in Figure 33. Intake conditions do not seem quite as favorable as those obtained for Alternative 1.

Bed topography and flow streamlines are shown at a discharge of 4,000 cfs in Figures 34a and 34b, respectively. In analogy to Alternative 2, the single spur dike truncates only the downstream edge of the bar. Adequate conditions are maintained at the intake, as shown in Figure 35. Flow streamline patterns are shown at discharges of 20,000 cfs and 40,000 cfs in Figures 36 and 37, respectively. The effect of the dike on flood flow appeared to be minimal.

The experience gained with Alternatives 1 ~ 3 suggests that appropriate constriction and flow deflection can indeed maintain adequate flow depths at the intake, and prevent the bar from migrating farther downstream. On the other hand, a single obstruction, whether a pad or a spur dike, cannot eliminate the bar. In addition, the turning of the flow from west to east bank provided by a single obstruction is quite abrupt. This results in deep scour along the base of the pad or dike on the upstream side, with possible failure of the dike and/or west bank levee to which it is attached. Finally, the local scour around the structure is associated with a strong oblique vortex, which is very effective in suspending sediment. This sediment then passes directly past the intake house.

As a result of these considerations, it was decided to attempt to provide a more gradual deflection of the flow by means of a field of spur dikes. The placement of the dikes was chosen so as to effectively restore the flow alignment near the intake that prevailed in 1961, in accordance with the results of the diagnostic study [6].

ALTERNATIVE 4. In this option, two spur dikes were placed rather than one. Their positions are shown in Figure 38. In Figures 39a and 39b, bed topography and flow streamline patterns are shown at a flow of 10,000 cfs. The brunt of the deflection is borne by the leading dike, again resulting in rather severe local scour along its upstream side. The flow pattern across the intake is seen to be parallel and smooth, indicating excellent conditions.

Bed topography and flow conditions are shown in Figures 40a and 40b at 4,000 cfs, 41a and 41b at 20,000 cfs, and 42a and 42b at 40,000 cfs. At 4,000 cfs, the bar of Figure 14a has been essentially removed, with only a remnant near section 11. The flow pattern is seen to be superior to that found for Alternatives 2 and 3 at 4,000 cfs. Local scour along the leading dike is most intense at 20,000 cfs, with an arc–like scour hole extending downstream past the tip of the trailing dike. Flow patterns at the intake again appear to be good.

At 40,000 cfs, some separation of surface flow appears along the east bank, in the approximate position of the bar of Figure 14b. There is a tendency for the bar to be reinstated, but its topography is subdued compared to that of the calibration run.

In Figure 43, water surface profiles measured at 20,000 and 40,000 cfs for Alternative 4 (west bank levee and two dikes in place) are compared with calibration values. The two sets are essentially indistinguishable, indicating that the effect of the dikes at such flows on flood water surface elevation is negligible.

The results of Alternative 4 were considered to be very favorable. The only problem was the observation that most of the deflection was done by the leading dike, causing deep local scour along it adjacent to the (proposed) west bank levee. It was then decided to adjust the length of the dikes appropriately, and add a third short leading dike.

ALTERNATIVE 5. This alternative was investigated only cursorily at a flow of 10,000 cfs because visual observation suggested some obvious improvements, later realized in Alternative 6. Bed topography and flow patterns are shown in Figures 44a and 44b. Conditions appear somewhat improved over Alternative 4. The effective flow channel was slightly wider than desirable near the middle dike, however. It was decided to lengthen the leading dike, and make the middle dike more nearly perpendicular to the west bank.

ALTERNATIVE 6. This is the first of the runs for which a complete set of data is available. The positioning of the three dikes is illustrated in Figure 45. The essentially negligible effect of the dikes and west bank levee on water surface elevations is illustrated in Figure 46. Other results are summarized below according to discharge.

Tests at 10,000 cfs. Bed topography and flow patterns are illustrated in Figures 47a and 47b, respectively. The results appear to be excellent. The bed topography at the intake is illustrated in Figure 48. The profile appears to be superior to that realized at the same discharge in Alternative 3 (Figure 33), for example. No central ridge appears in Figure 48, and a wider area of deep flow is maintained near the intake. On the other hand, excessive scour of the bed immediately adjacent to the intake is not realized.

The bed topography is illustrated in detail in Figure 49. Scour at the junction of the leading dike and the (proposed) west bank levee is clearly not excessive. The deepest scour appears at the tip of the middle dike, at a safe distance from the west bank. Considerable deposition of sediment occurred between the middle and trailing dike. Only a trace of the bar seen in Figure 14 remains; it is located between sections 11 and 12, well upstream of the intake.

Tests at 4,000 cfs. Bed topography and flow patterns are again seen to be excellent in Figures 50a and 50b. The intake bed profile, seen in Figure 51, is similarly good. A contour map of the bed topography is given in Figure 52; the results parallel those at 10,000 cfs.

Tests at 20,000 cfs. Bed topography and flow patterns are shown in Figures 53a and 53b. A coutour map of the bed topography is given in Figure 54. Comparison with Figure 13c reveals a lowering of the bed by 4 ~ 5 ft in comparison with the calibration run, in the vicinity of the intake. The bar remains subdued.

Tests at 40,000 cfs. Bed topography and flow patterns are shown in Figures 55a and 55b. A tendency for the bed level to rise on the average is realized, as was the case for the calibration run.

A contour map of bed topography is shown in Figure 56. Comparison with Figure 13d reveals that in this case alone, bed elevations at the intake are higher than their corresponding values for the calibration run. In fact, bed elevations are found almost everywhere to be higher than in the case of the calibration run. This is likely due to the somewhat unrealistic nature of the tests at this discharge, as discussed earlier. That is, a flow of 40,000 cfs cannot be expected to continue in the field for the long duration it was run in the model. In any case, at the intake section, the flow depth immediately adjacent to the intake is substantially lower than the depth near the center of the channel.

In summary, the results for Alternative 6 indicate excellent performance at discharges of 4,000, 10,000, and 20,000 cfs, and adequate performance at 40,000 cfs.

ALTERNATIVE 7. In this option, an attempt was made to reproduce the good results of Alternative 6 using only two carefully–positioned dikes. The intent was to find a more cost–effective solution. The position of the spur dikes is denoted on Figure 57.

Water surface profiles are shown in Figure 58 at all flows. Again, the dikes and levees do not raise flood stage measurably over calibration values.

Tests at 10,000 cfs. Bed topography and flow are illustrated in Figures 59a and 59b, respectively. Flow patterns are seen to be similar to those of Alternative 6. The surface streamlines are, however, somewhat less regular, as can be seen by comparing Figures 59b and 47b.

Bed elevation contours are shown in Figure 60. Intake bed elevations differ only slightly between Alternative 6 and Alternative 7, as can be seen from a comparison with Figure 49. The bar on the east bank is seen to be rather larger, however, and patterns of bed scour are more irregular. On the whole, the results were judged to be good, but not quite as good as those obtained for Alternative 6.

Tests at 4,000 cfs. Bed topography and flow patterns are shown in Figures 61a and 61b. Flow patterns are again not quite as good as those realized in Alternative 6.

Bed elevation contours are shown in Figure 62. The bar on the east bank between sections 11 and 12 is seen to be higher than that realized in Alternative 6. Intake conditions are slightly worse than in the case of Alternative 6, in that higher bed elevations are realized adjacent to the intake.

Tests at 20,000 cfs. Bed topography and flow patterns are shown in Figures 63a and 63b. Bed elevation contours are shown in Figure 64. At this flow, the performance of Alternative 7 appears to be as good as Alternative 6.

Tests at 40,000 cfs. Bed topography and flow patterns are shown in Figures 65a and 65b. Bed elevation contours are shown in Figure 66. In terms of bed elevation near the intake, Alternative 7 appears to be slightly superior to Alternative 6 at this flow. The surface streamlines of Alternative 7 are not, however, as regular as those of Alternative 6.

In summary, the scheme of Alternative 6 is found to perform somewhat better than Alternative 7 at 4,000 and 10,000 cfs. Performance is similar at 20,000 cfs; at 40,000 cfs Alternative 7 may perform slightly better. Insofar as the lower flows are the more frequent ones, Alternative 6 is judged to be the better of the two in an overall sense. Either, however, appears to be adequate in terms of removing the bar and maintaining good intake conditions.

ALTERNATIVE 8. In this alternative, three spur dikes are again used. They are shortened in comparison with Alternative 6, however, in the hopes of making the design more cost–effective. The positioning of the dikes is shown in Figure 67. Water surface profiles at all flows are shown in Figure 68. It is again confirmed that the dikes and levee have a negligible effect on flood flow elevations.

Tests at 10,000 cfs. Photographs of bed configuration and flow streamlines are given in Figures 69a and 69b. Contours of bed elevation are given in Figure 70. The results compare very well with those of Alternative 6. A rather deep scour hole appears at the intake, however.

Tests at 4,000 cfs. The bed configuration and flow patterns are illustrated photographically in Figures 71a and 71b. The results are indistinguishable from those for Alternative 6. Contours of bed elevation are provided in Figure 72. These are again very similar to those of Alternative 6. The intake section is more uniform than Alternative 6, suggesting that Alternative 8 is slightly superior in this regard.

Tests at 20,000 cfs. Photographs of the bed configuration and surface flow streamlines are shown in Figures 73a and 73b; the visual pattern is essentially identical to that obtained for Alternative 6. Bed elevation contours are presented in Figure 74. .The intake section is somewhat deeper than that of Alternative 6. This advantage is partially counterbalanced by the presence of a point of high elevation, apparently a remnant of the bar, at section 14. This high point was less pronounced in the case of Alternative 6.

Tests at 40,000 cfs. The bed configuration and surface flow patterns are illustrated photographically in Figures 75a and 75b. Lines of constant bed elevation are shown in Figure 76. An undesirable high point is apparent in the center of the channel at section 13. Intake conditions, however, appear to be slightly better than in the case of Alternative 6.

It may be concluded that the best overall performance was obtained with either Alternative 6 or Alternative 8. Alternative 6 provides a more complete removal of the bar presently upstream of the intake. On the other hand, Alternative 8 provides a slightly better cross–section at the intake house. Either appears acceptable for the rectification of the sedimentation problem in the Minnesota River adjacent to the Wilmarth Power Plant.

VIII. CONCLUSIONS AND RECOMMENDATIONS

Based on the information obtained from both the physical model study and the diagnostic study [6], the following recommendations can be made.

1. The construction of a levee along the west bank of the Minnesota River near the intake would help stabilize the river channel in its present configuration, and would aid in preventing the bar from shifting farther downstream.

2. The removal of the floodplain spur dike shown in Figure 5 has important implications for the intake. In its absence, and without reconstruction of the west bank, a substantial amount of flow would leave the channel during floods, enter the excavation, and flow over the floodplain before re–entering the channel (Figure 17). As a result, the possibility of a channel avulsion away from the intake cannot be ignored.

3. A properly designed levee would substantially reduce the possibility of channel avulsion.

4. The levee would neither eliminate, nor reduce the size of, the existing bar that is feeding sediment past the intake.

5. The levee will be more effective the higher it is. A height of 764 ft (232.9 m) would render it no higher than much of the surrounding floodplain, and thus acceptable in terms of the potential for raising flood stages.

6. The levee should extend downstream from point A (70 ft downstream from cross–section no. 8) to point C (80 ft downstream from cross–section no. 15) in Figure 18. This gives a levee with a total length of approximately 1600 ft. Any existing natural levees along this way should be excavated back at least to the depth of placement of the riprap. In the model study, point A was originally midway between sections 9 and 10, as shown in Fig. 18. The results of the diagnostic study indicated that the bank protection should extend as far upstream as cross–section 9. The final position of point A takes this into account and allows for the possibility of tying the upstream end of the levee to the existing natural terrain.

7. The model study does not provide a definitive basis for choosing between Options 1 and 2, in that the results for flow and bed topography are quite similar. Option 1 for the levee, however, seems to be marginally better than Option 2 (Figure 18) in terms of flow patterns. Option 1 would allow for the placement of a filter layer or geotextile under not only the riprap above the water

line, but also that portion extending down the river bank. It would also allow the placement of an extra stockpile of riprap at the toe of the bank. This would provide added safety, as compared to Option 2, for which the bank riprap is self-launching, but might be more expensive.

8. Two different design criteria for the riprap gradations were considered. The first is that of Neill [7] and the second is based on the procedure of the U.S. Army Corps of Engineers [8].

Neill recommends the following riprap gradation for local velocities up to 10 ft/s.

100%	smaller than	18 in or 300 lbs
≥ 20%	larger than	14 in or 150 lbs
≥ 50%	larger than	12 in or 80 lbs
≥ 80%	larger than	8 in or 25 lbs

The U.S. Army Corps of Engineers recommends the following riprap gradations for the same hydraulic conditions.

Percent lighter by weight	Weight limits (lbs)	Size (inches)
100	86–35	12–9
50	26–17	8–7
15	13–5	6–5

Based on the results of Figure 19, both of the above gradations would be more than adequate for the present case, at least up to 40,000 cfs (1130 cumecs). This discharge corresponds to a flood with a recurrence interval near one in ten years. If the levee were to be designed for the highest flow on record, coarser riprap might be required. In this case, the issue of cost-effectiveness needs to be considered.

9. A possible cross-section for the levee is suggested in Figures 22 and 23, based upon Option 1. It is important to note that the design based upon the recommendation of the U.S. Army Corps of Engineers gives considerably less volume of riprap than the one obtained following Neill. This is due to the difference in riprap thickness. The diagrams in Figures 22 and 23 should provide the basis for design and consultation with a contractor, rather than a final result.

10. The diagnostic study [6] indicates that restoration of channel width and alignment near the intake to the configuration prevailing in 1961 should result in both the removal of the bulk of the bar visible in Figure 14, and the maintenance of appropriate flow depths at the intake as well.

11. The above result of the diagnostic study was confirmed in the model study. A field of three impermeable in–channel spur dikes was found to restore effective channel width and alignment, remove most of the bar, and maintain sufficient depth in the vicinity of the intake.

12. Based on experimental results, Alternatives 6 and 8 were found to provide the best configuration of three spur dikes for correction of the sedimentation problem at Wilmarth Power Plant. Alternative 6 provides somewhat more complete removal of the bar. Intake conditions seem to be slightly better in the case of Alternative 8. Alternative 8 is likely the less expensive of the two options, insofar as the total length of dikes is shorter.

13. It is recommended that the three spur dikes be built out from the west bank levee from appropriately selected rock. A top width of 13 ft was tested herein; in the field, this value will be controlled by construction techniques (e.g. width of haul road if end–dumping from trucks is employed). The spur dikes should be covered with a layer of riprap sufficient to prevent erosion. An extra stockpike of riprap should be placed along the base of each spur dike in order to provide protection against expected local scour during floods. Special attention needs to be paid to the upstream side of the spur dikes in this regard. An extra stockpile of riprap and/or a larger size is advisable around the tip of each dike, and where each dike joins the west bank levee. Useful information as regards design can be found in refs. [7] and [8].

14. An overall mean top elevation of the spur dikes of 759 ft provides for adequate submergence of the spur dikes during floods. It is appropriate to taper the spur dikes, so that each is slightly higher near the west bank and lower near the tip. Experiments indicate that the effect of the dikes and levee as proposed herein on flood stages is negligible.

15. It should be remembered that a finite amount of time will be required to wash out the bar and restore favorable conditions at the intake. The amount of time required is dependent on the sequence of floods. Frequent periods of high, but in–channel flows should induce the most rapid restoration. During the adjustment period, conditions may temporarily worsen. Dredging may thus be required in the interim.

IX. REFERENCES

1. Internal correspondence, Northern States Power Co., from J. Mike Pappenfus, Plant Superintendent, Wilmarth Power Plant, to E. H. Schentzel, Adm. Regulatory Liaison, ERAD, October 21, 1983.

2. Johannesson, H., and G. Parker, Realignment of the Minnesota River at the NSP – Wilmarth Plant Intake, Report presented to NSP by St. Anthony Falls Hydraulic Laboratory, University of Minnesota, transmitted August 27, 1986.

3. Diplas, P., Johannesson, H., and H. Stefan, A Survey of Some Conceptual Design Alternatives for the Wilmarth Power Plant Cooling Intake on the Minnesota River, External Memorandum No. 203, St Anthony Falls Hydraulic Laboratory, University of Minnesota, December, 1986.

4. Johannesson, H., and G. Parker, Computer Simulated Migration of Rivers in Minnesota, Project Report No. 242, St. Anthony Falls Hydraulic Laboratory, University of Minnesota, September, 1985.

5. Parker, G, Martinez, I. and R. Hills, Model Study of the Minnesota River near Trunk Highway No. 169 Bridge, Minnesota, Project Report No. 213, St. Anthony Falls Hydraulic Laboratory, University of Minnesota, September, 1982.

6. Johannesson, H., Parker, G., Garcia, M., and Okabe, K, Diagnostic Study of the Siltation Problem at the Wilmarth Power Plant Cooling Water Intake on the Minnesota River, Project Report No. 277, St. Anthony Falls Hydraulic Laboratory, University of Minnesota, August, 1988.

7. Neill, C. R. (editor), Guide to Bridge Hydraulics, Project Committee on Bridge Hydraulics, Roads and Transportation Association of Canada, University of Toronto Press, 191 p, 1973.

8. U.S. Army Corps of Engineers, Additional Guidance for Riprap Channel Protection, Engineer Technical Letter No. 1120–2–120, May, 1971.

REFERENCES

1. Molinas, A. and C. T. Yang, "Computer Program User's Manual for GSTARS (Generalized Stream Tube Model for Alluvial River Simulation)," U.S. Bureau of Reclamation, Denver, Colorado, November 1986.

2. Song, C. C. S. and Yifan Zheng, "Application of Bureau of Reclamation GSTARS to Willow Creek Unprotected Spillway," St. Anthony Falls Hydraulic Laboratory, Technical Report No. 251, April 1987.

3. Molinas, Albert and C. T. Yang, "Generalized Water Surface Profile Computation," J. of Hydraulic Engineering, ASCE, Vol. 111, No. 3, March 1983.

4. Kikkawa, M., S. Ikeda, and A. Kitagawa, "Flow and Bed Topography in Curved Open Channels," J. of the Hydraulic Division, ASCE, Vol. 102, No. 9, Sept. 1976.

5. Doddiah, Doddiah, M. Albertson, and R. Thomas, "Scour from Jets," Minnesota International Hydraulic Convention, 1953.

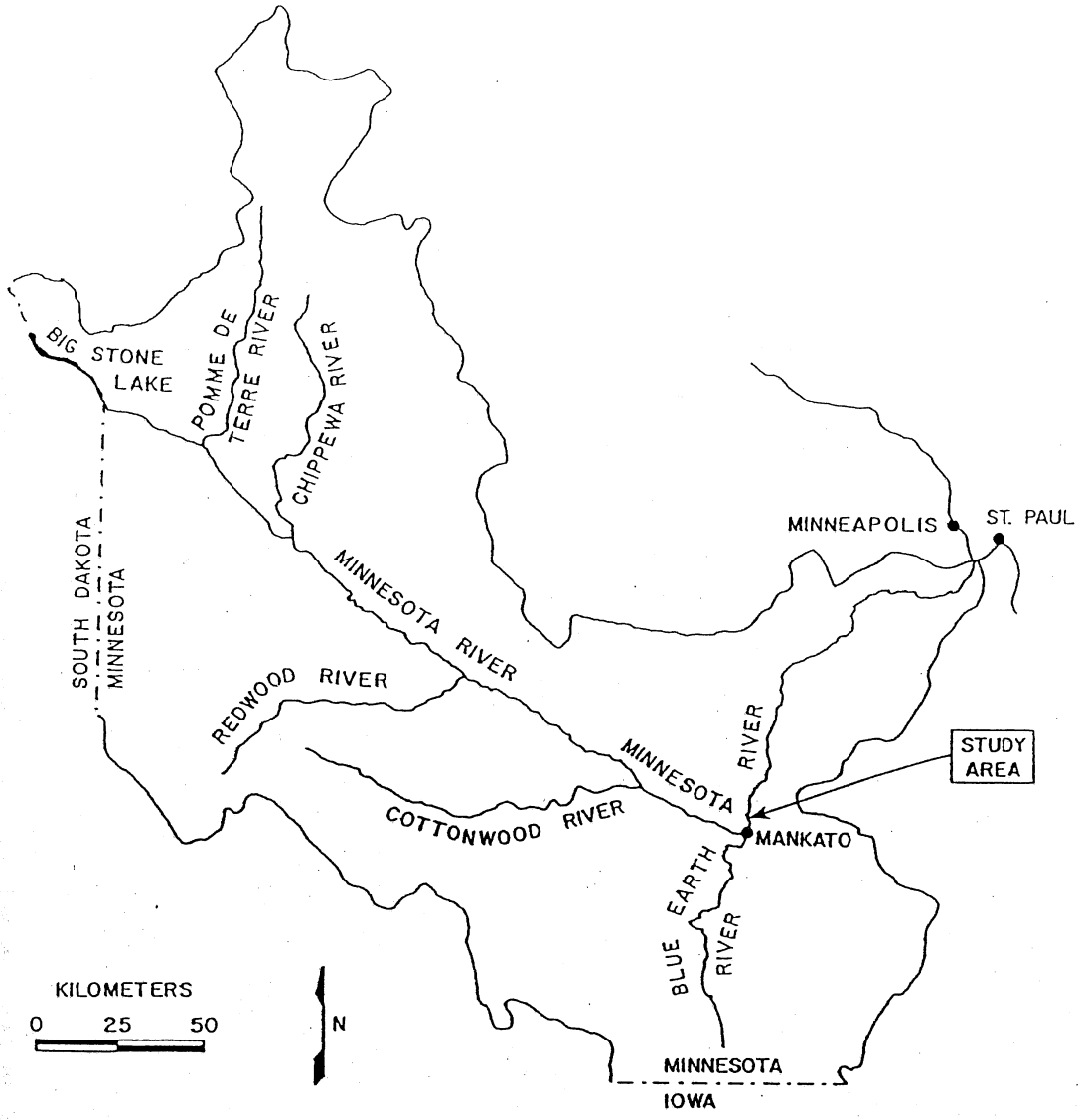

Fig. 1. Minnesota River Watershed.

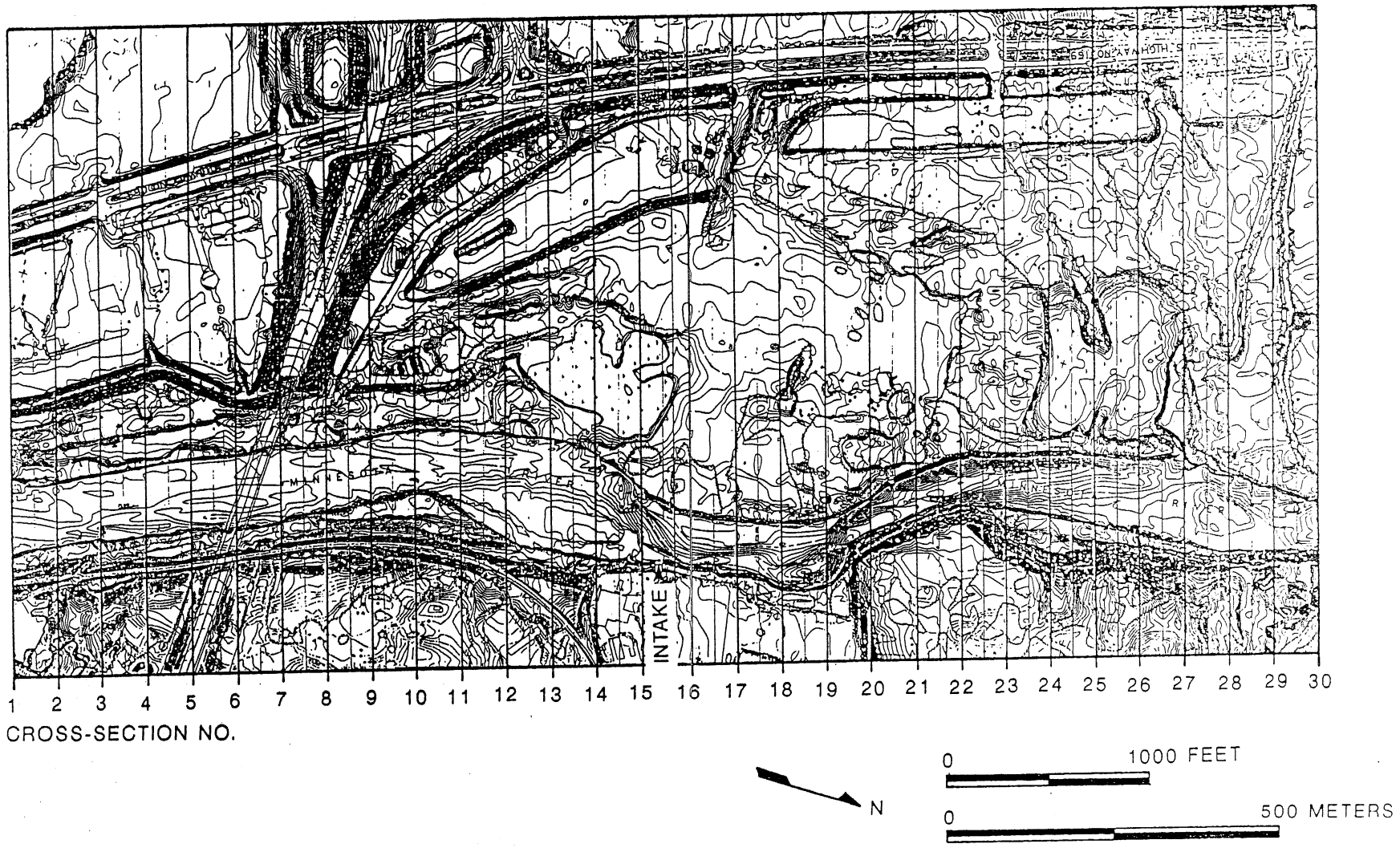

Fig. 2 Topographical map of the channel and floodplain of the Minnesota River near the Wilmarth Power Plant.

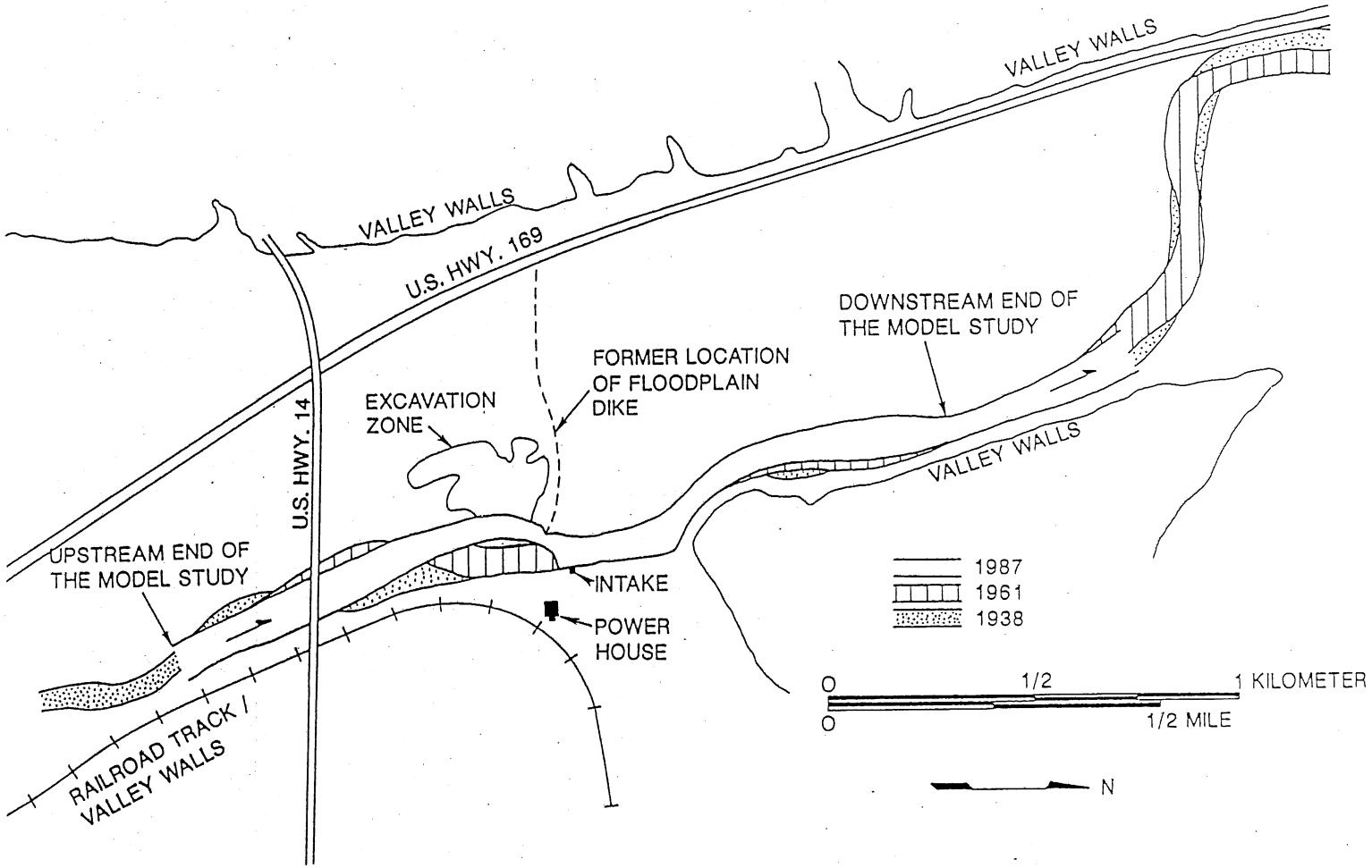

Fig. 3. Plot of the history of channel shift near the power plant, along with the location of the excavation opposite the intake, and the location of the former floodplain spur dike.

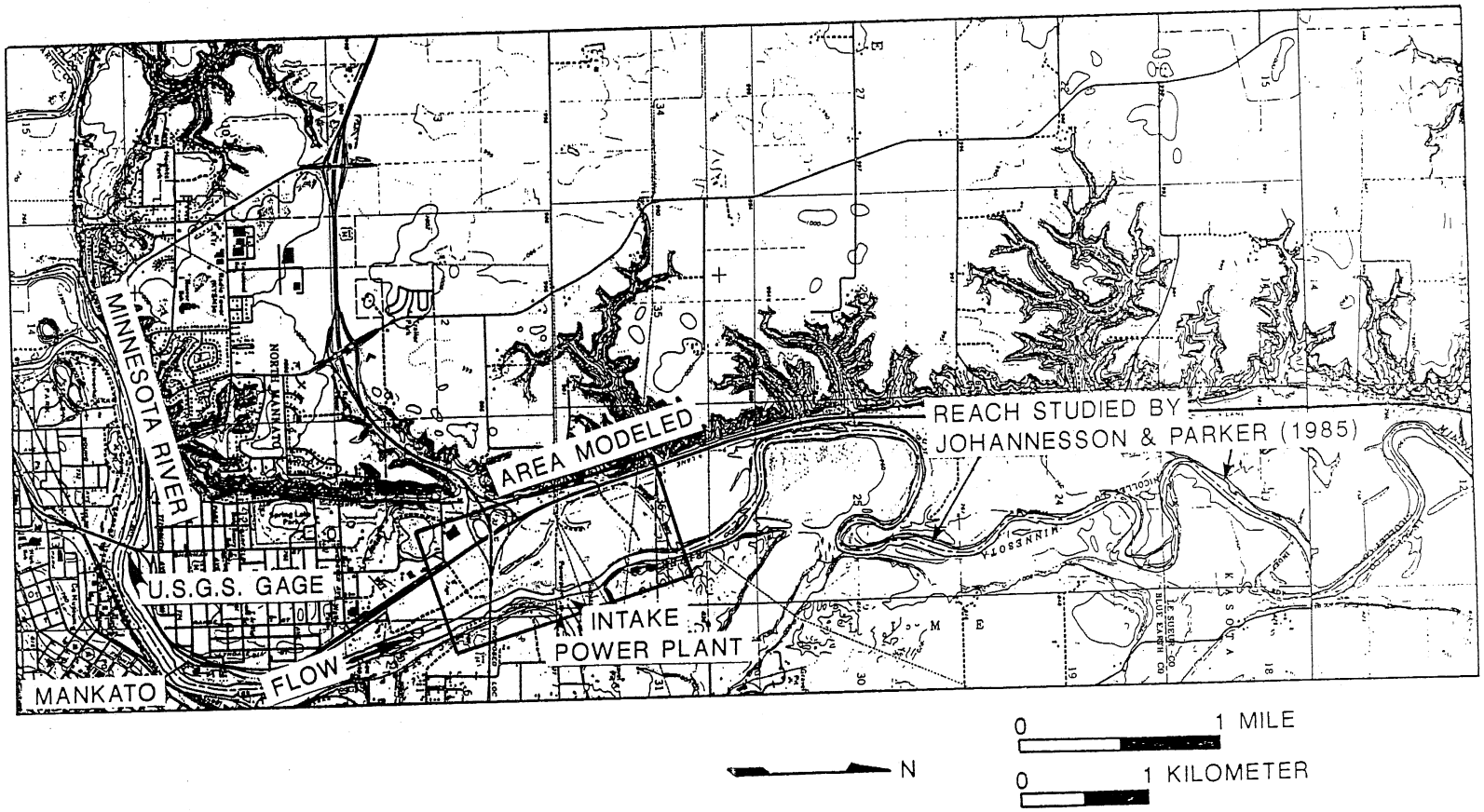

Fig. 4. Area near the power plant included in the physical model.

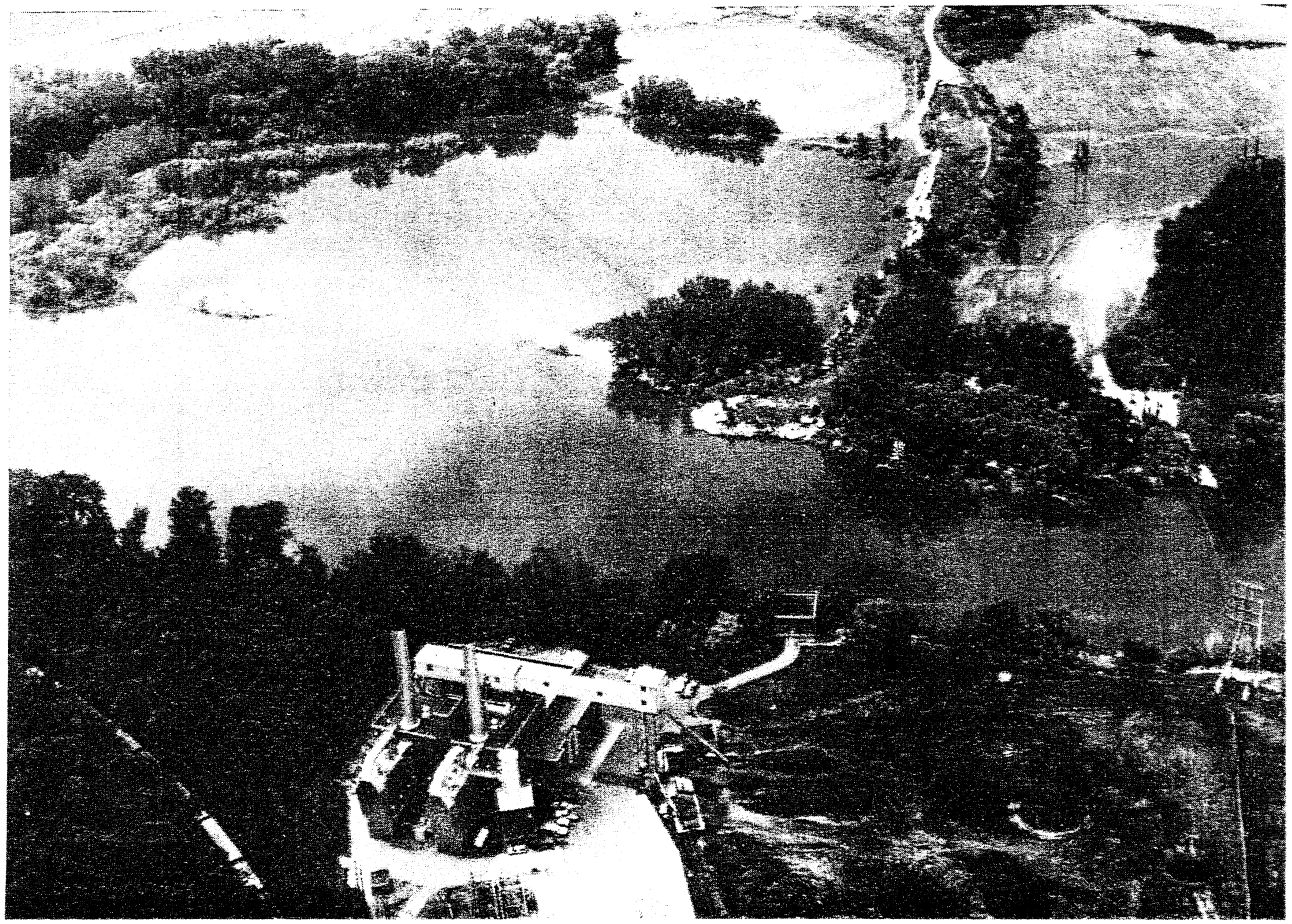

Fig. 5. Photograph of the former spur dike shown in Figure 3. Flow is near bankfull; the excavation is to the left.

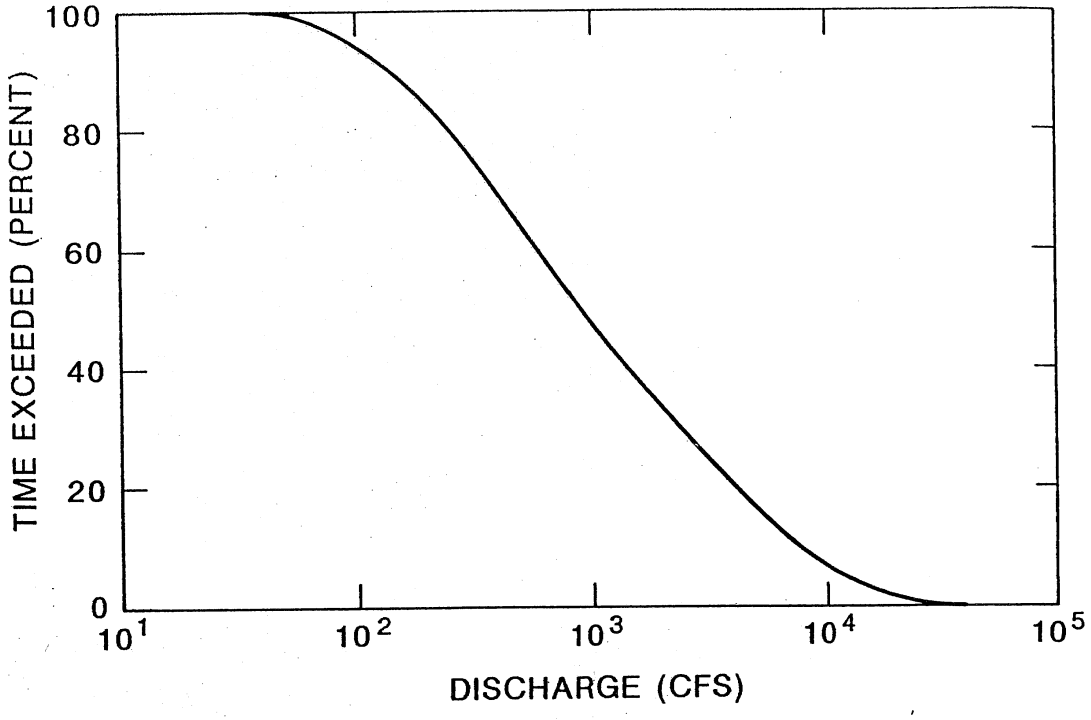

Fig. 6. Flow duration curve for the Minnesota River at Mankato.

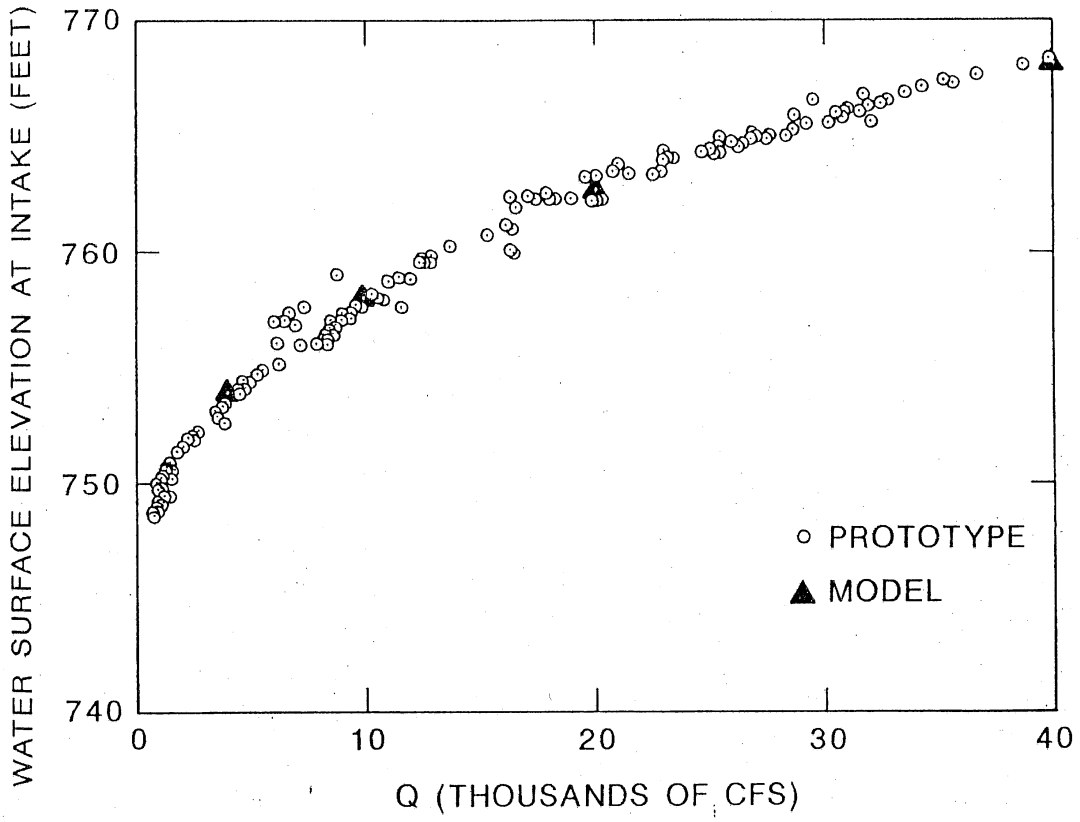

Fig. 7. Plot of observed water surface elevation at the Wilmarth Power Plant as a function of water discharge at Mankato. The open circles denote field measurements; the triangles denote results from the model.

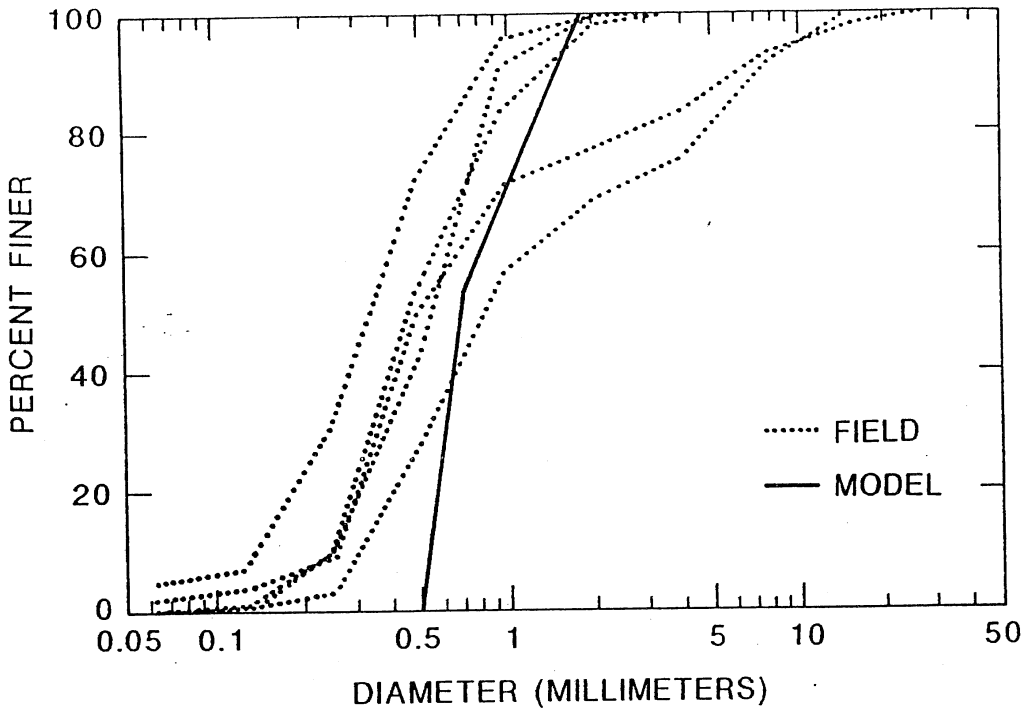

Fig. 8. Several size distributions of: a) bed material of the Minnesota River at Mankato; b) the crushed walnut shells used in the model.

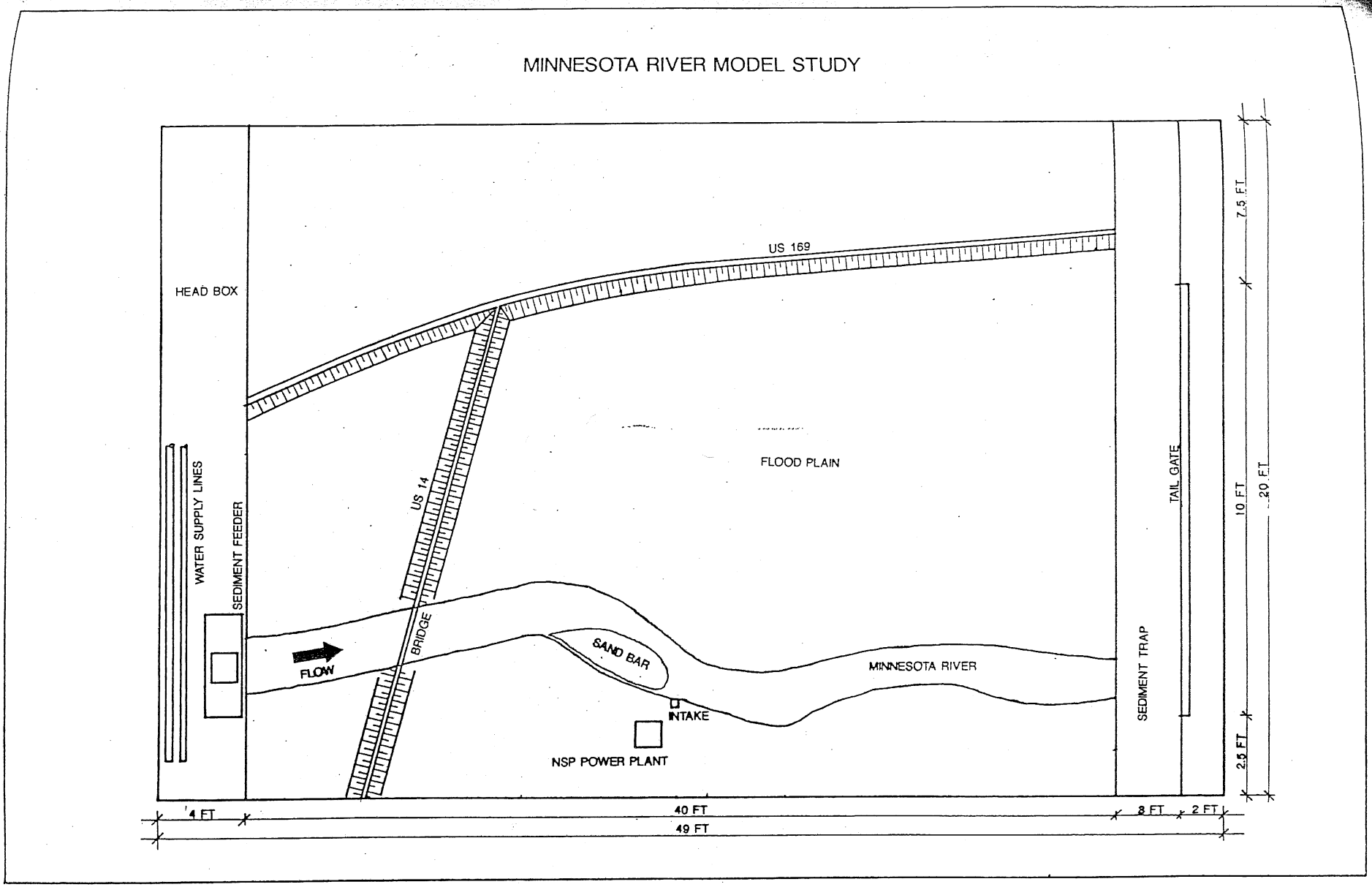

Fig. 9. Schematic diagram of the model basin.

MODEL STUDY OF THE MINNESOTA RIVER NEAR WILMARTH POWER PLANT

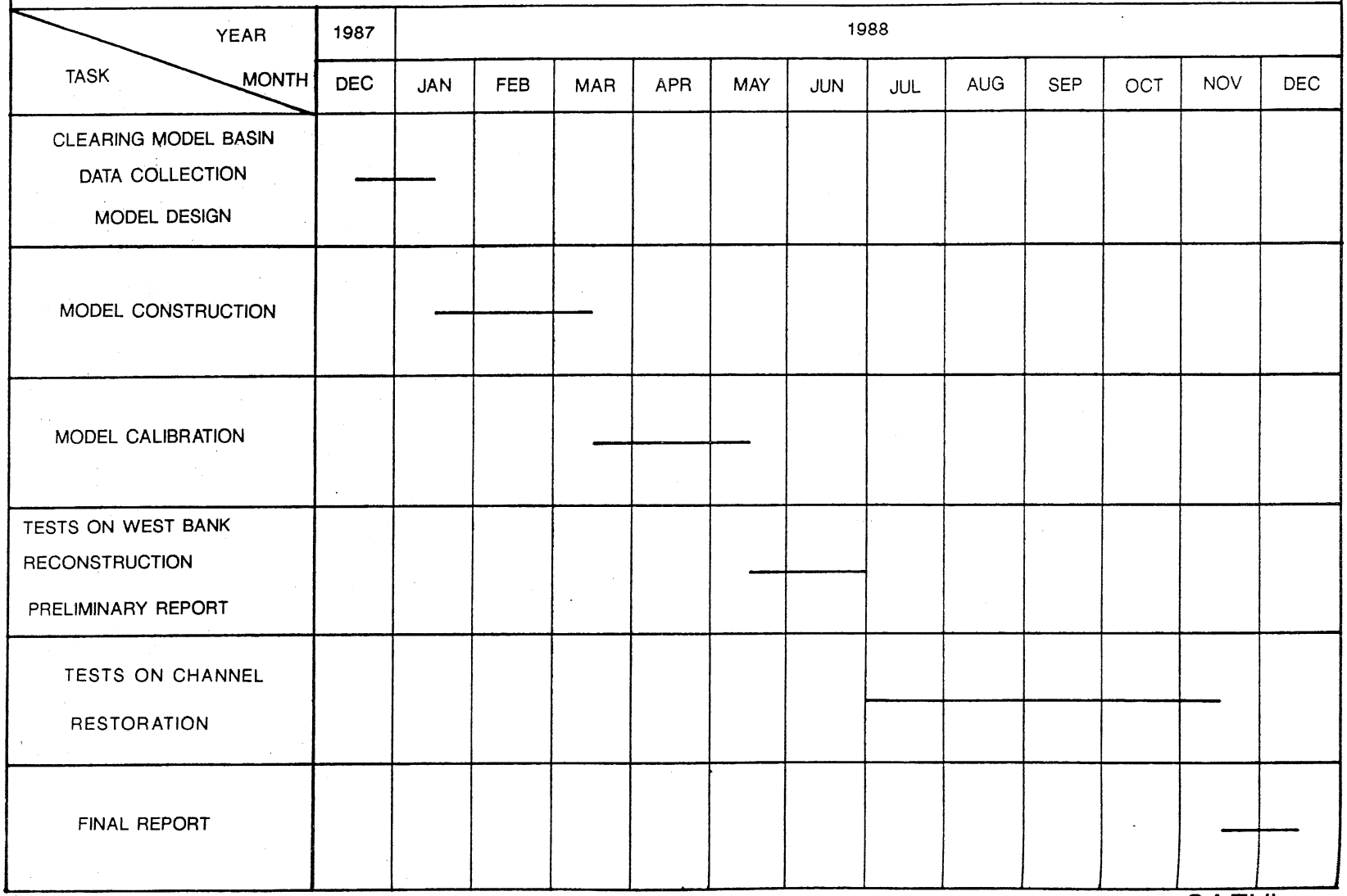

SAFHL

FIGURE 10

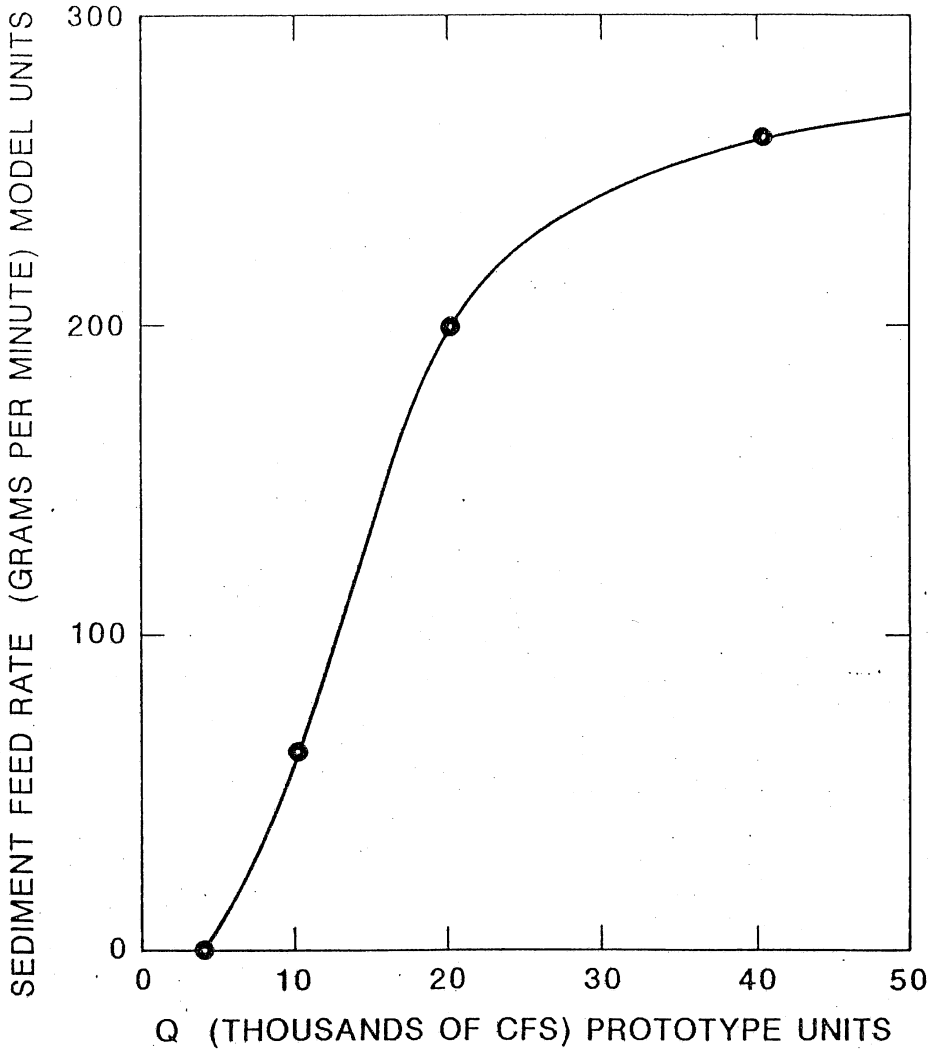

Fig. 11. Sediment feed rate (model values) versus water discharge (prototype values in the calibrated model.

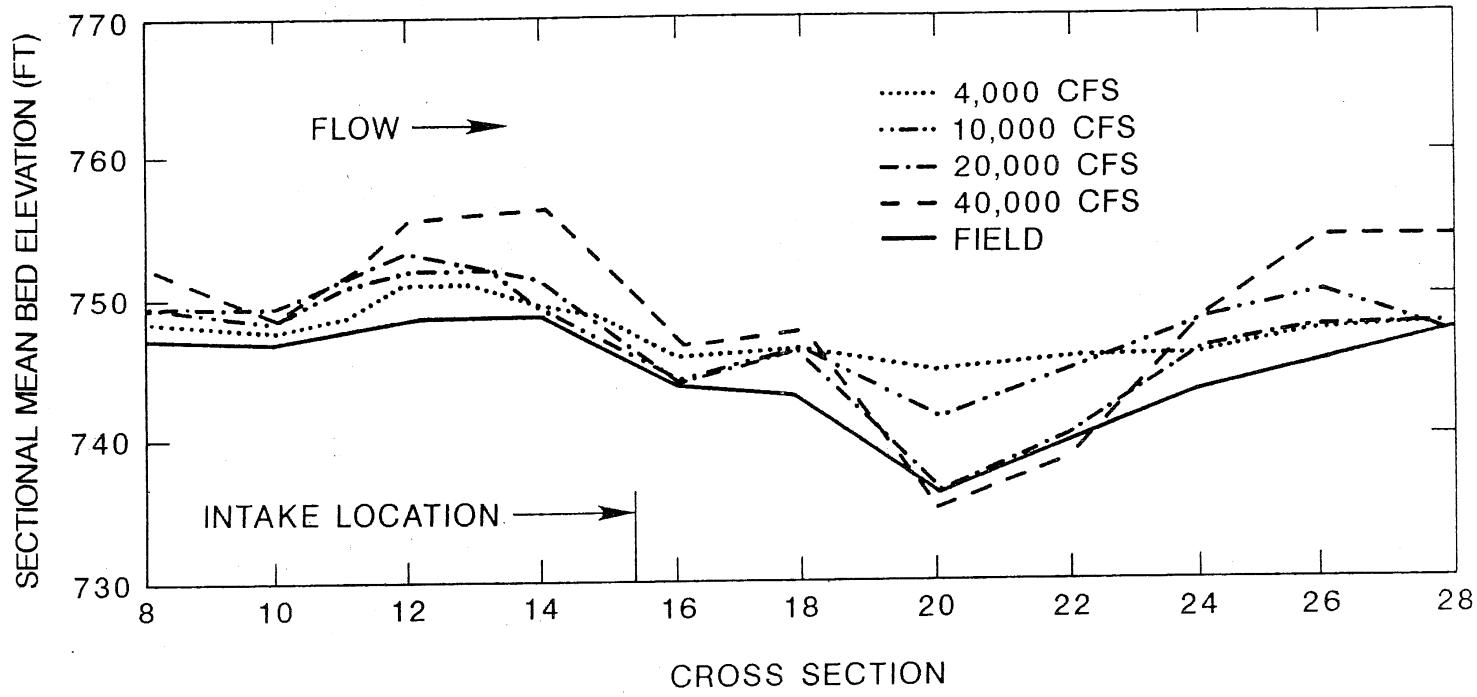

Fig. 12. Mean sectional bed elevation as a function of distance downvalley. Curves are shown for the field measurements, and for the measurements obtained for each calibration. The locations of the sections are shown in Figure 2.

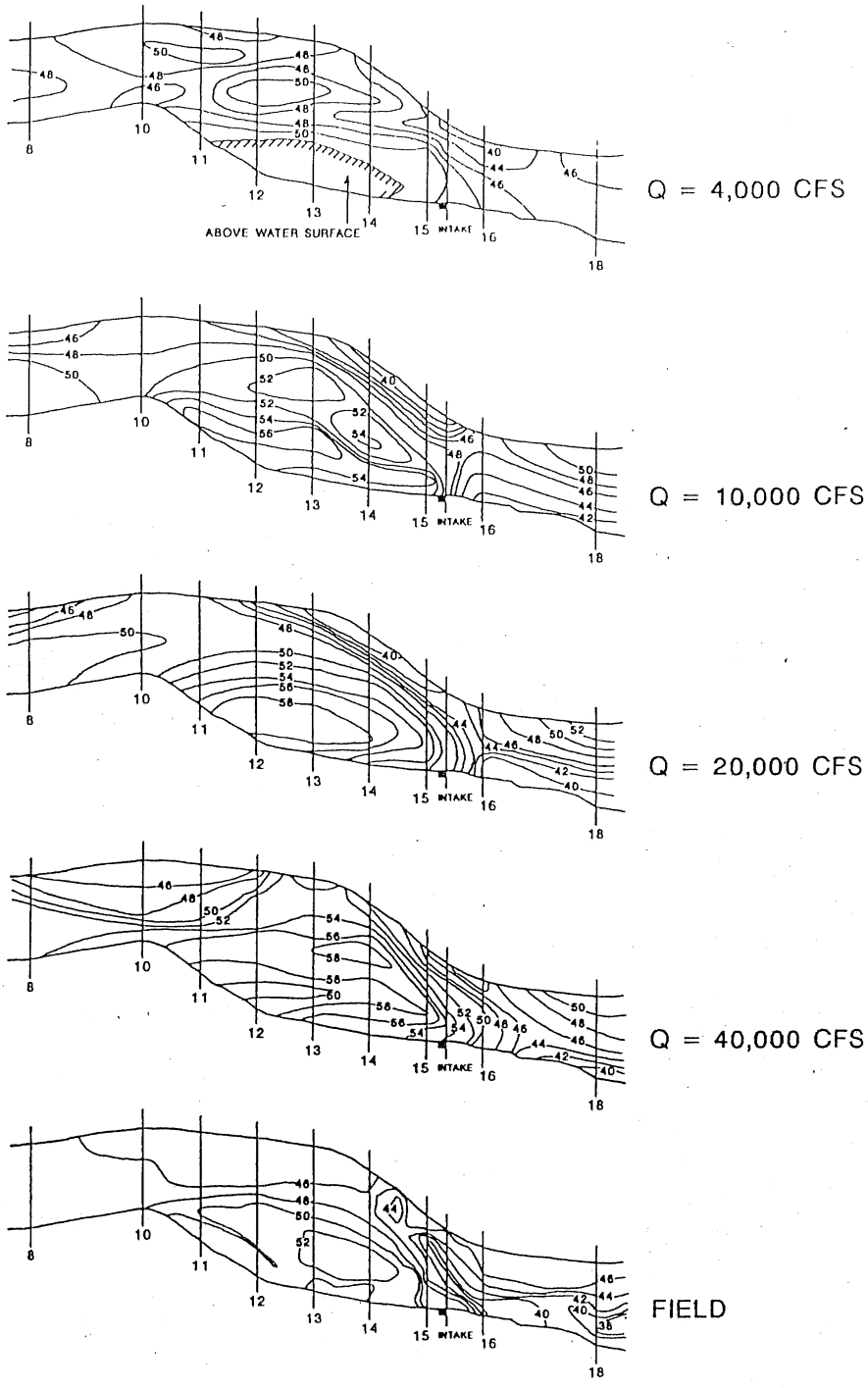

Fig. 13. River bathymetry for the following cases: a) 40,000 cfs (model); b) 20,000 cfs (model); c) 10,000 cfs (model); d) 4,000 cfs (model); e) prototype.

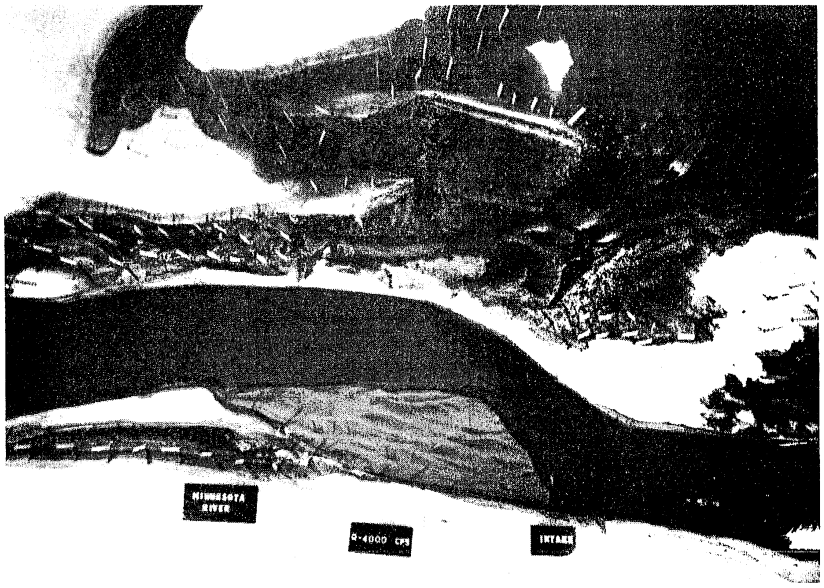

Fig. 14a. The exposed bar upstream of the intake at 4,000 cfs in the model.

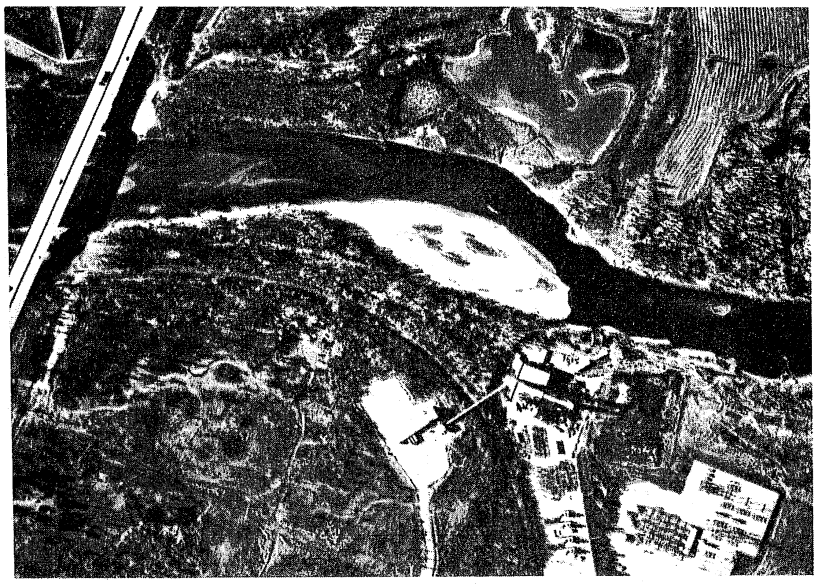

Fig. 14b. The exposed bar upstream of the intake at 5,000 cfs in the prototype.

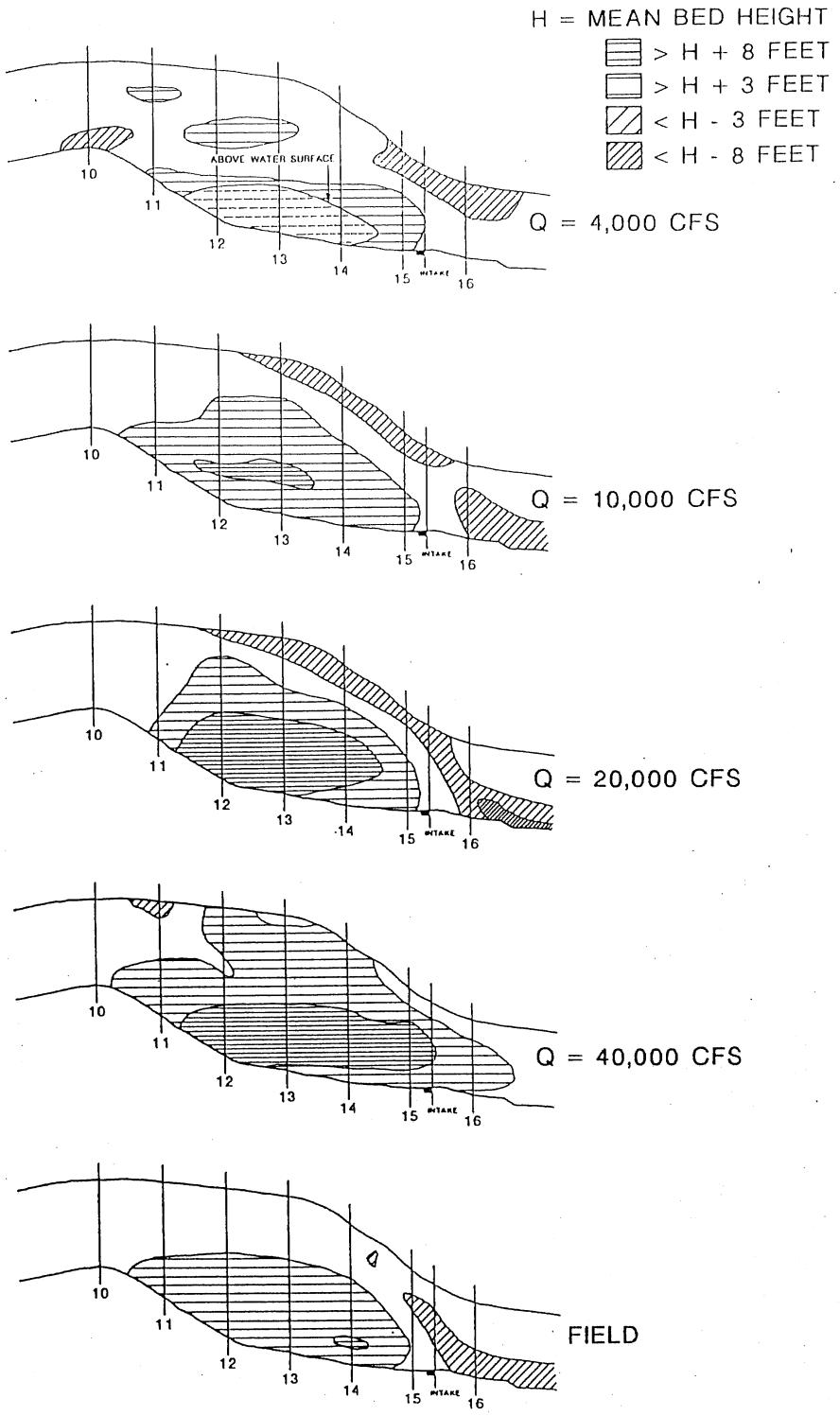

Fig. 15. Plots of relative bed topography, such that elevation 0 corresponds to the mean bed elevation between sections 10 and 16, for: a) 40,000 cfs (model); b) 20,000 cfs (model); c) 10,000 cfs (model); d) 4,000 cfs (model); e) prototype.

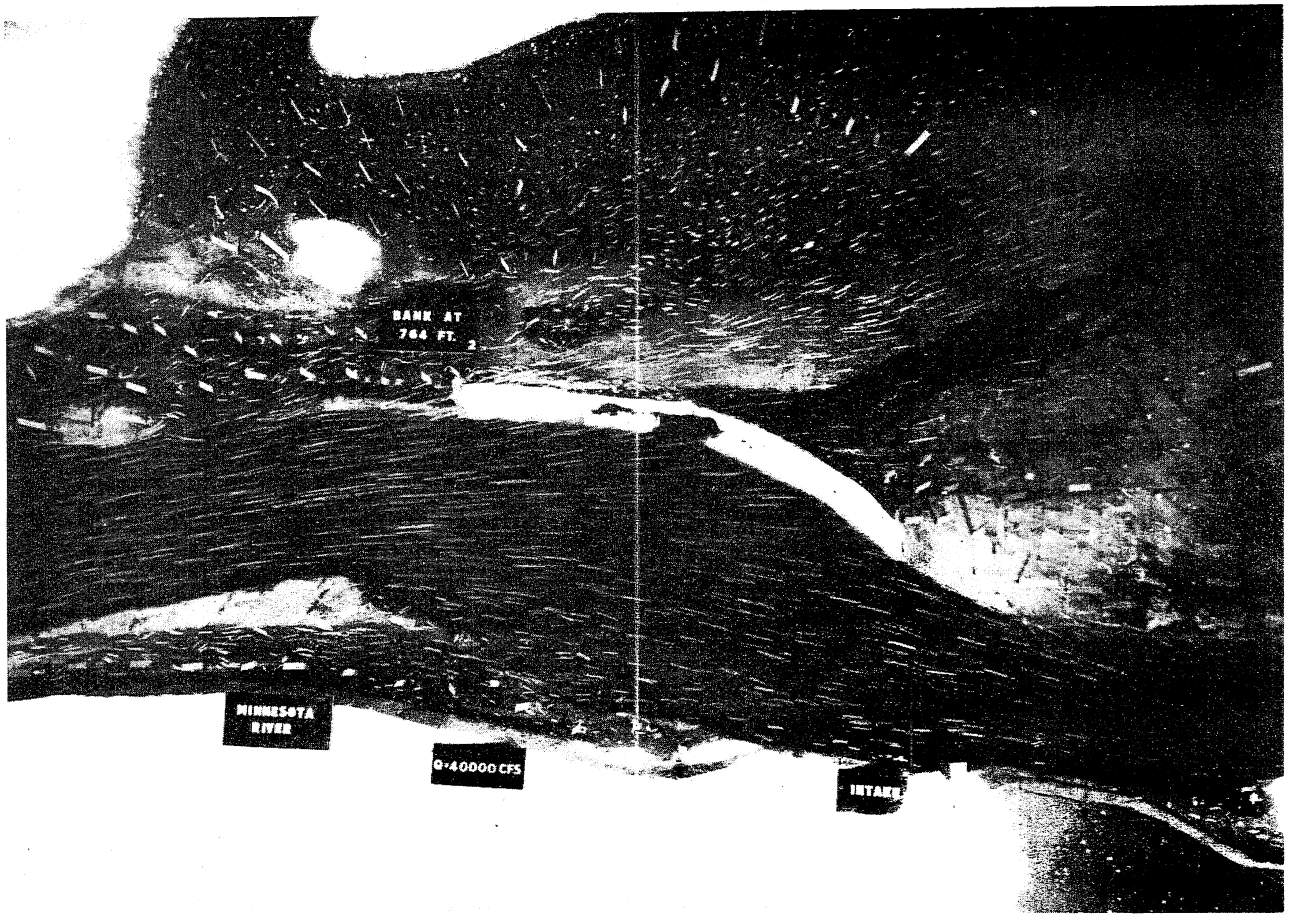

Fig. 16. Photograph illustrating flow patterns in the channel and on the floodplain near the intake at 40,000 cfs in the model.

40,000 cfs in the model.

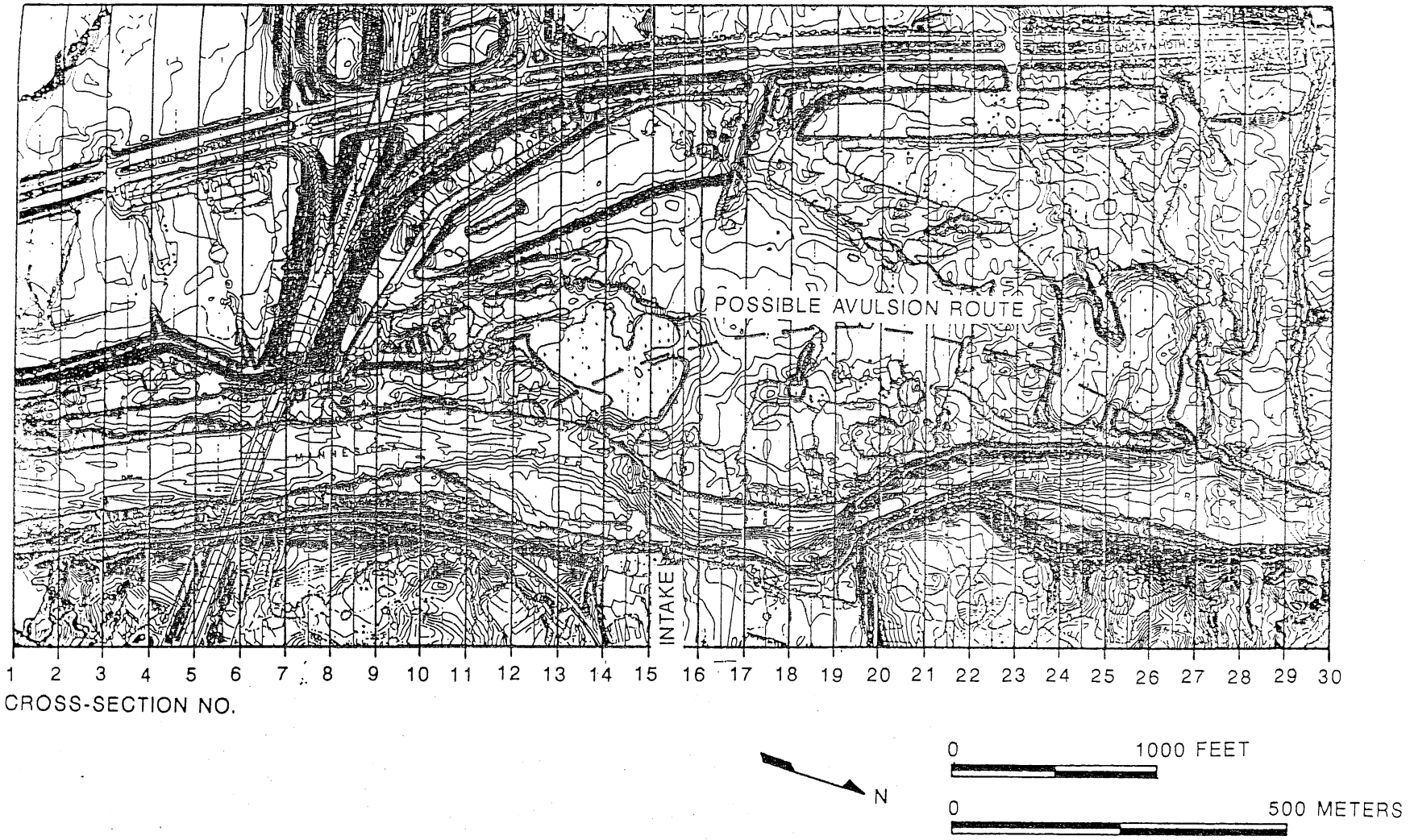

Fig. 17. Sketch of possible avulsion route inferred from observations of flow patterns at 40,000 cfs in the model.

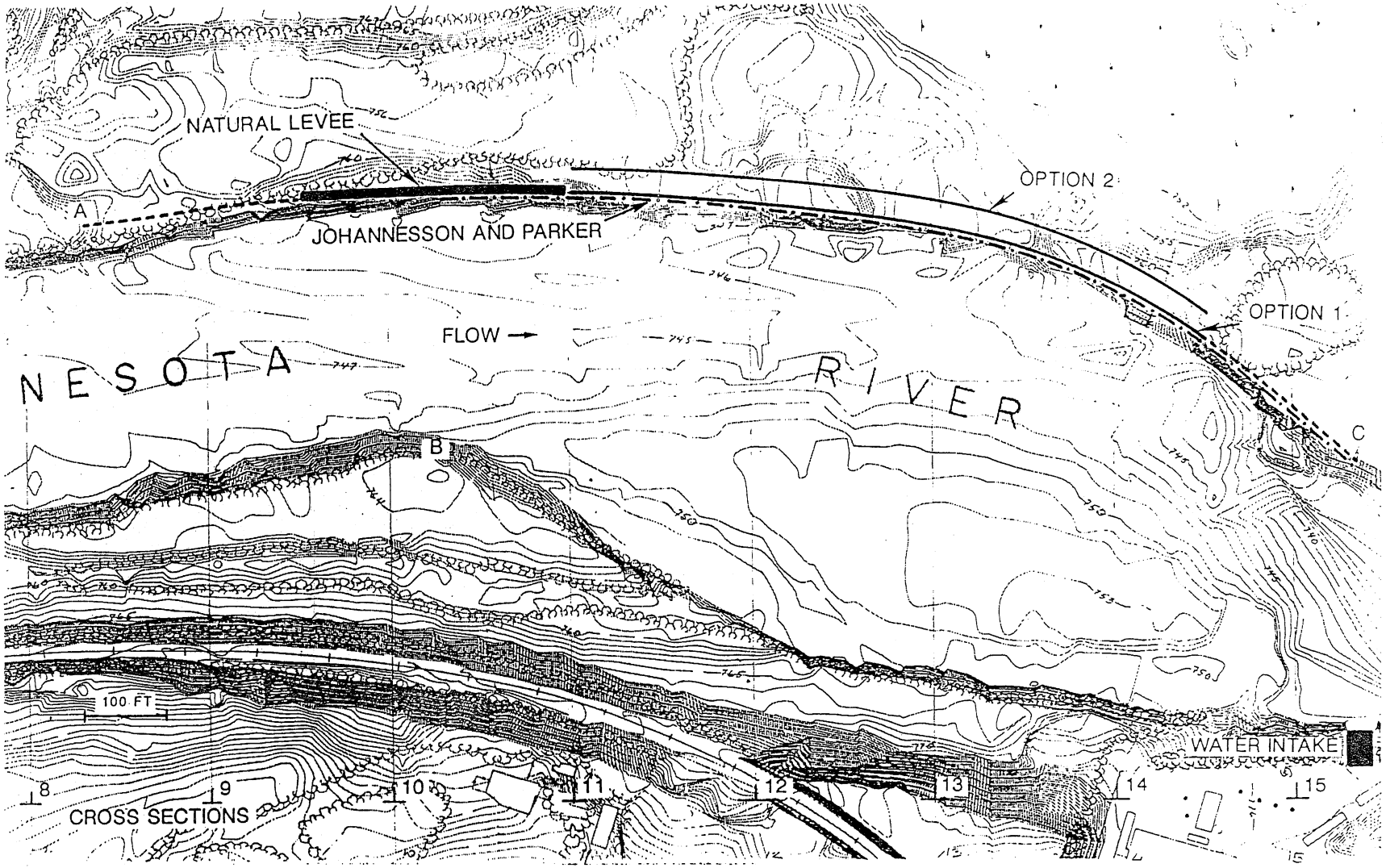

Fig. 18. Various options shown in plan for rebuilding the west bank with a levee.

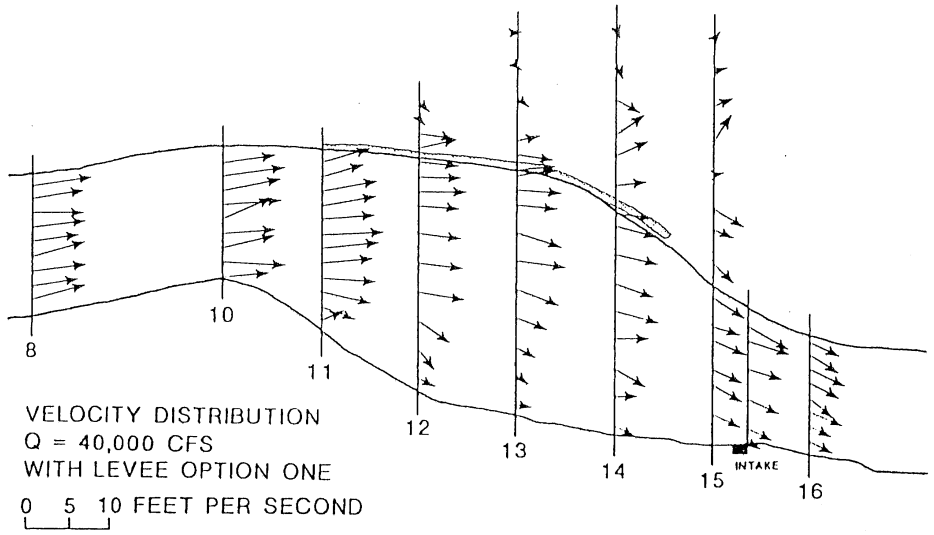

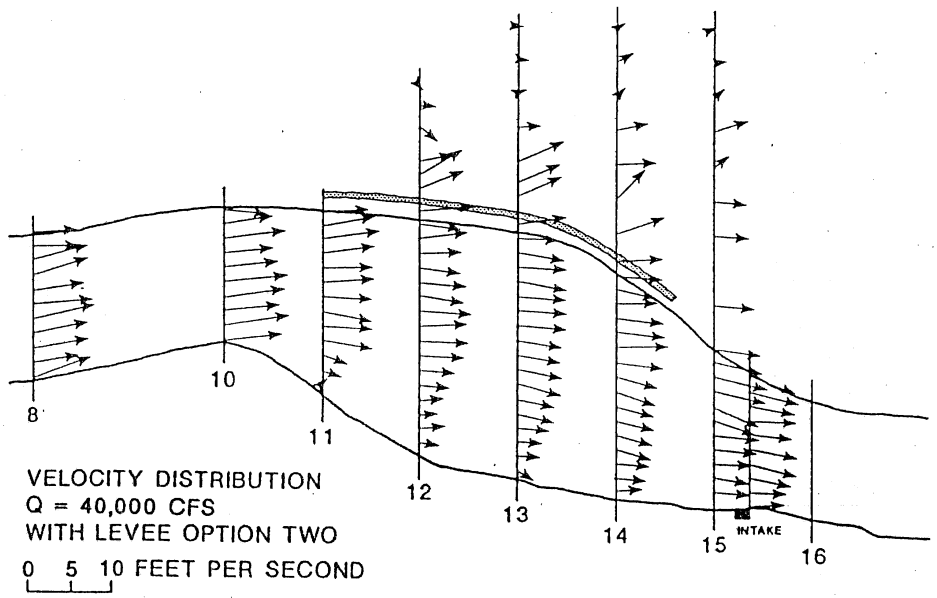

Fig. 19. Patterns of water surface velocity vectors measured in the model for the following two options for the reconstructed west bank: a) Option 1: b) Option 2.

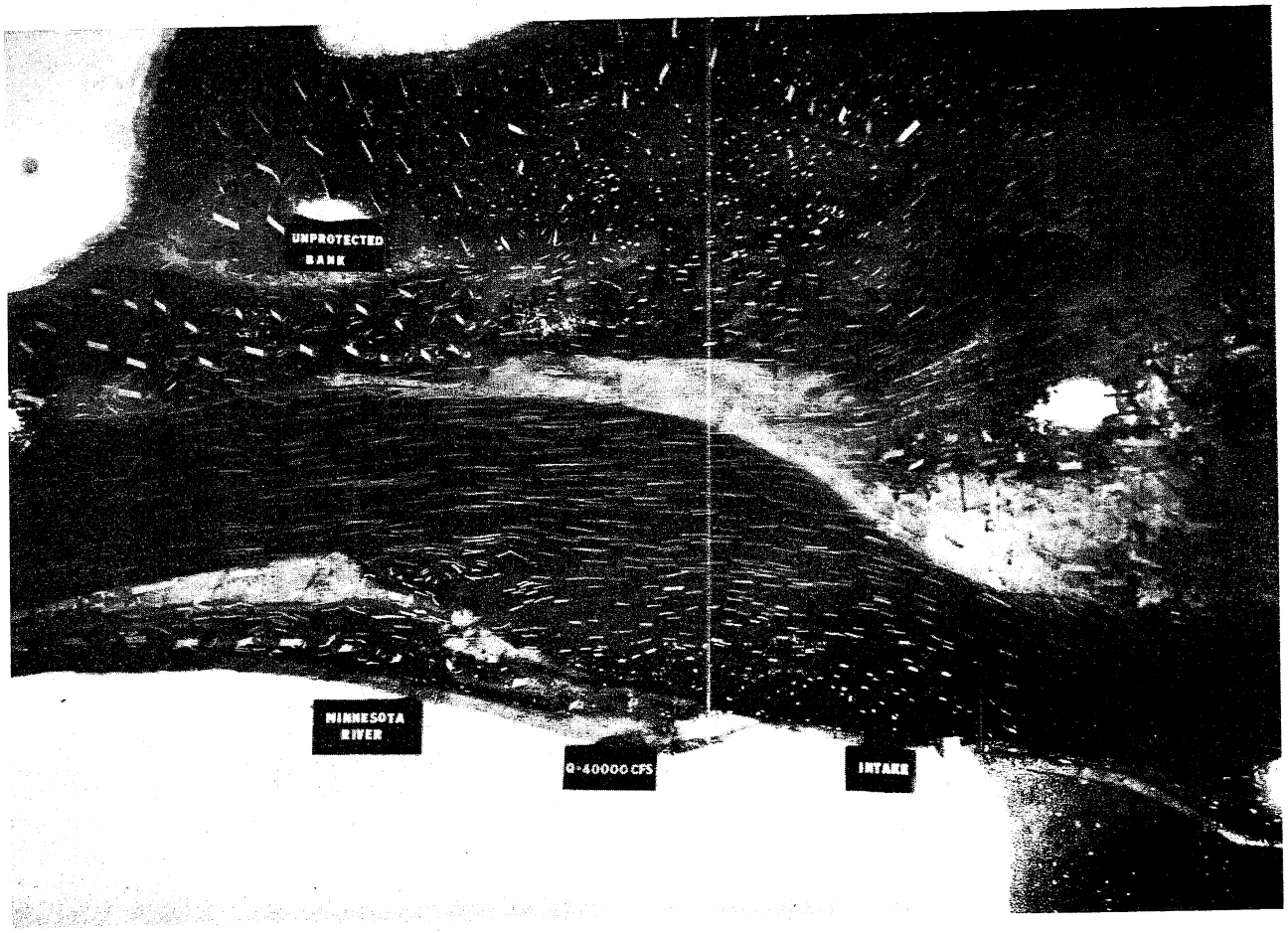

Fig. 20. Photograph illustrating the pattern of flow of water and sediment over the floodplain, for the case of Option 2 for the levee, at 40,000 cfs.

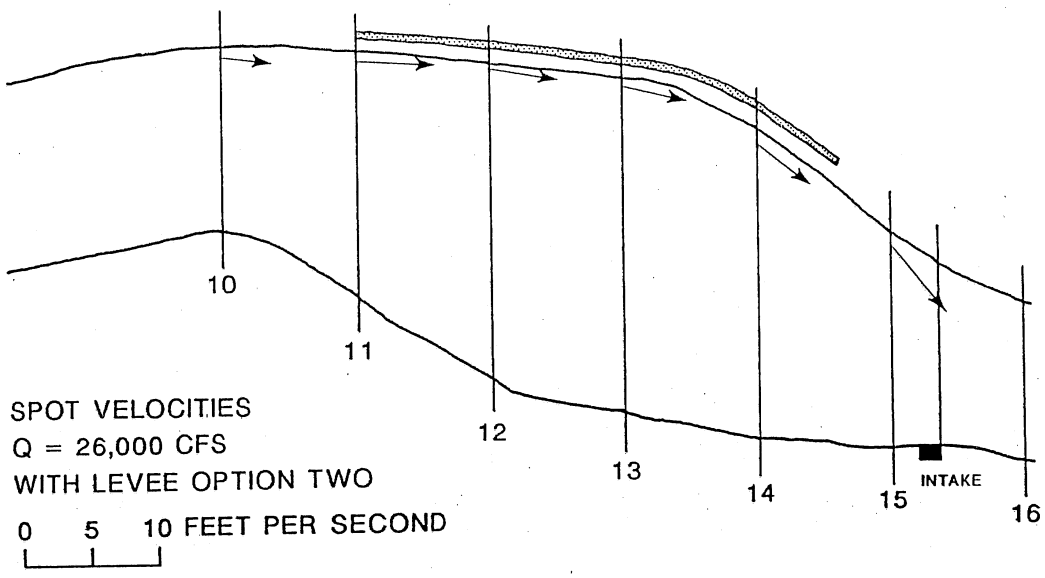

Fig. 21. Plot of near–bank water surface velocity vectors at incipient overtopping conditions for Option 2. The velocities were measured in the channel rather than tlie offset.

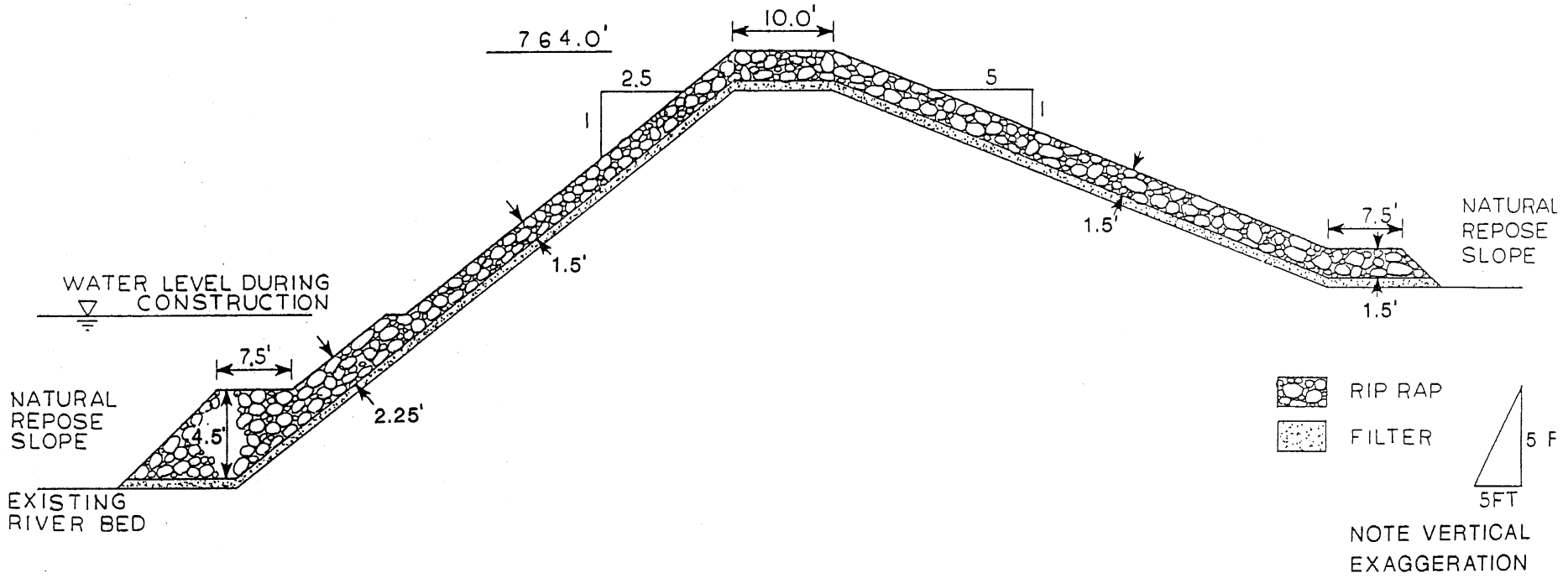

Fig. 22. Possible cross–section for the levee along the west bank, following Neill's recommendations.

Fig. 22. Possible cross–section for the levee along the west bank, following Nem's recommendations.

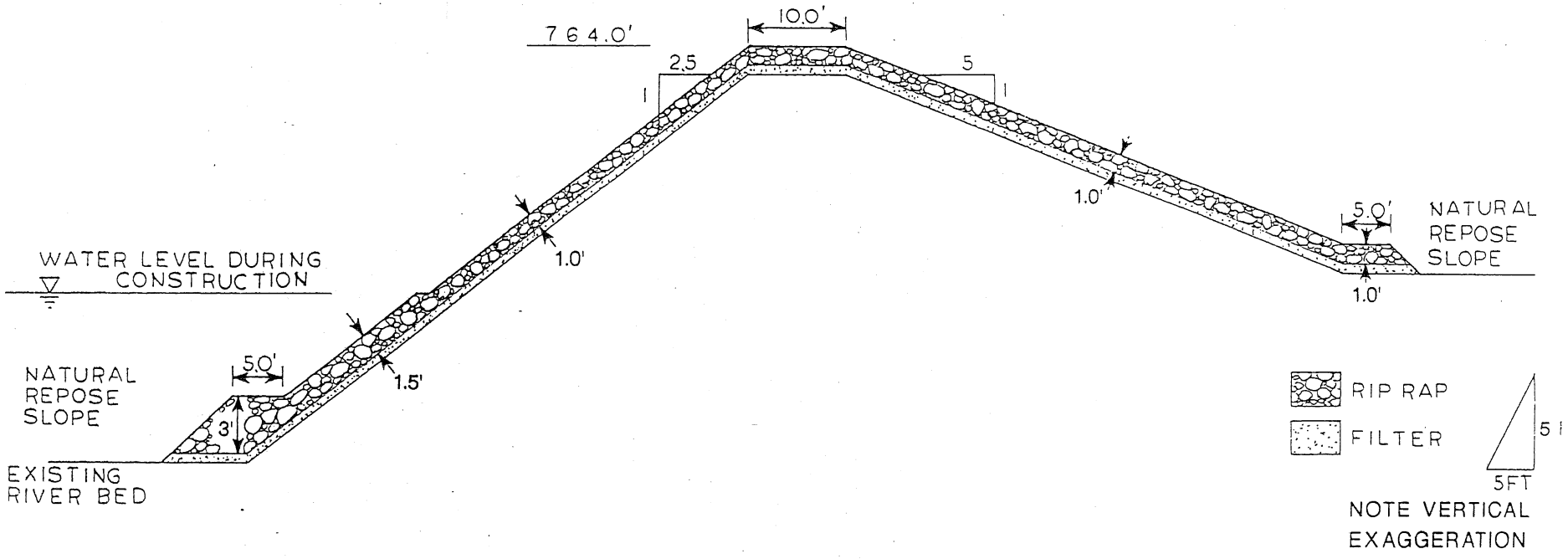

Fig. 23. Possible cross–section for the levee along the west bank, following the U.S. Army Corps of Engineers' procedure.

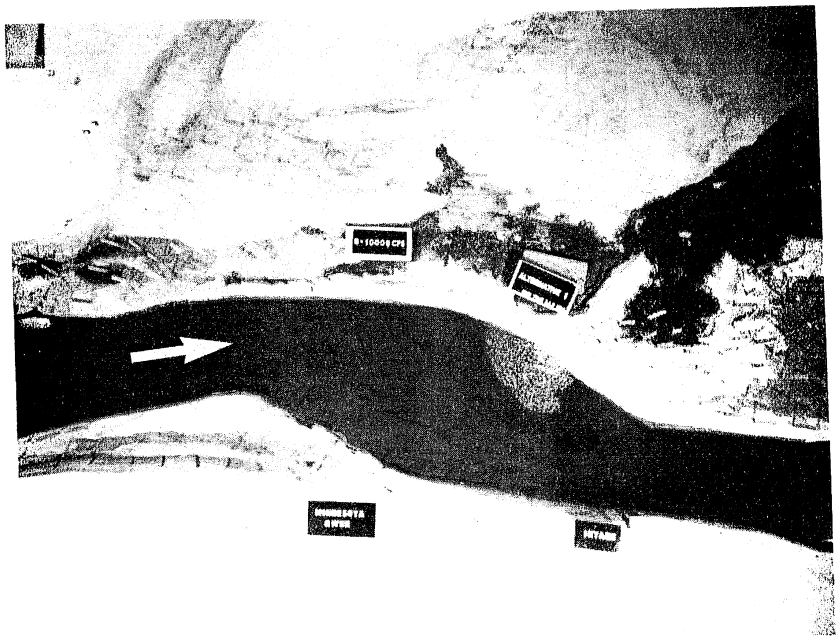

Fig. 24a. Bed configuration at Q = 10,000 cfs for Alternative 1.

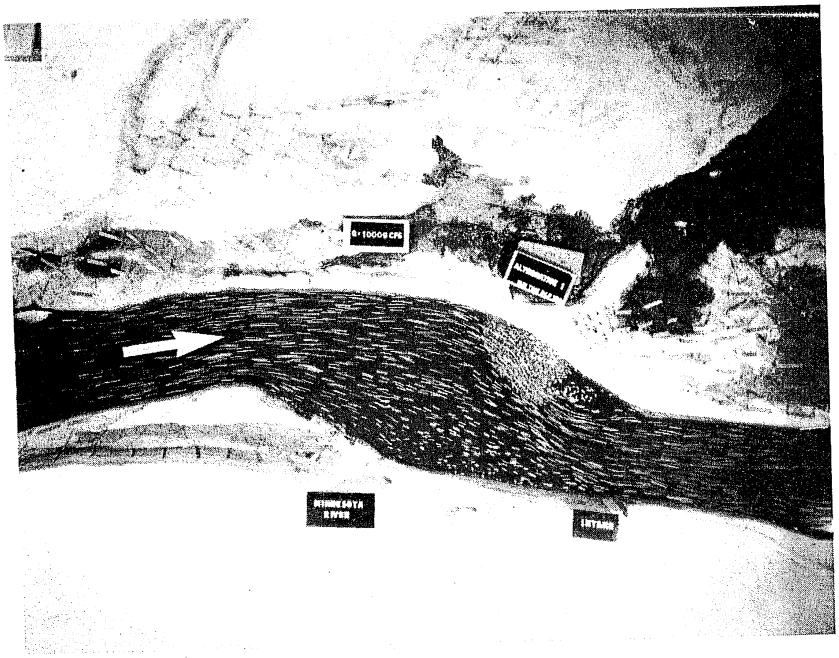

Fig. 24b. Streamline patterns at Q = 10,000 cfs for Alternative 1.

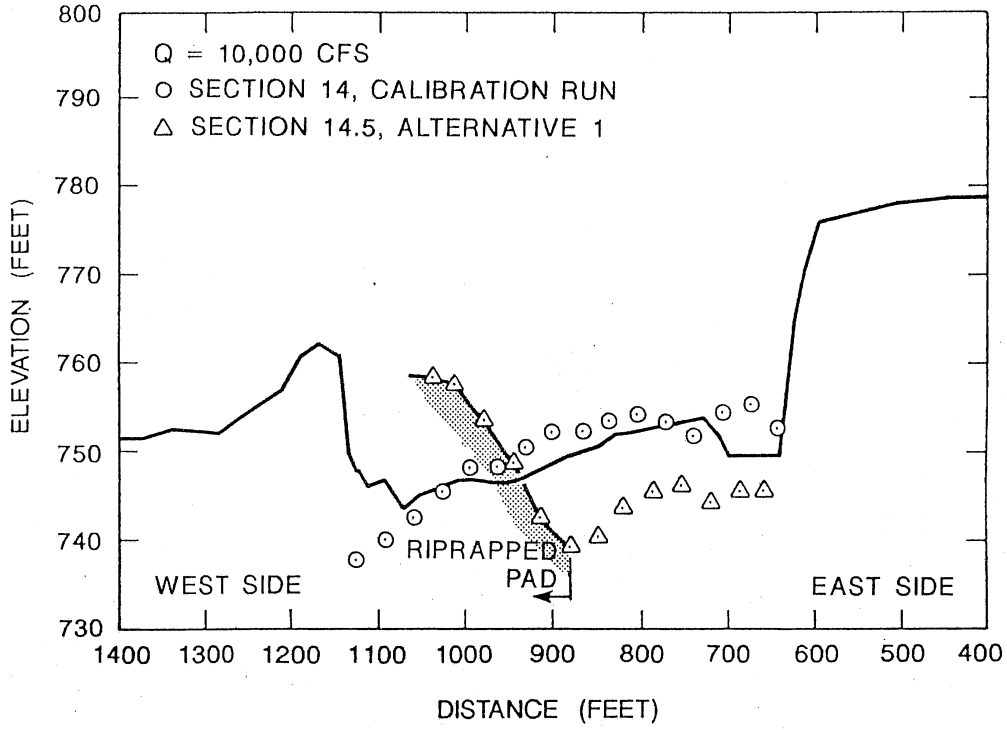

Fig. 25a. Comparison of Section 14 of the calibration run with that of Section 14.5 of Alternative 1; Q = 10,000 cfs.

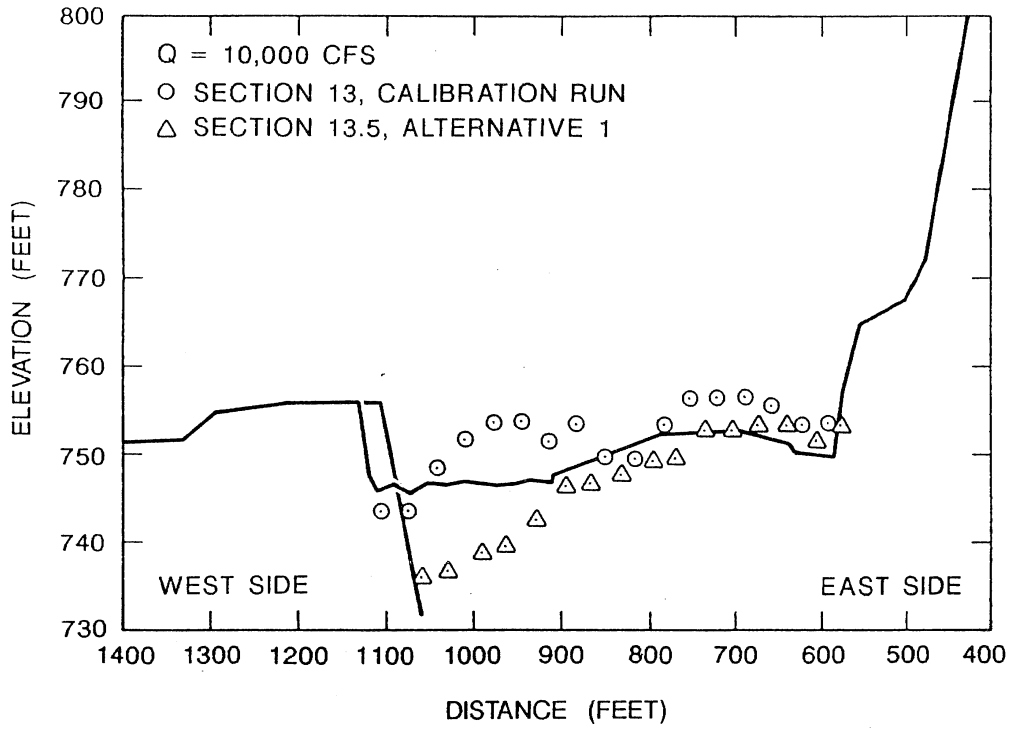

Fig. 25b. Comparison of the bed topography of Section 13 of the calibration run with that of Section 13.5 of Alternative 1; Q = 10,000 cfs.

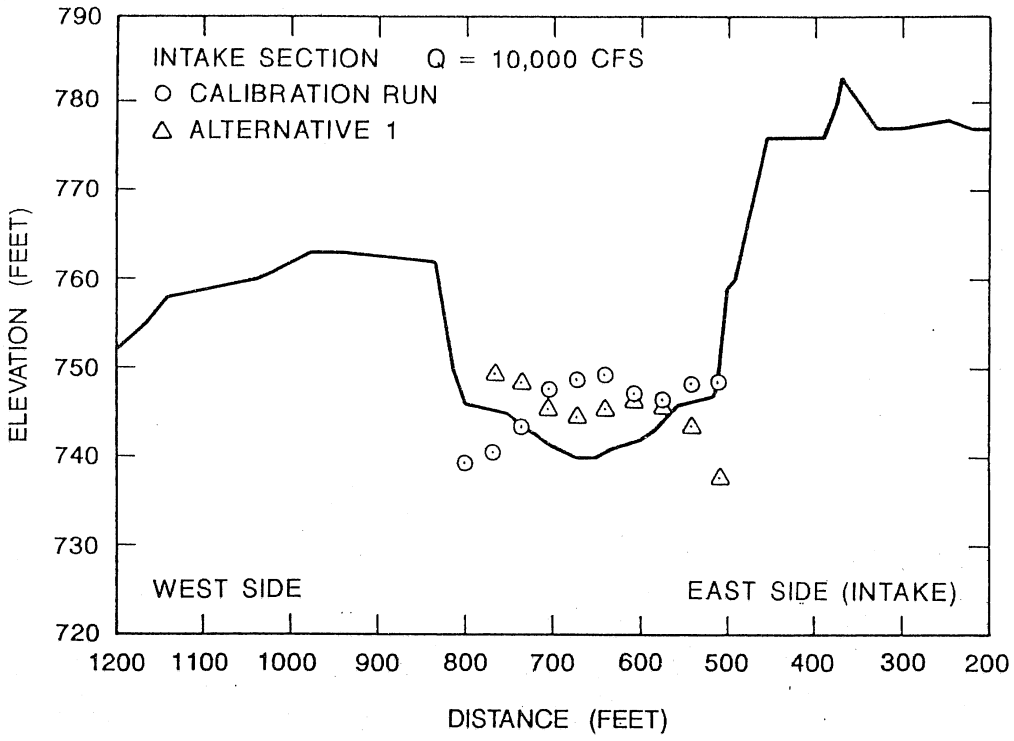

Fig. 25c. Comparison of the bed topography at the intake section of the calibration run with that in Alternative 1: Q = 10,000 cfs

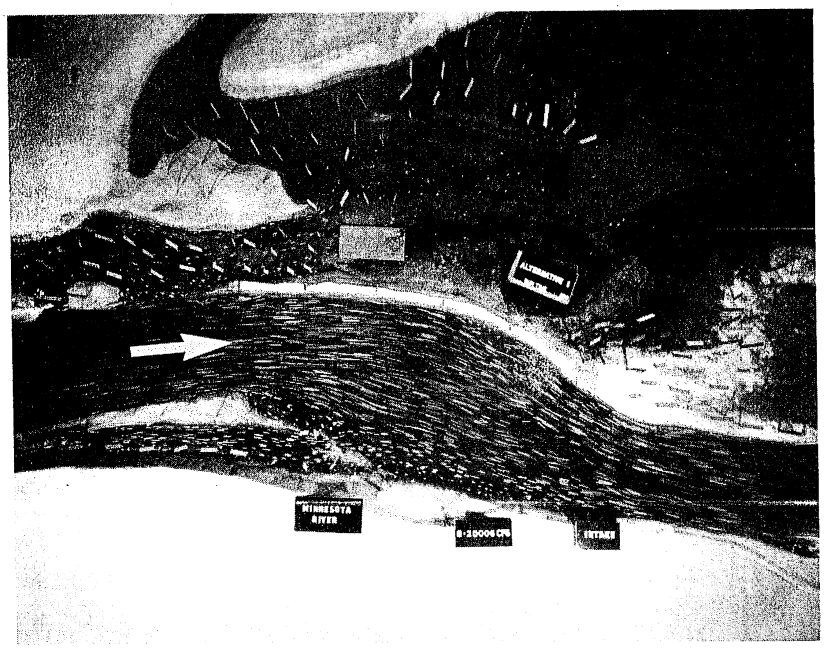

Fig. 26. Streamline patterns at Q = 20,000 cfs for Alternative 1.

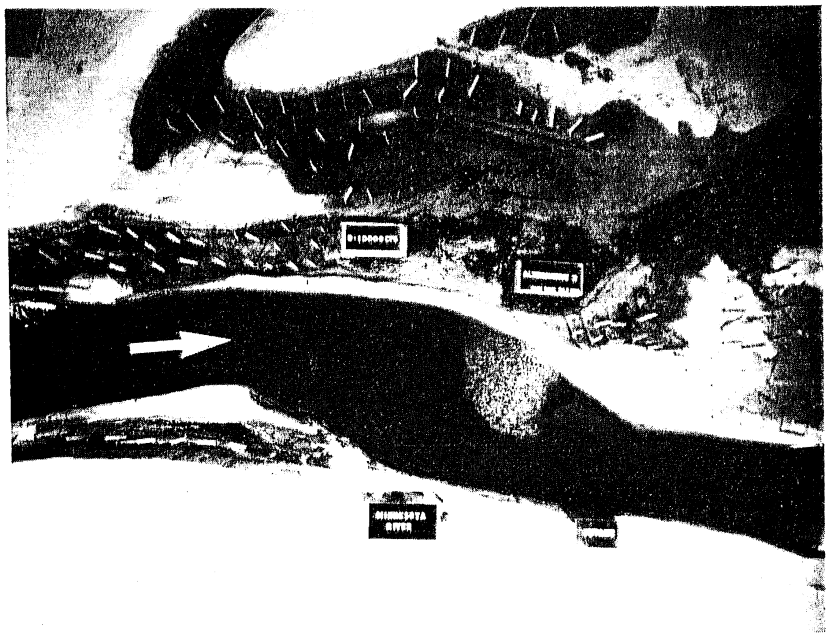

Fig. 27a. Bed configuration at Q = 10,000 cfs for Alternative 2.

Fig. 27b. Streamline patterns at Q = 10,000 cfs for Alternative 2.

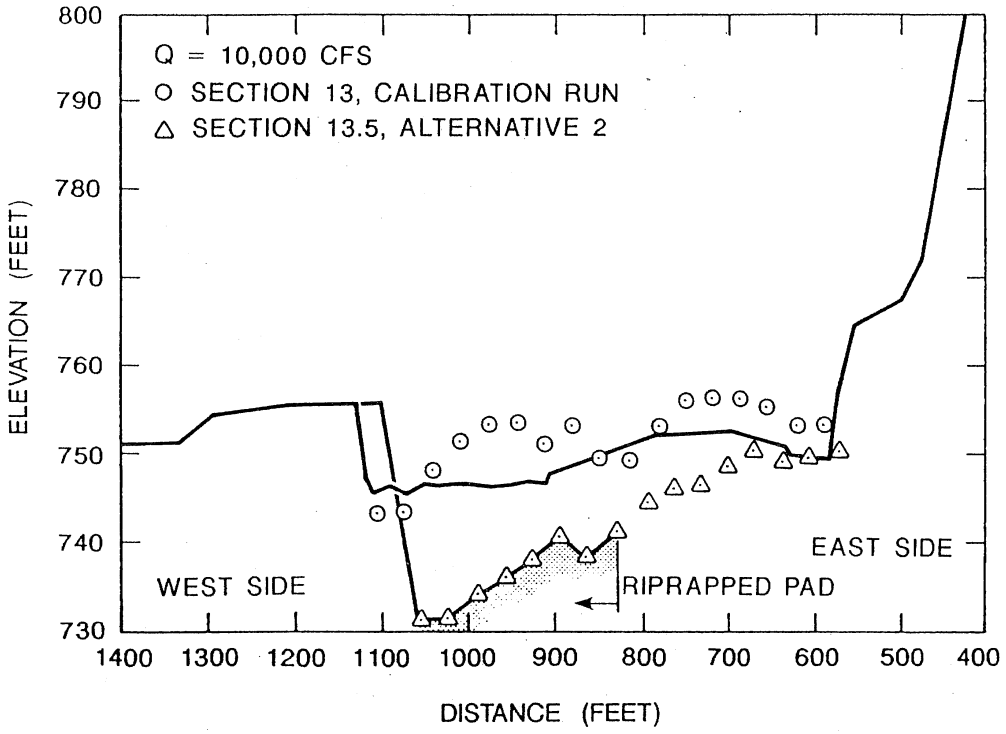

Fig. 28a. Comparison of the bed topography of Section 13 of the calibration run with that of Section 13.5 of Alternative 2; Q = 10,000 cfs.

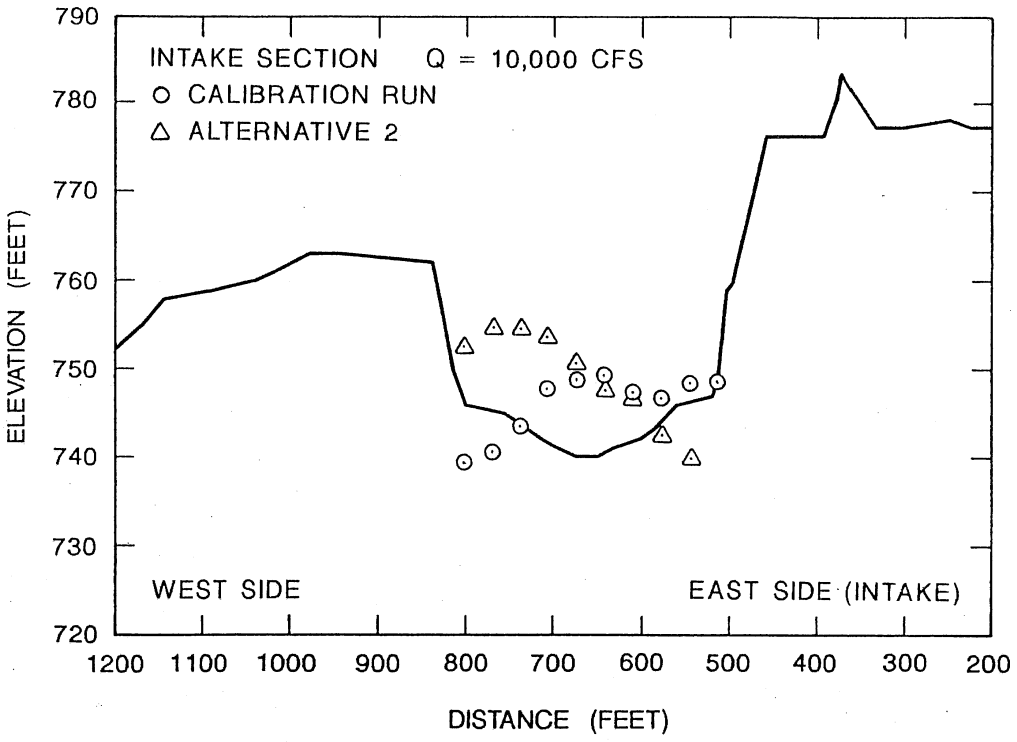

Fig. 28b. Comparison of the bed topography of the intake section in the calibration run with that of Alternative 2; Q = 10,000 cfs.

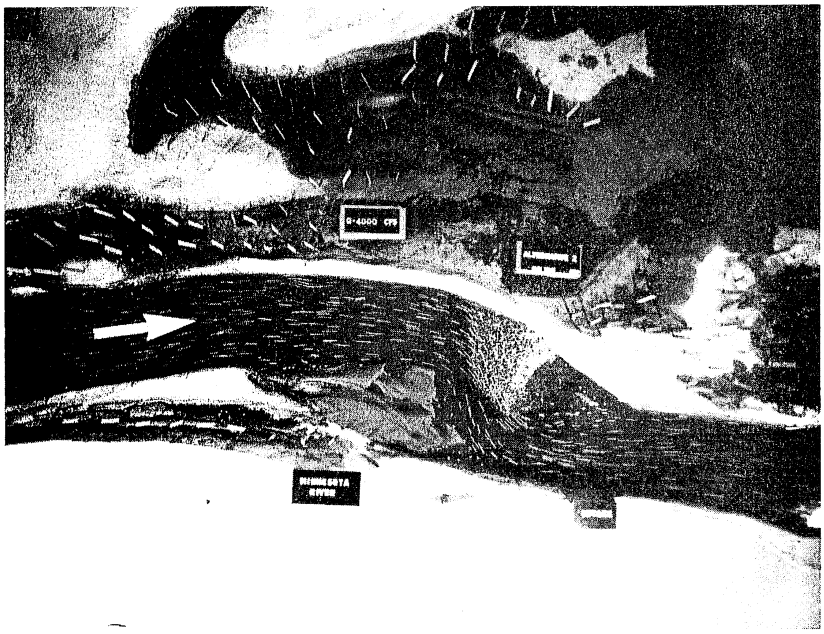

Fig. 29. Streamline patterns at Q = 4,000 cfs for Alternative 2.

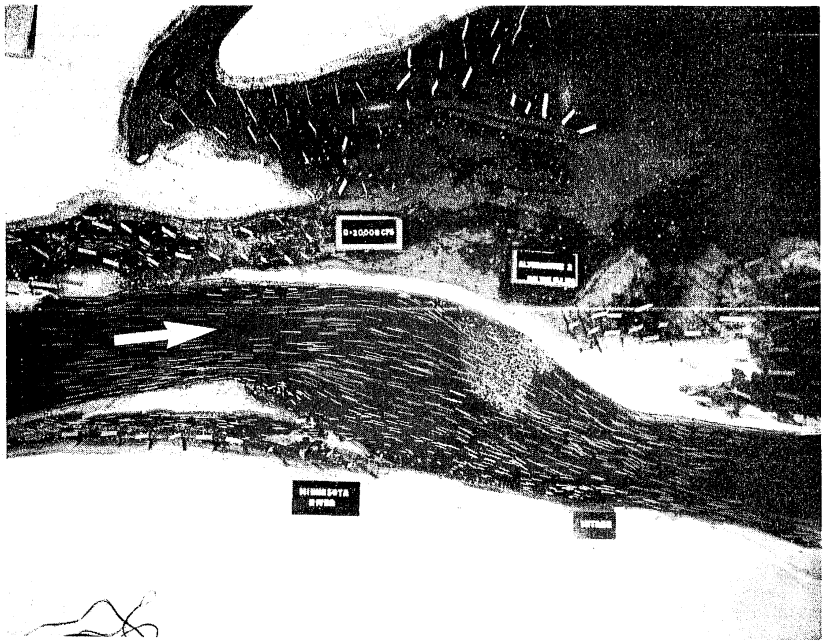

Fig. 30. Streamline patterns at Q = 20,000 cfs for Alternative 2.

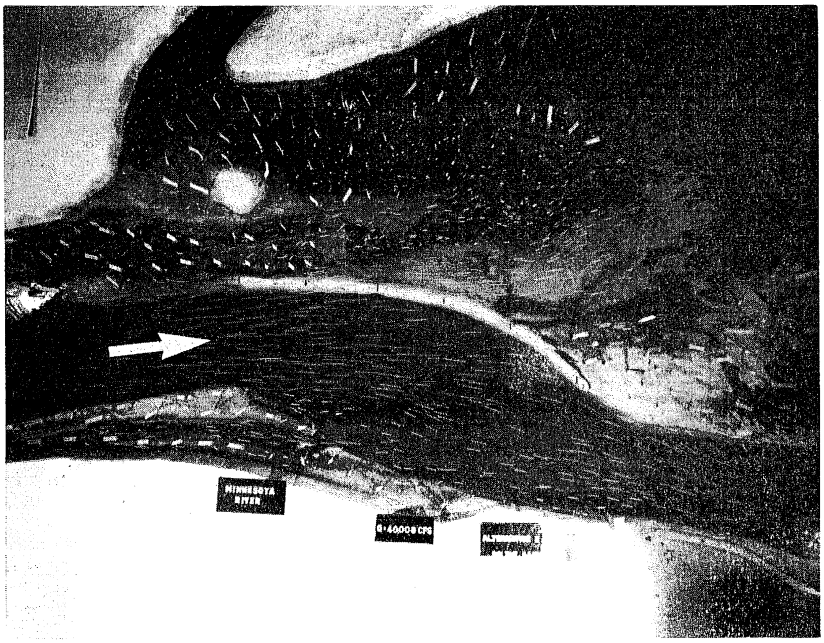

Fig. 31. Streamline patterns at Q = 40,000 cfs for Alternative 2.

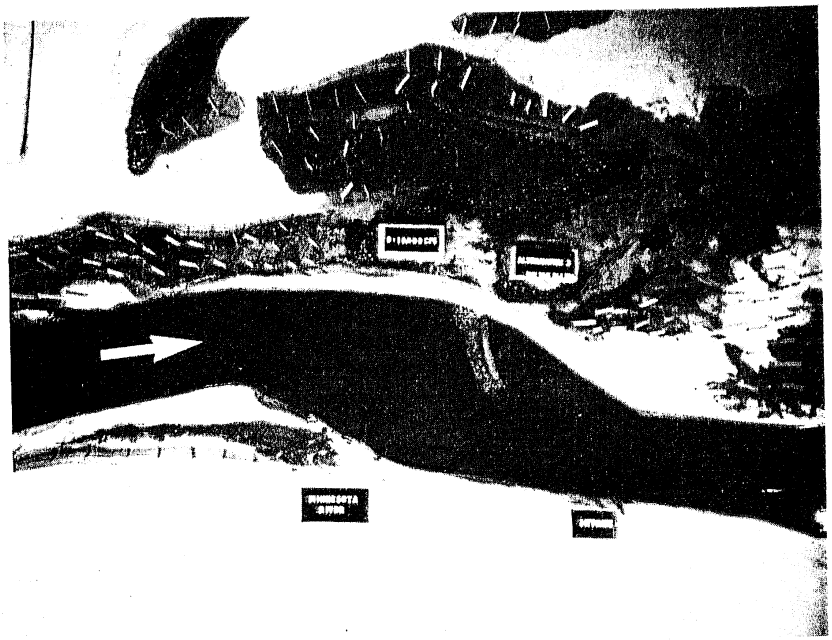

Fig. 32a. Bed configuration at Q = 10,000 cfs for Alternative 3.

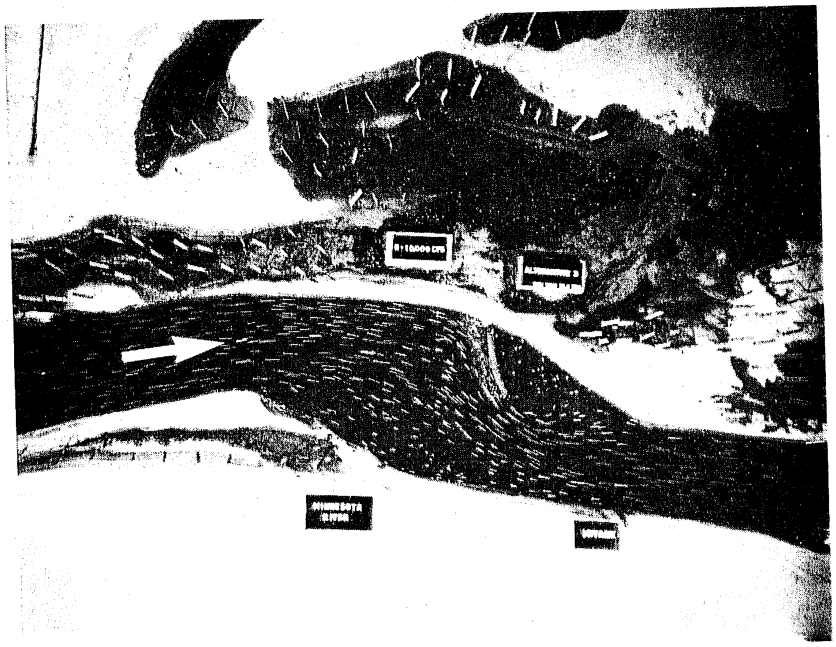

Fig. 32b. Streamline patterns at Q = 10,000 cfs for Alternative 3.

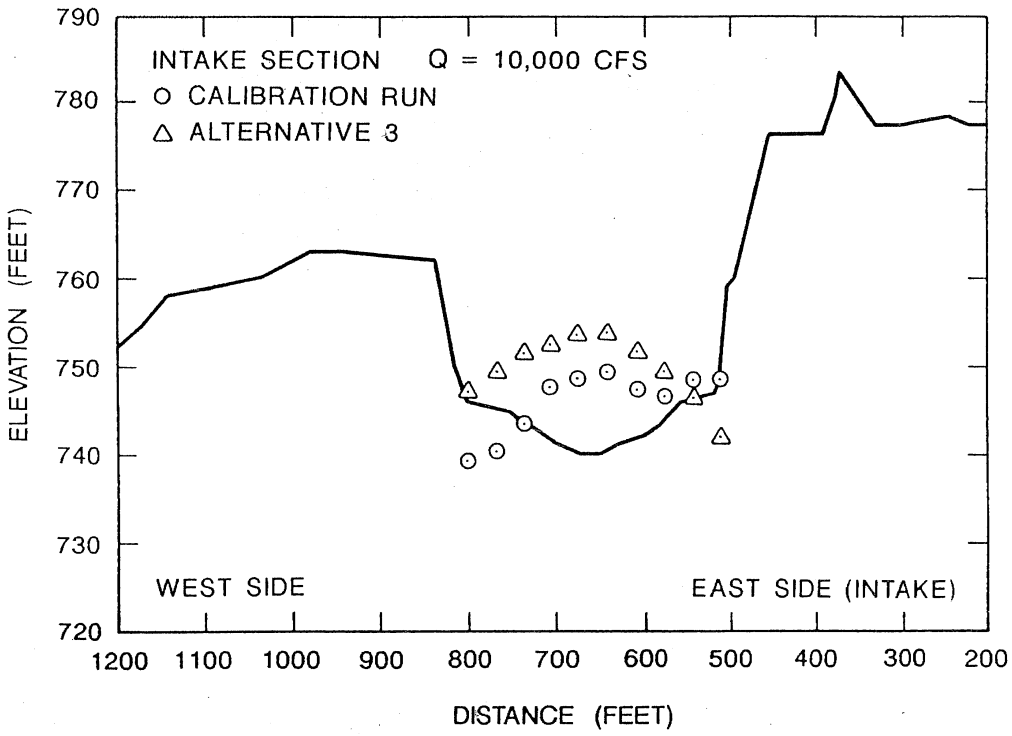

Fig. 33. Comparison of the bed topography at the intake section in the calibration run with that in Alternative 3; Q = 10,000 cfs.

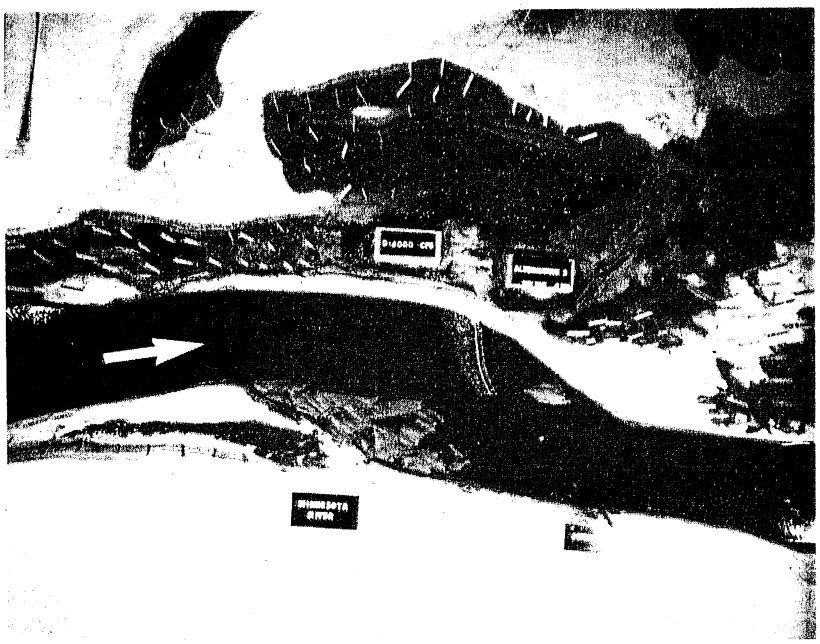

Fig. 34a. Bed configuration at Q = 4,000 cfs for Alternative 3.

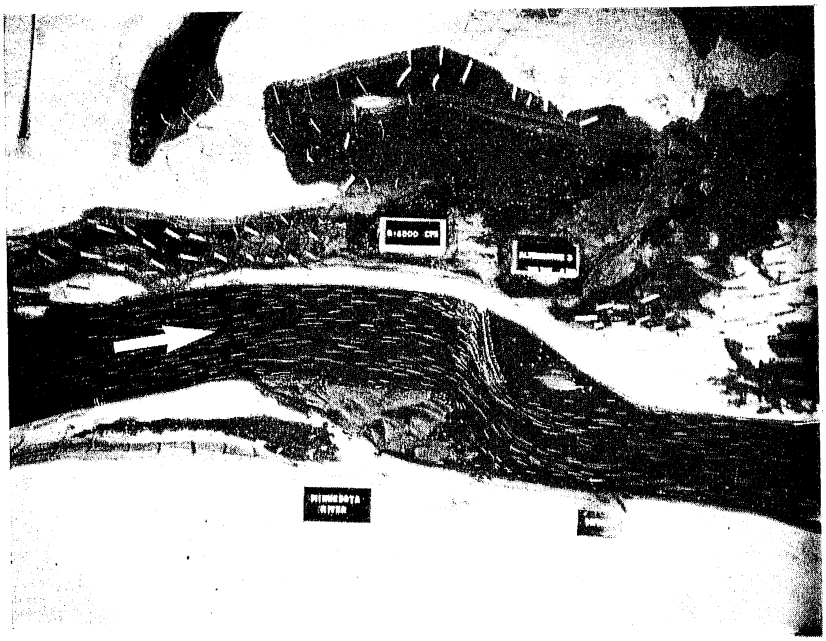

Fig. 34b. Streamline patterns at Q = 4,000 cfs for Alternative 3.

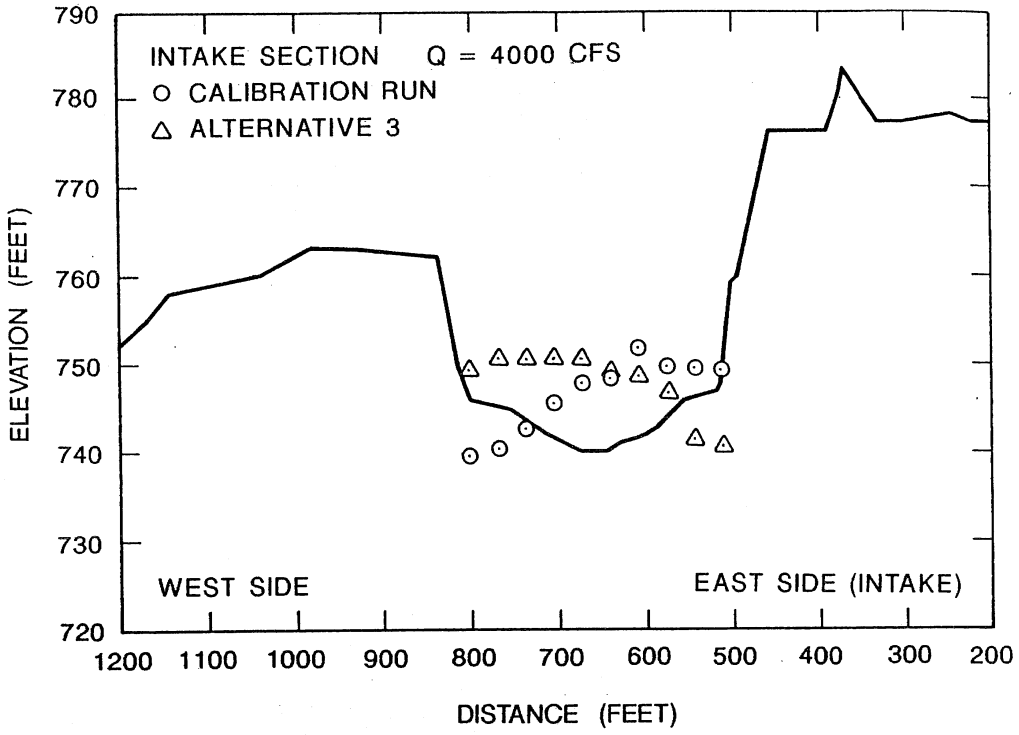

Fig. 35. Comparison of the bed topography at the intake section in the calibration run with that of Alternative 3; Q = 4,000 cfs.

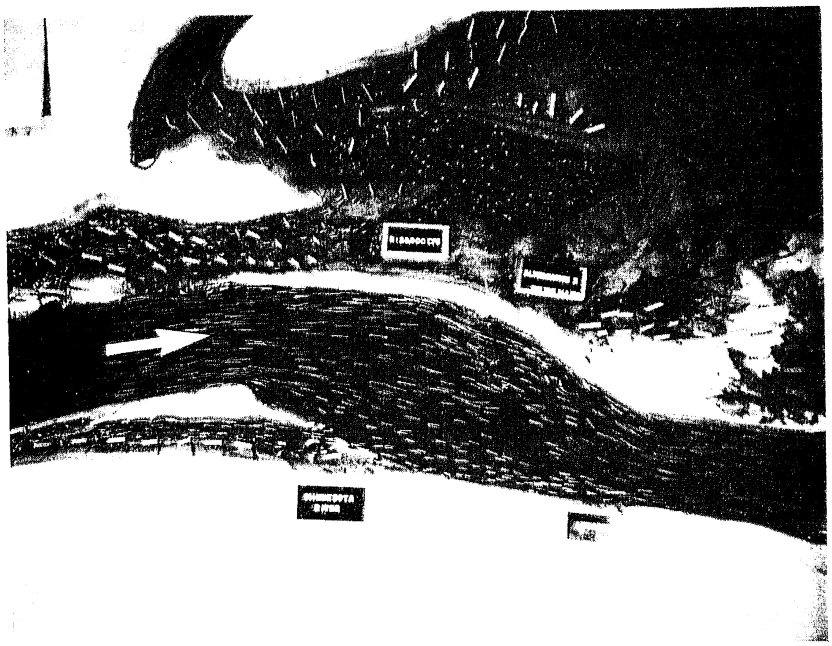

Fig. 36. Streamline patterns for Q = 20,000 cfs for Alternative 3.

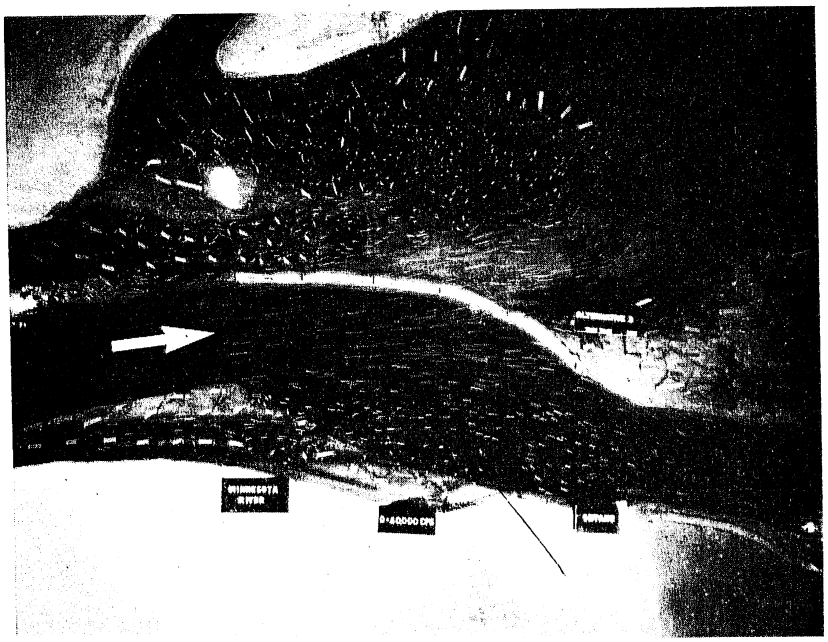

Fig. 37. Streamline patterns at Q = 40,000 cfs for Alternative 3.

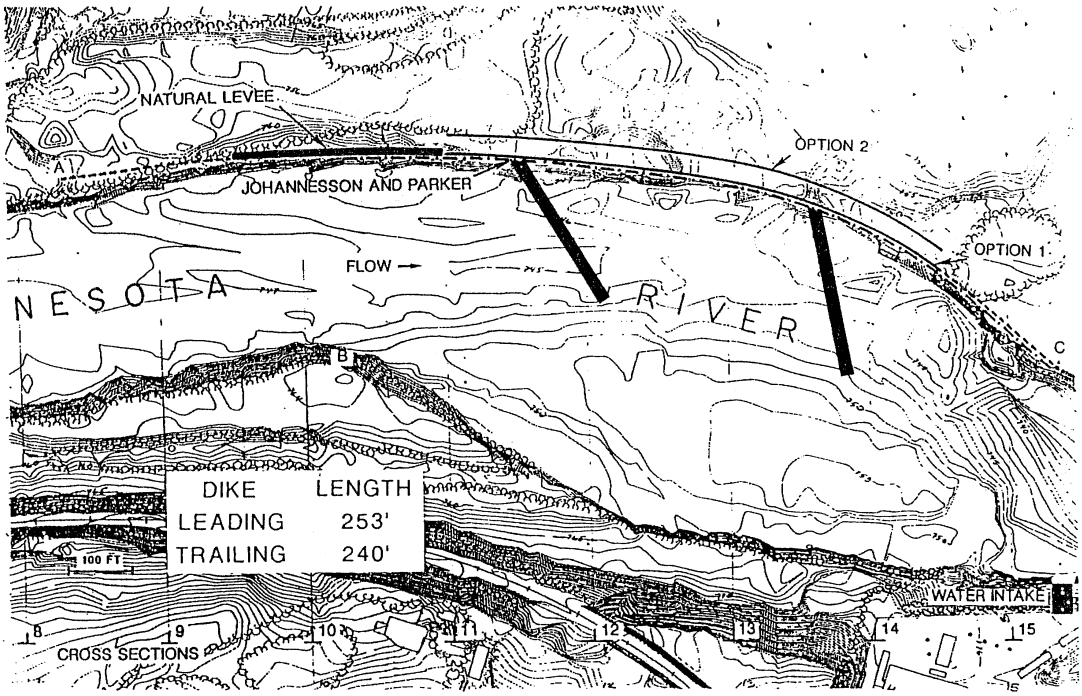

Fig. 38. Schematic diagram illustrating placement of spur dikes for Alternative 4. Bed topography is that of Figure 18.

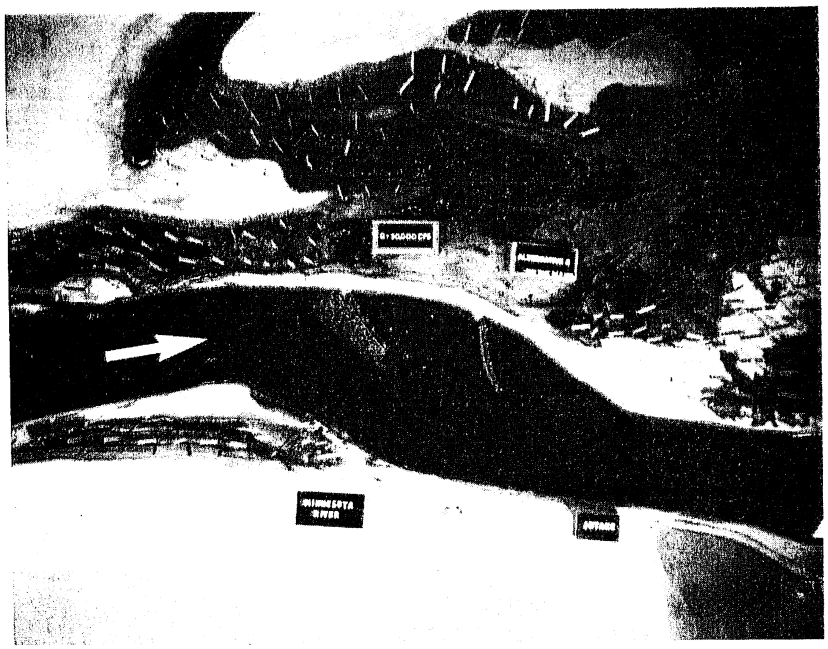

Fig. 39a. Bed configuration at Q = 10,000 cfs for Alternative 4.

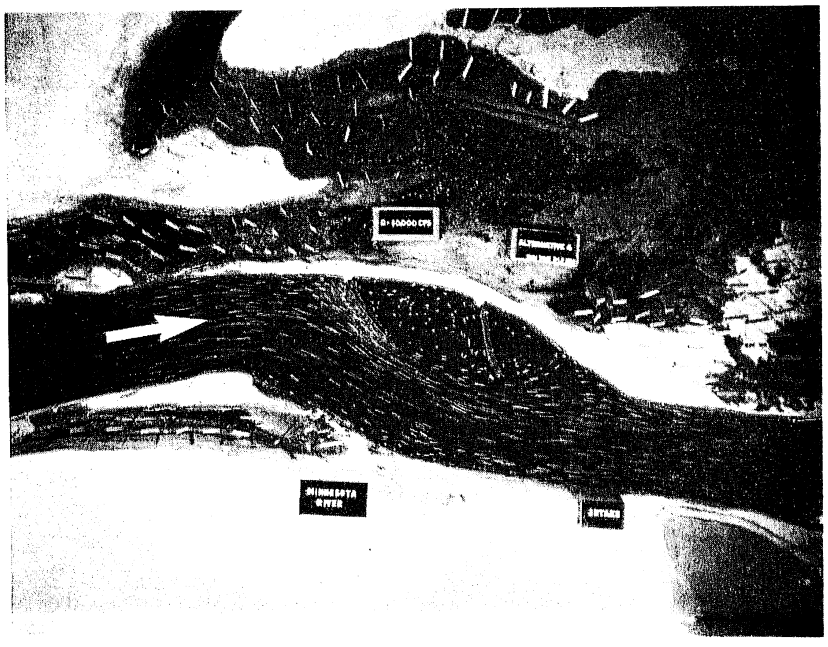

Fig. 39b. Streamline patterns at Q = 10,000 cfs for Alternative 4.

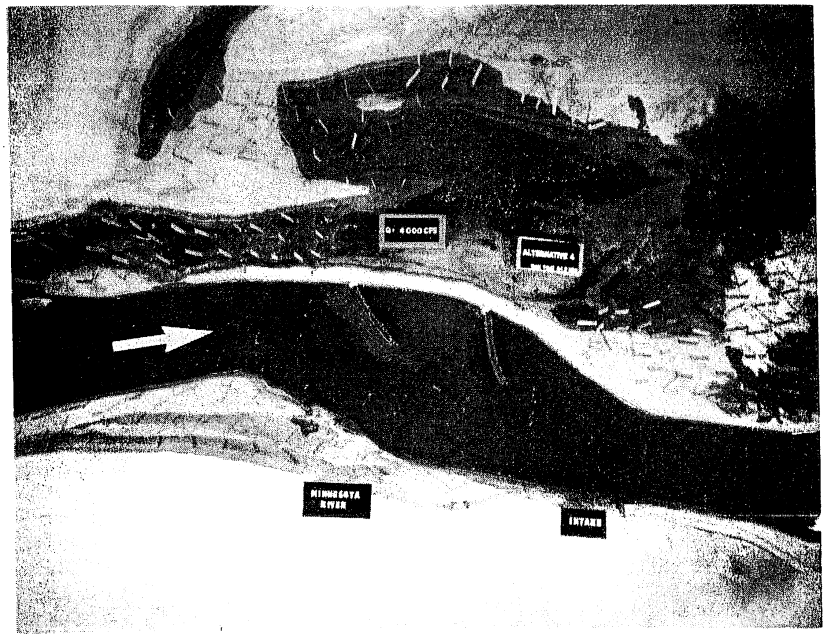

Fig. 40a. Bed configuration at Q = 4,000 cfs at Alternative 4.

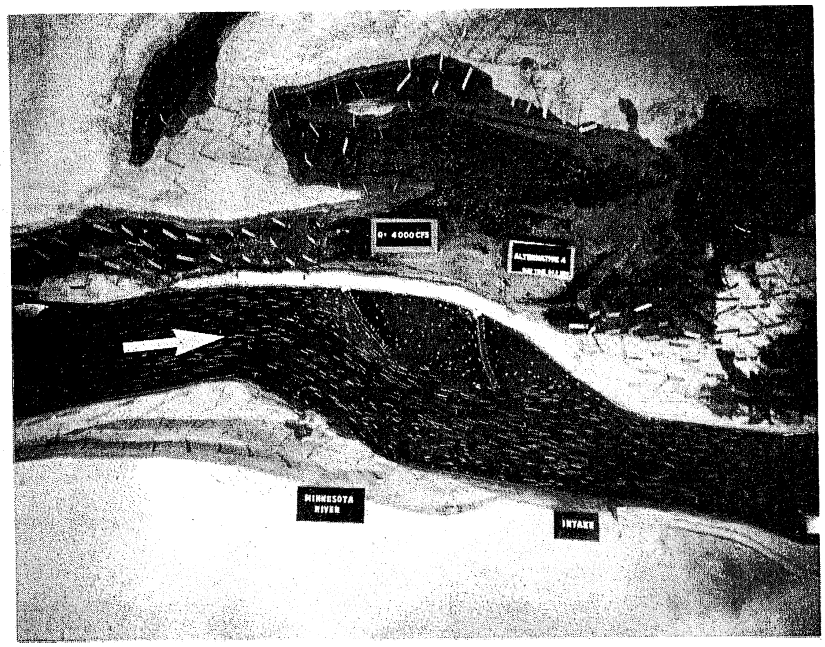

Fig. 40b. Streamline patterns at Q = 4,000 cfs for Alternative 4.

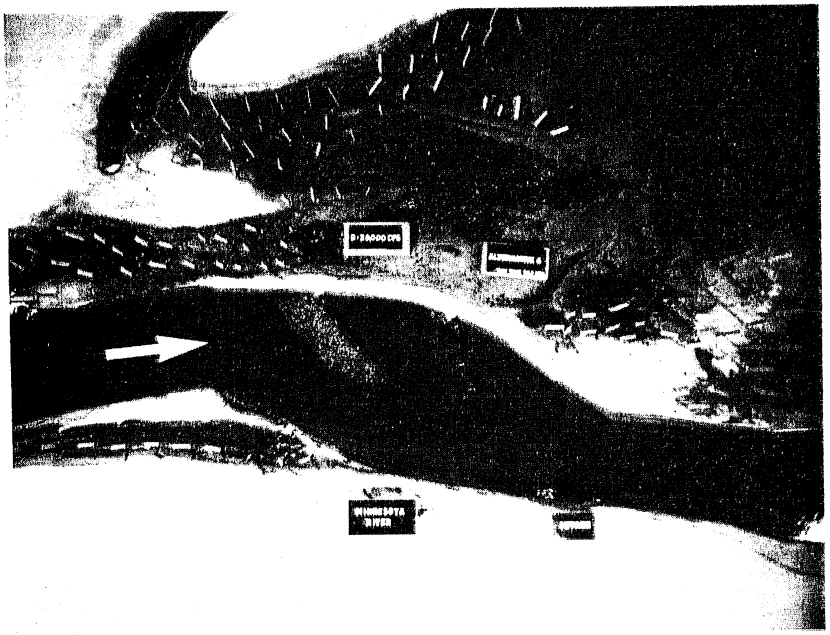

Fig. 41a. Bed configuration at Q = 20,000 cfs for Alternative 4.

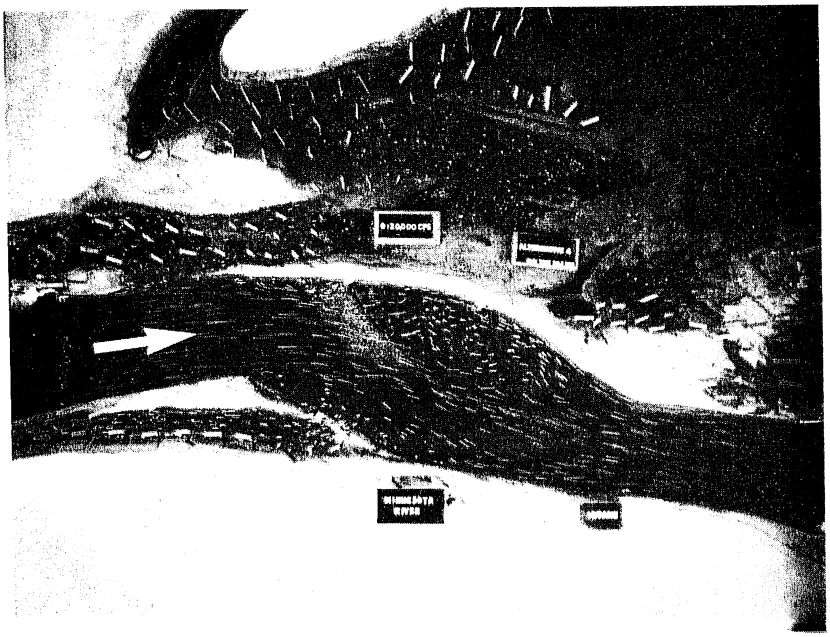

Fig. 41b. Streamline patterns at Q = 20,000 cfs for Alternative 4.

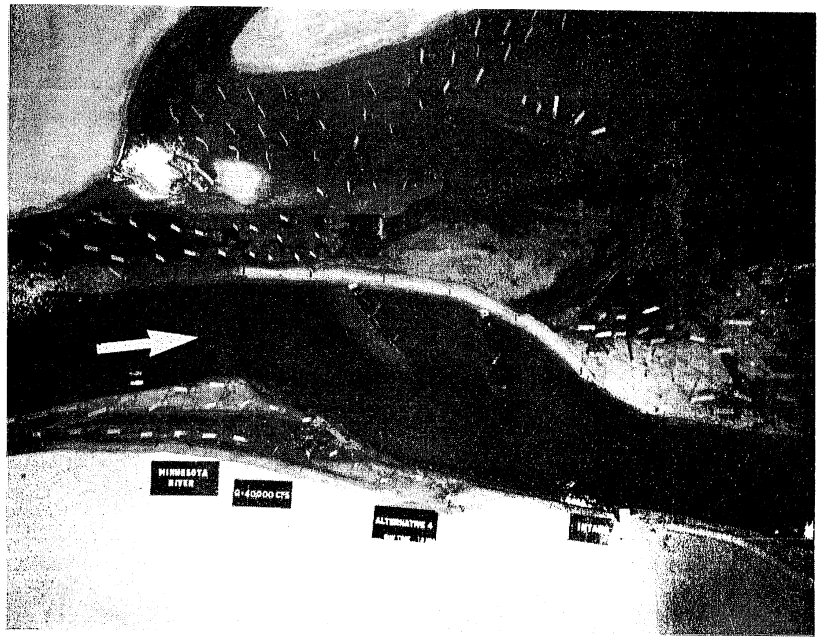

Fig. 42a. Bed configuration at Q = 40,000 cfs for Alternative 4.

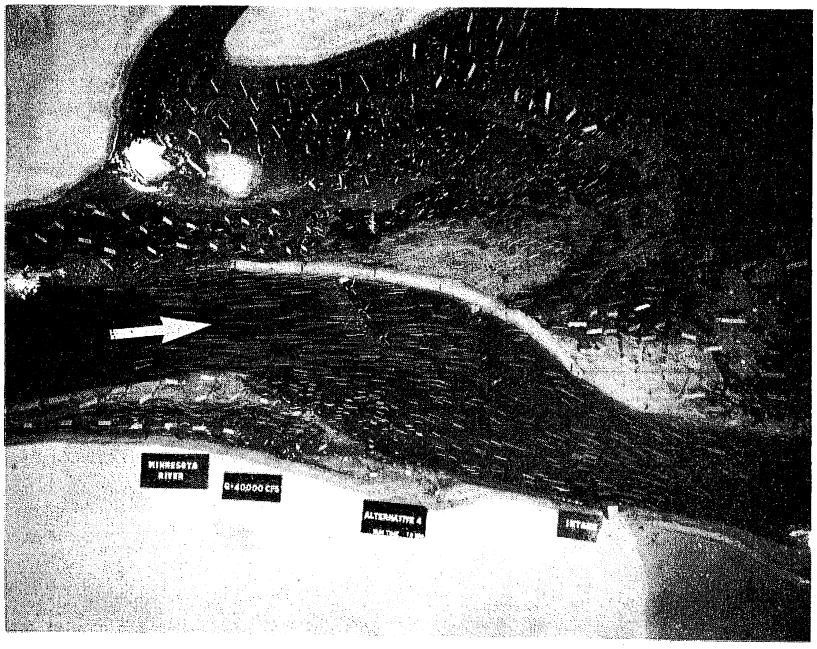

Fig. 42b. Streamline patterns at Q = 40,000 for Alternative 4.

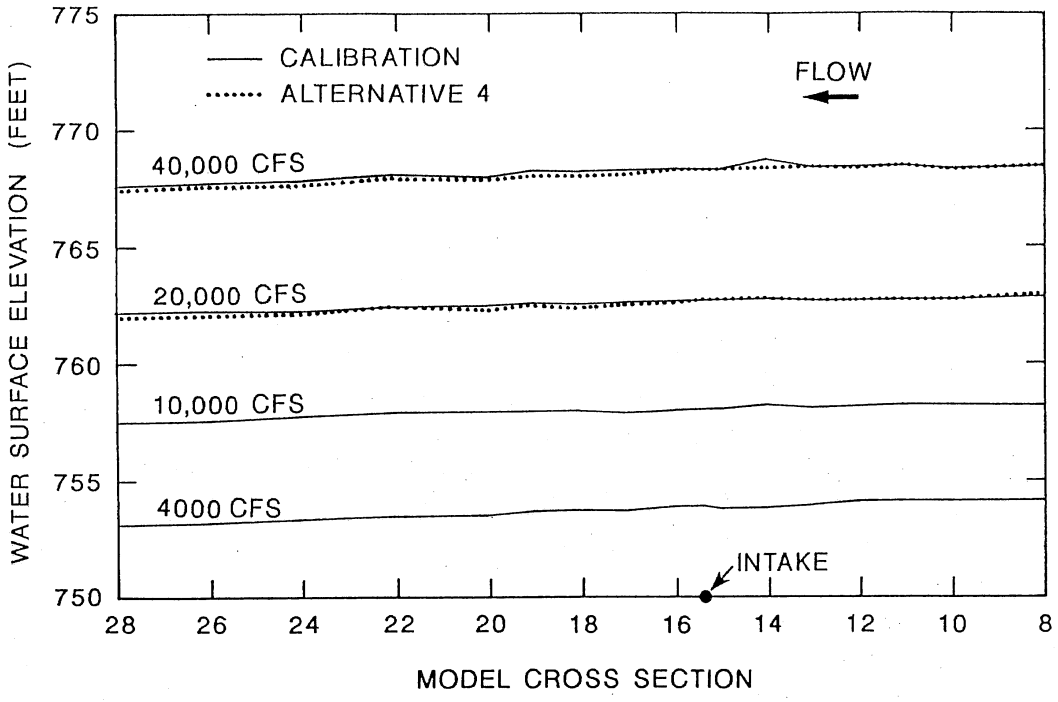

Fig. 43. Water surface profiles in the calibration runs and for Alternative 4.

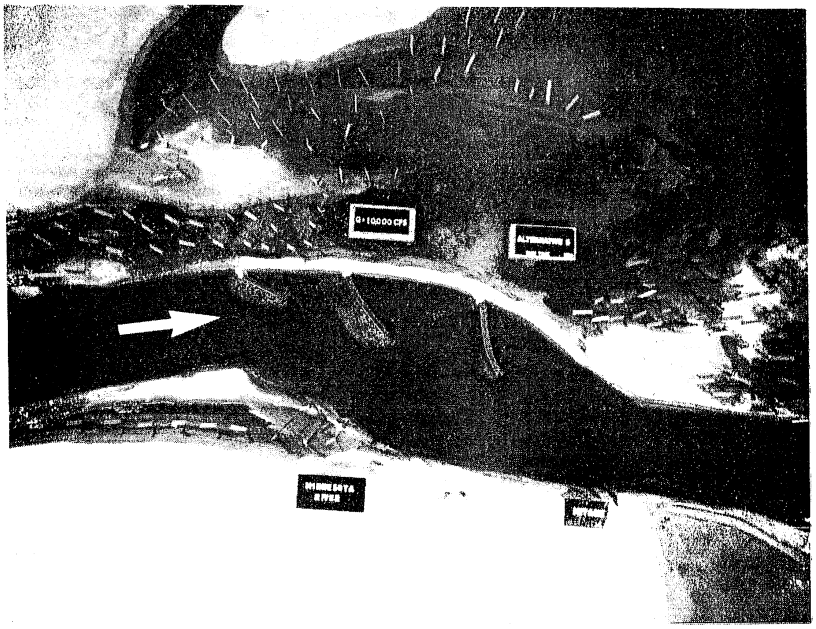

Fig. 44a. Bed configuration at Q = 10,000 for Alternative 5.

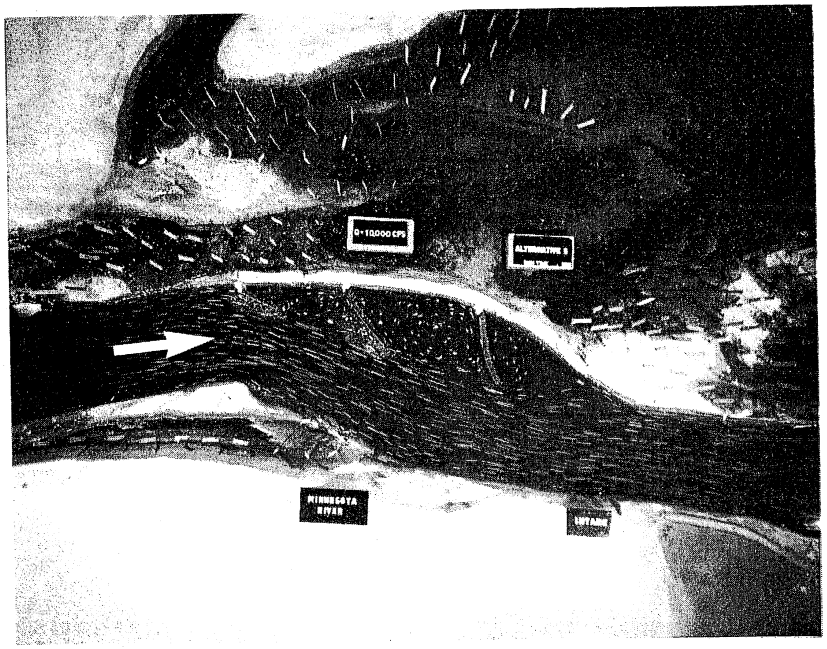

Fig. 44b. Streamline patterns at Q = 10,000 cfs for Alternative 5.

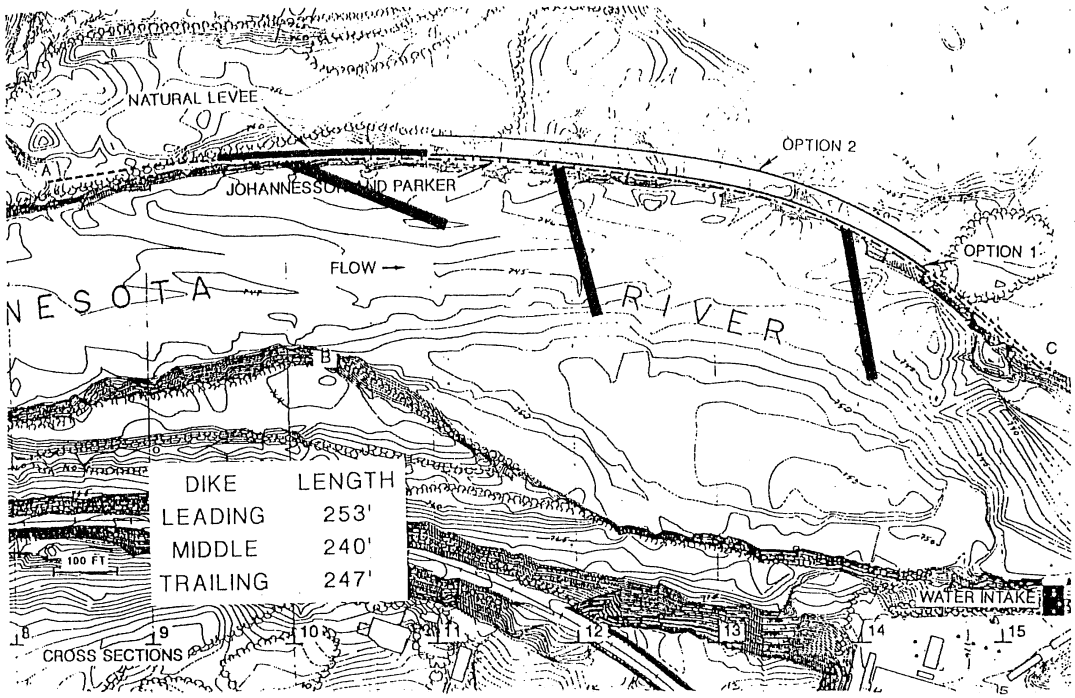

Fig. 45. Schematic diagram illustrating placement of dikes for Alternative 6. Bed topography is that of Figure 18.

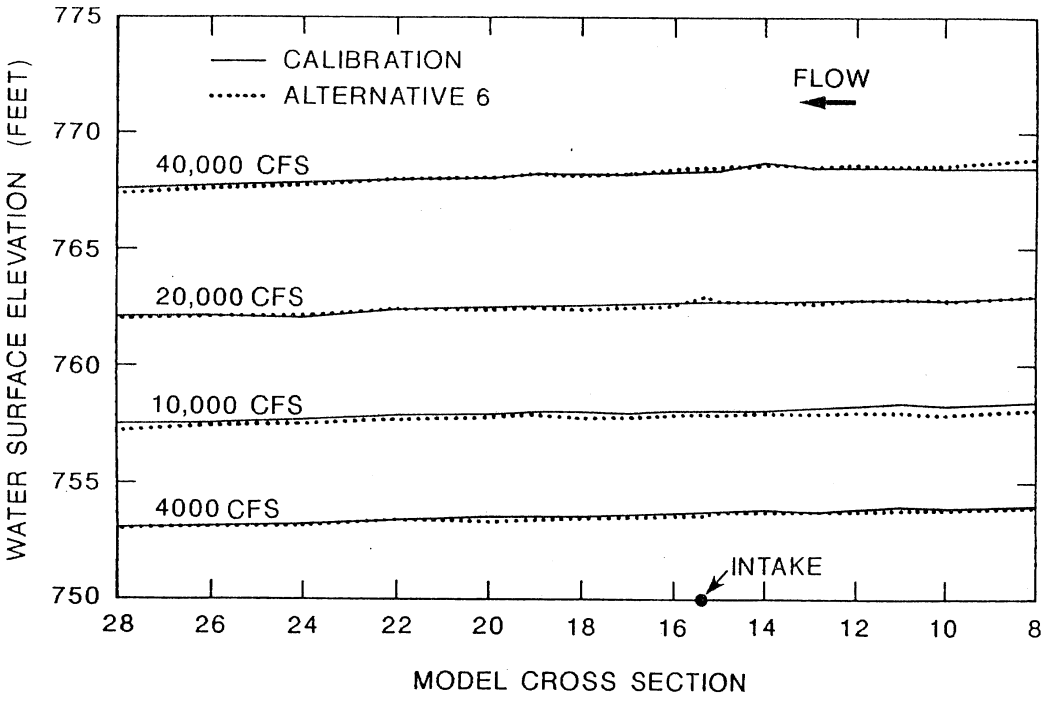

Fig. 46. Water surface profiles in the calibration runs and for Alternative 6.

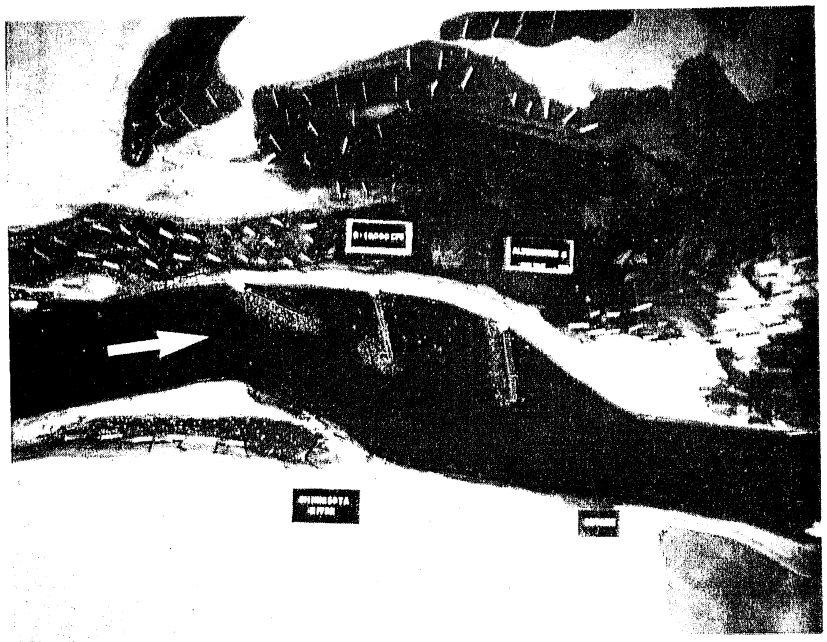

Fig. 47a. Bed configuration at Q = 10,000 cfs for Alternative 6.

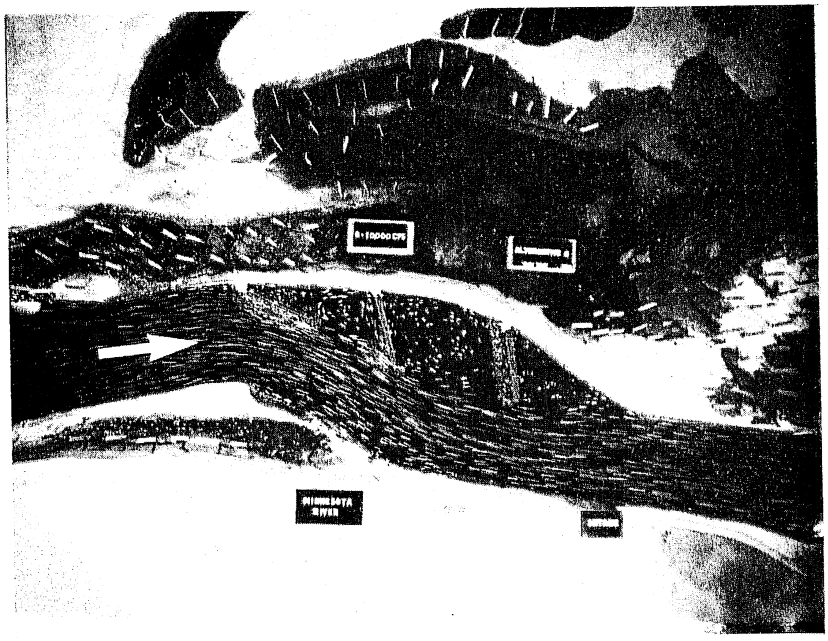

Fig. 47b. Streamline patterns at Q = 10,000 cfs for Alternative 6.

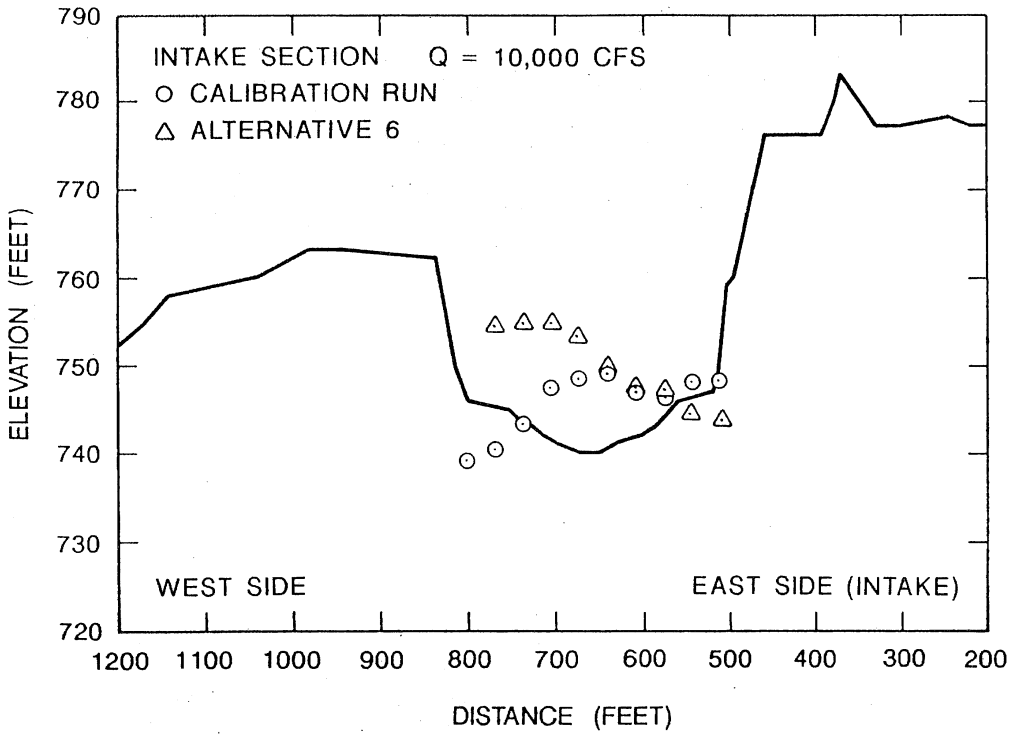

Fig. 48. Bed topography at the intake for Alternative 6; Q = 10,000 cfs.

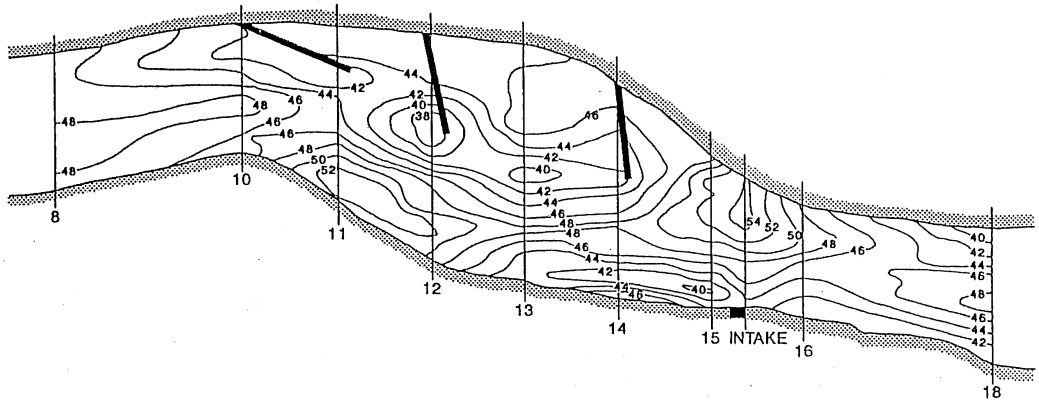

Fig. 49. Bed contours for Alternative 6; Q = 10,000 cfs.

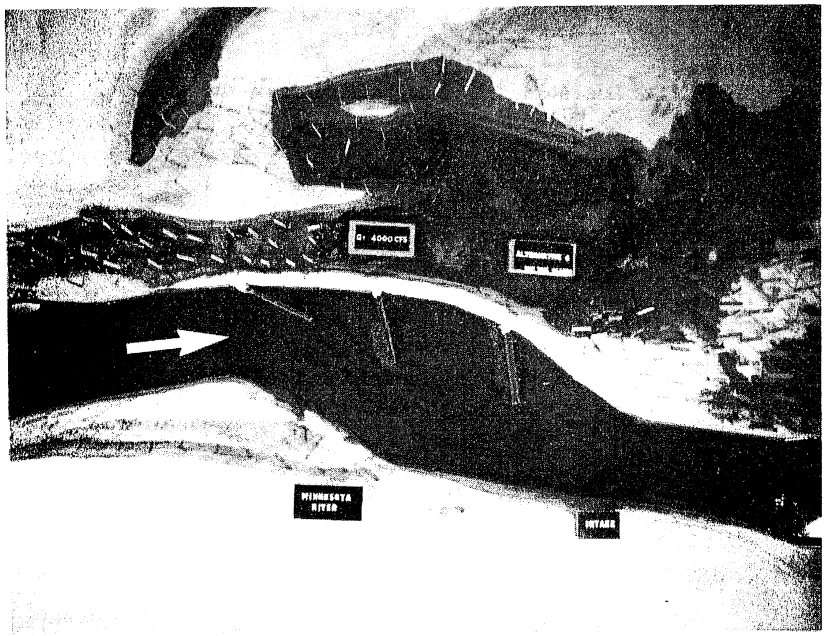

Fig. 50a. Bed configuration at Q = 4,000 cfs for Alternative 6.

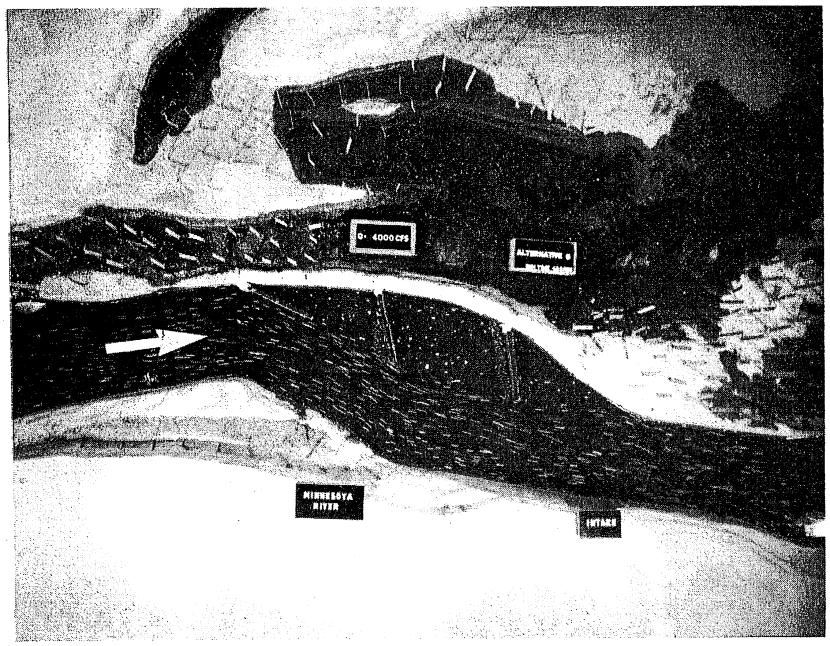

Fig. 50b. Streamline patterns at Q = 4,000 cfs for Alternative 6.

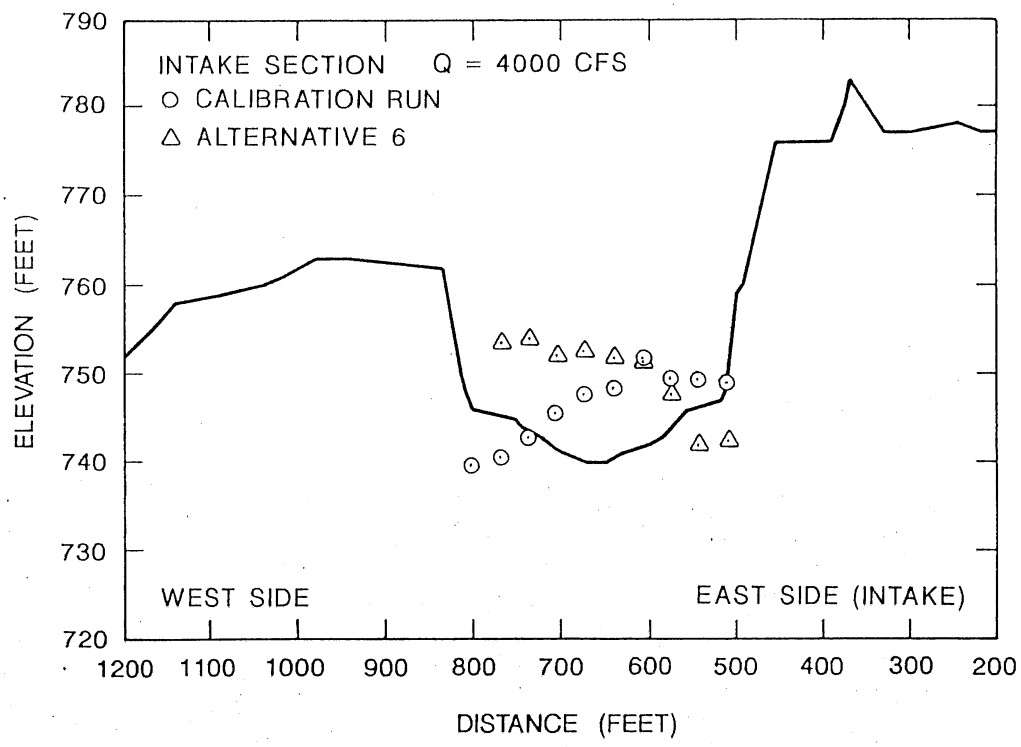

Fig. 51. Bed topography at the intake for Alternative 6; Q = 4,000 cfs.

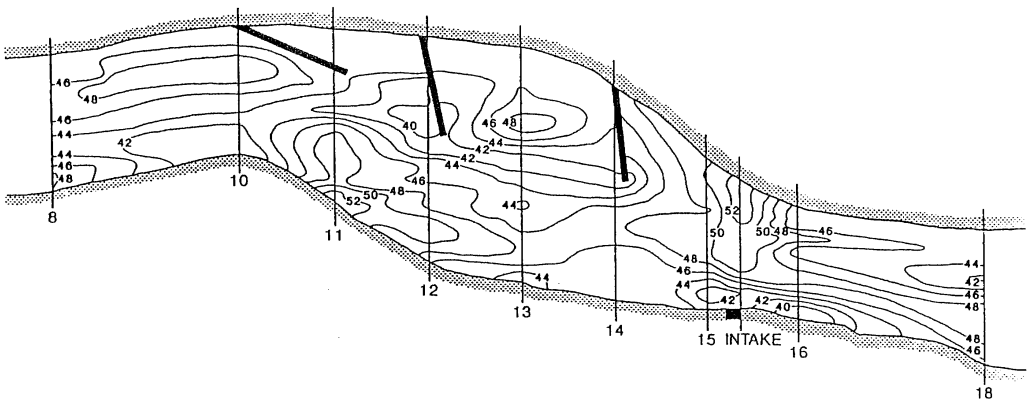

Fig. 52. Bed contours for Alternative 6; Q = 4,000 cfs.

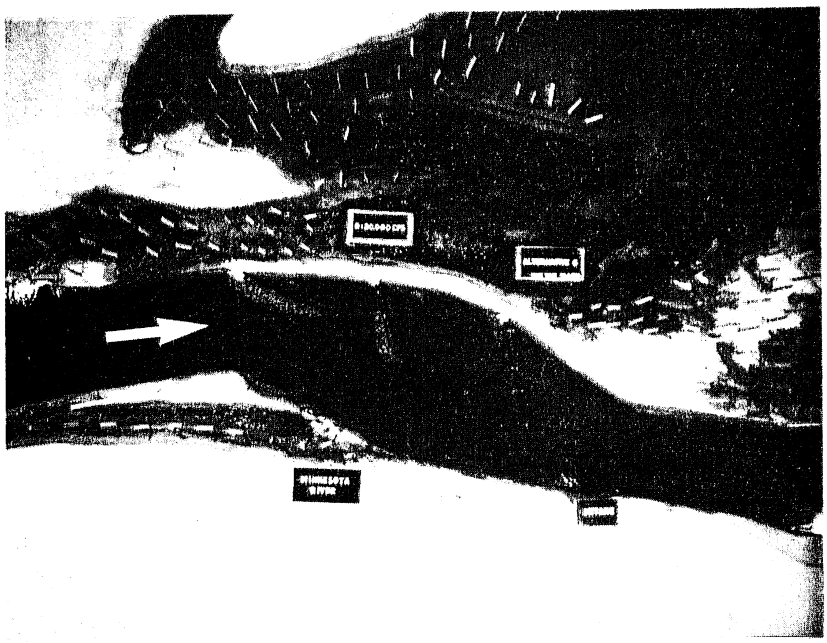

Fig. 53a. Bed configuration at Q = 20,000 cfs for Alternative 6.

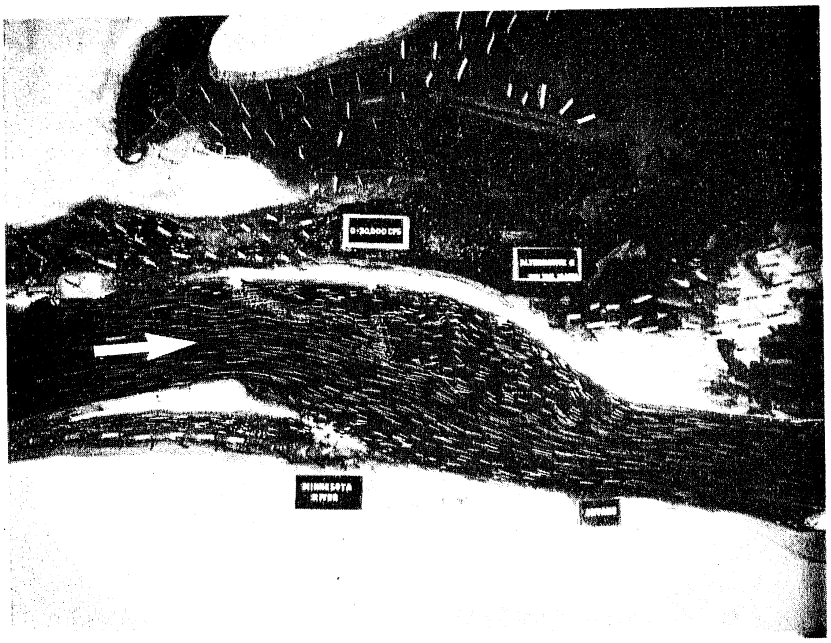

Fig. 53b. Streamline patterns at Q = 20,000 cfs for Alternative 6.

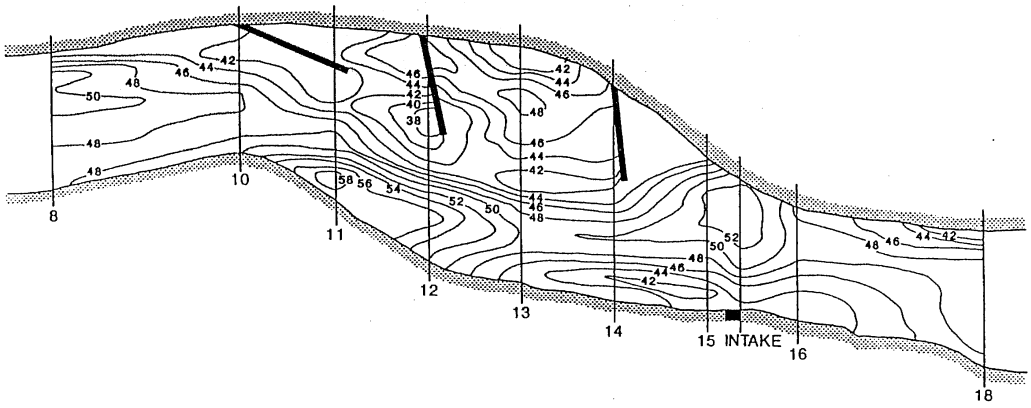

Fig. 54. Bed contours for Alternative 6; Q = 20,000 cfs

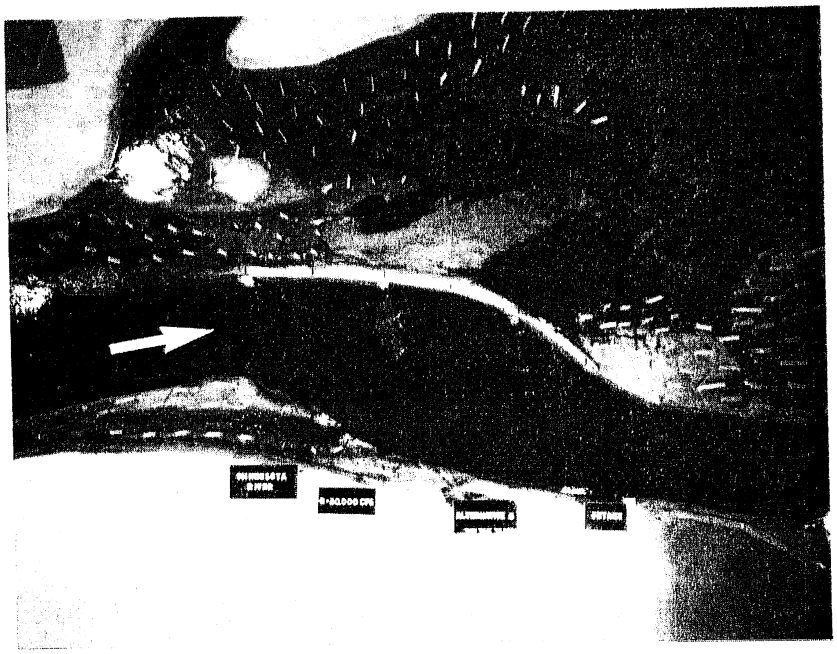

Fig. 55a. Bed configuration at 40,000 cfs for Alternative 6.

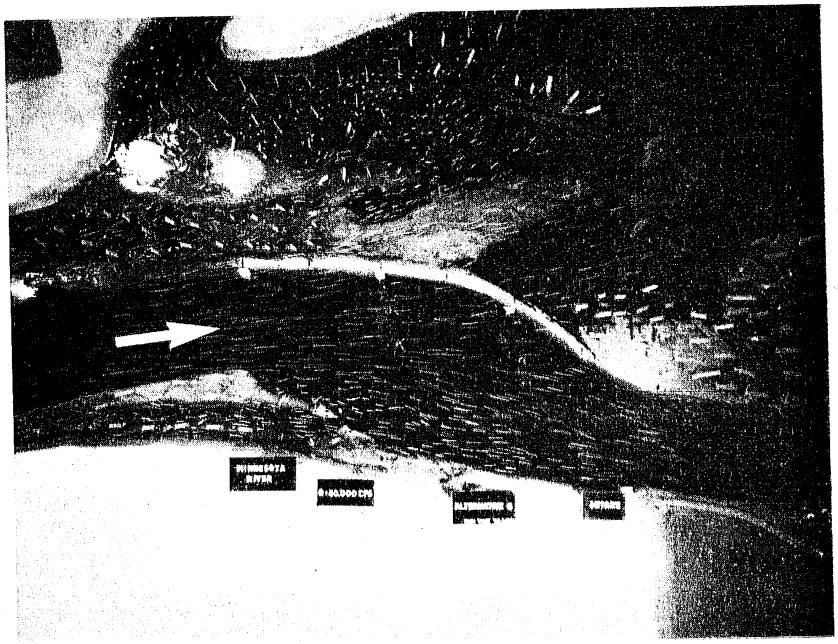

Fig. 55b. Streamline patterns at Q = 40,000 cfs for Alternative 6.

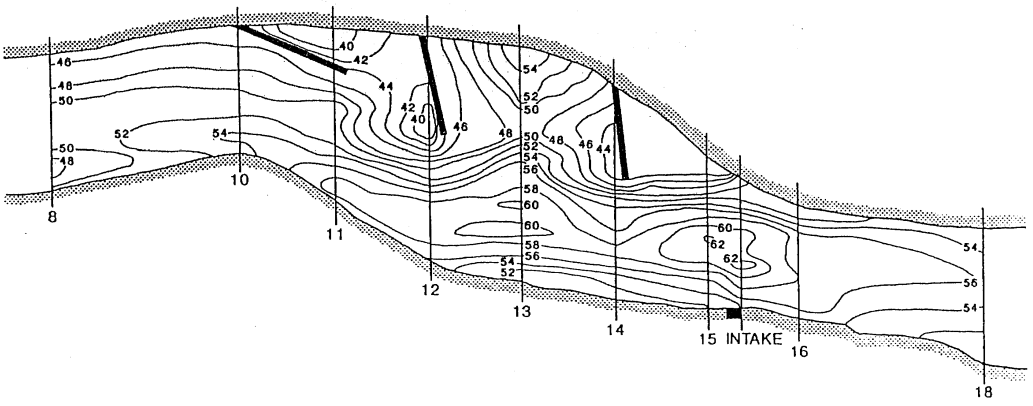

Fig. 56. Bed contours for Alternative 6; Q = 40,000 cfs.

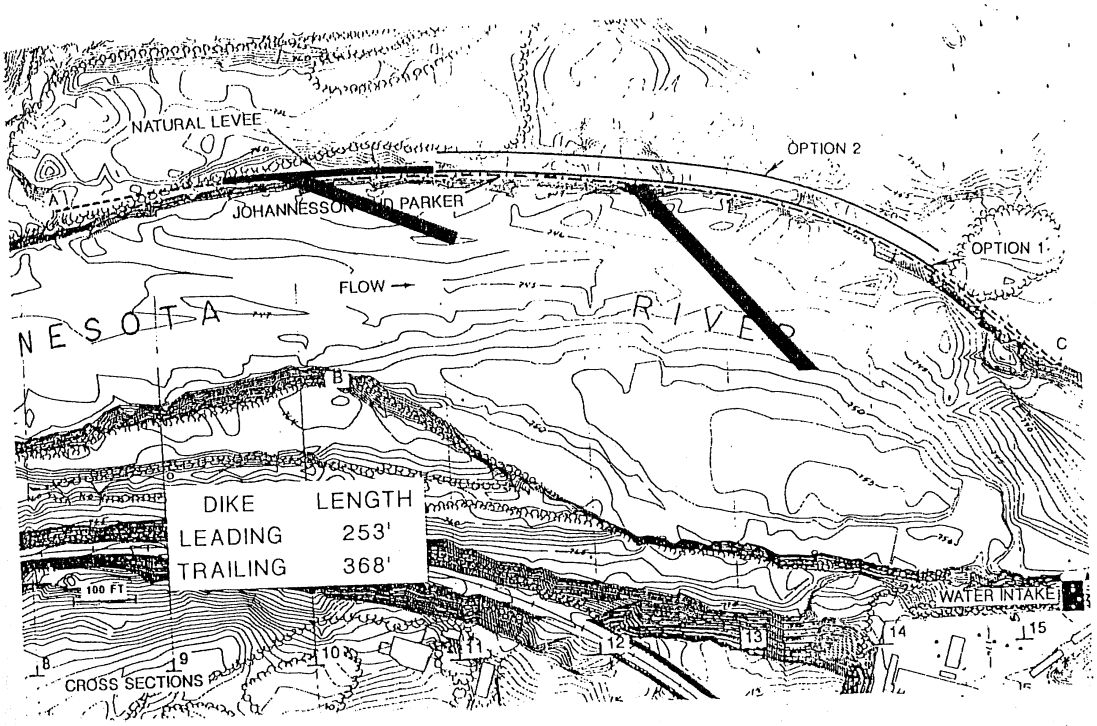

Fig. 57. Schematic diagram illustrating placement of spur dikes for Alternative 7. Bed topography is that of Figure 18.

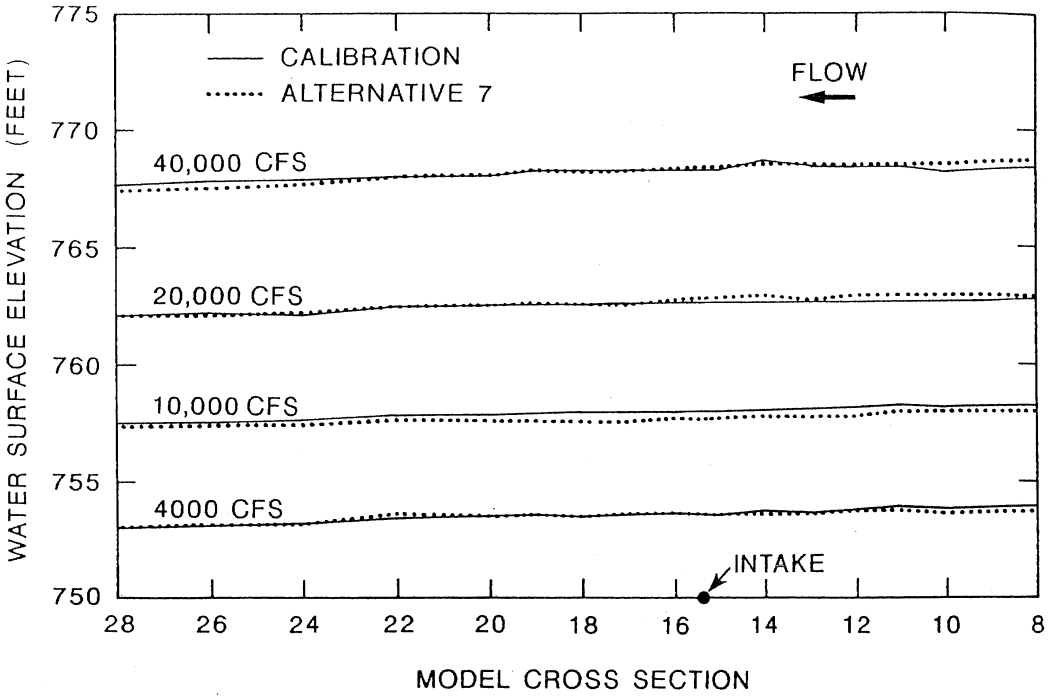

Fig. 58. Water surface profiles in the calibration run and for Alternative 7.

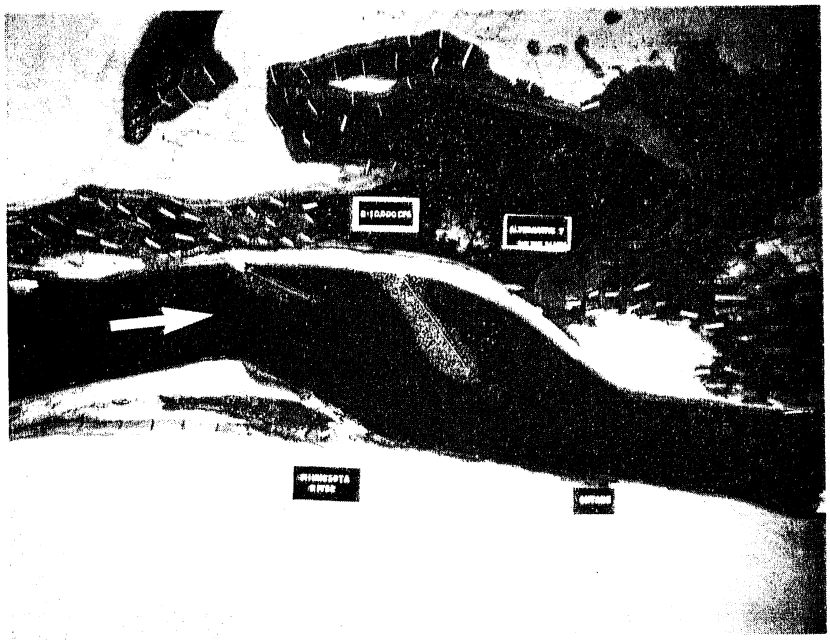

Fig. 59a. Bed configuration at Q = 10,000 cfs for Alternative 7.

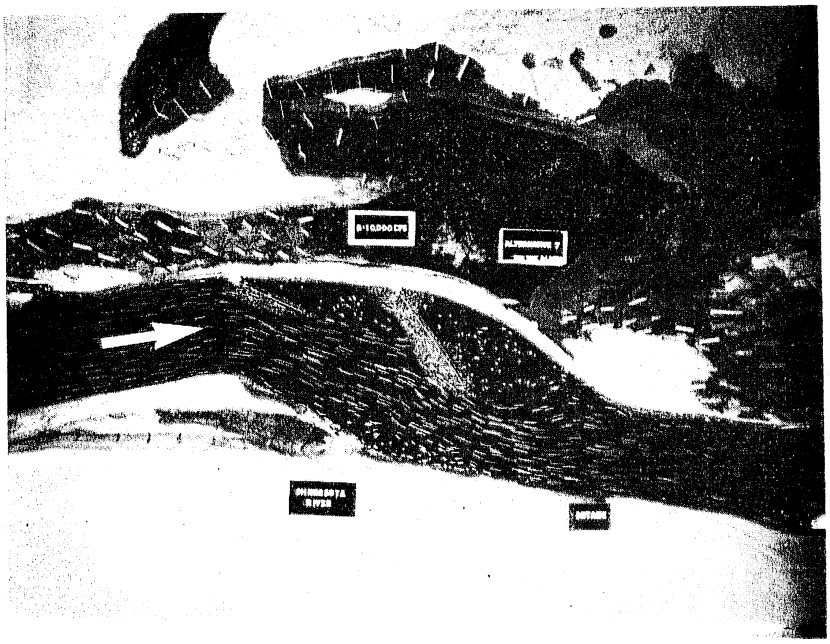

Fig. 59b. Streamline patterns at Q = 10,000 cfs for Alternative 7.

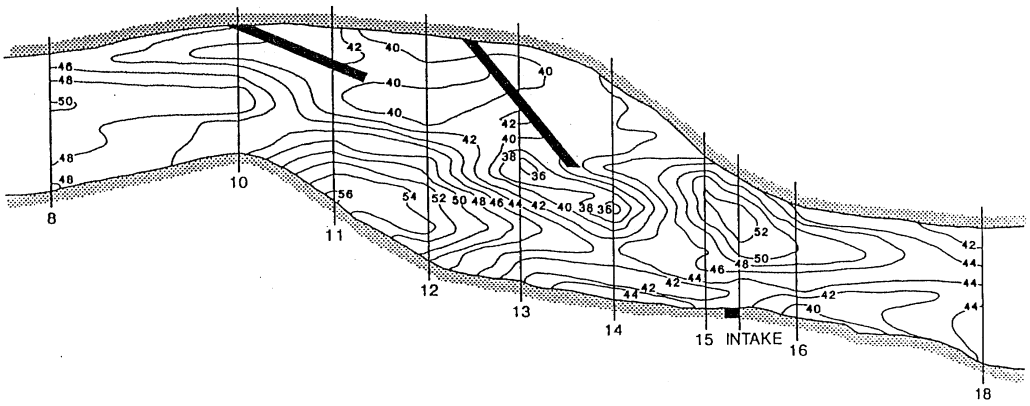

Fig. 60. Bed contours for Alternative 7; Q = 10,000 cfs.

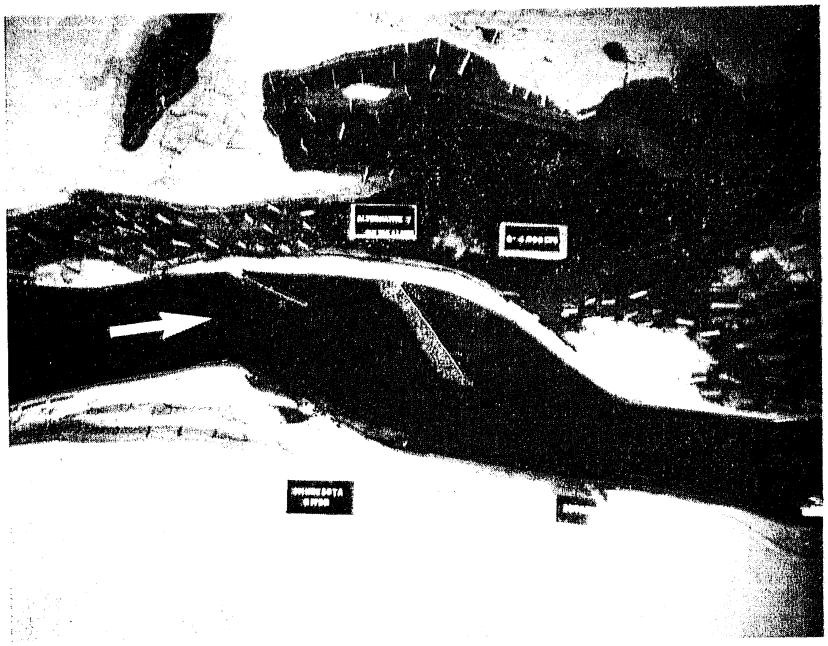

Fig. 61a. Bed configuration at Q = 4,000 cfs for Alternative 7.

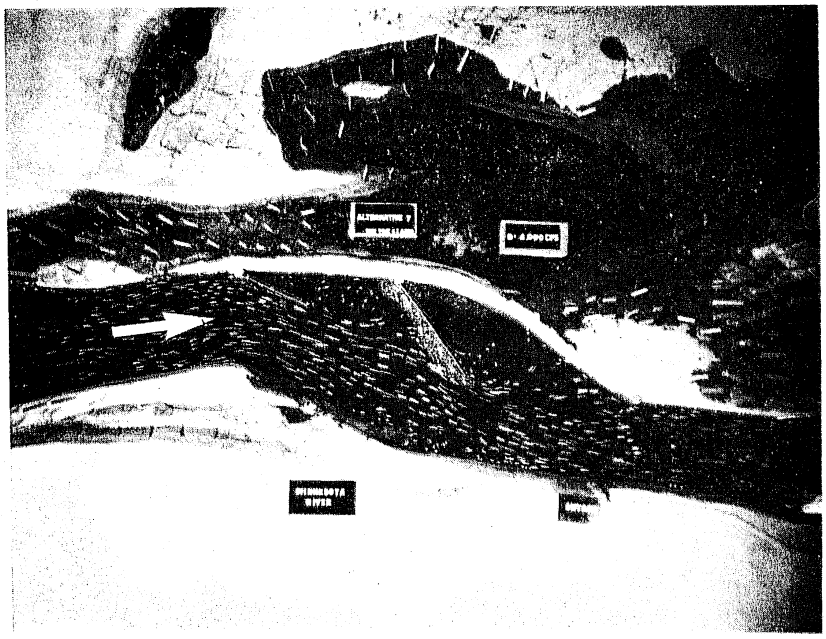

Fig. 61b. Streamline patterns at Q = 4,000 cfs for Alternative 7.

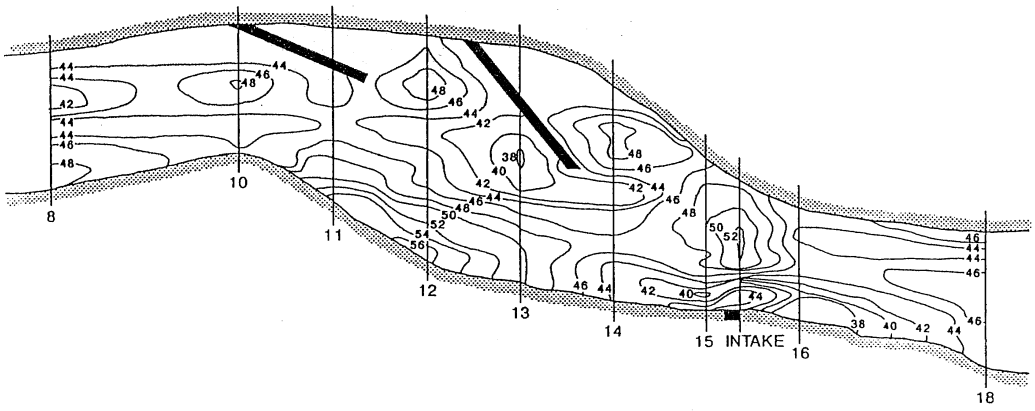

Fig. 62. Bed contours for Alternative 7; Q = 4,000 cfs.

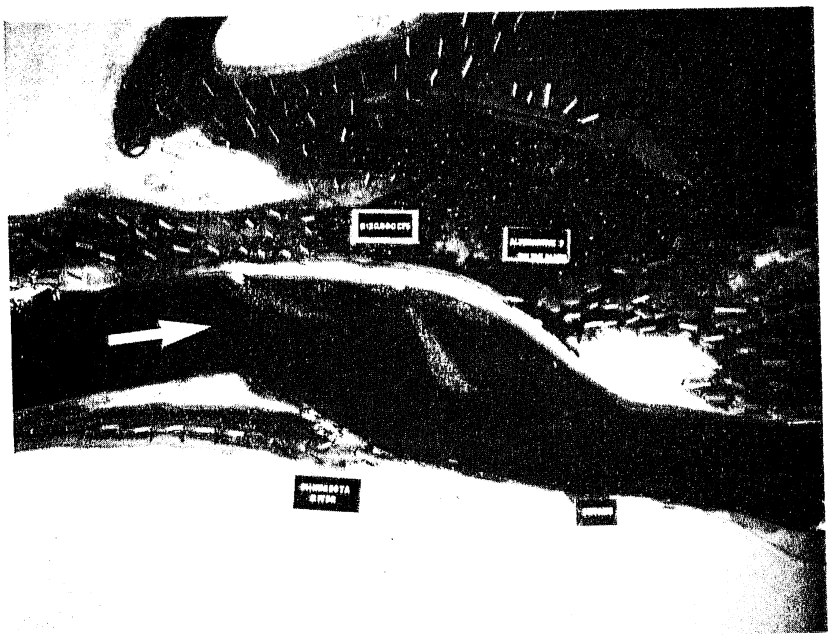

Fig. 63a. Bed configuration at Q = 20,000 cfs for Alternative 7.

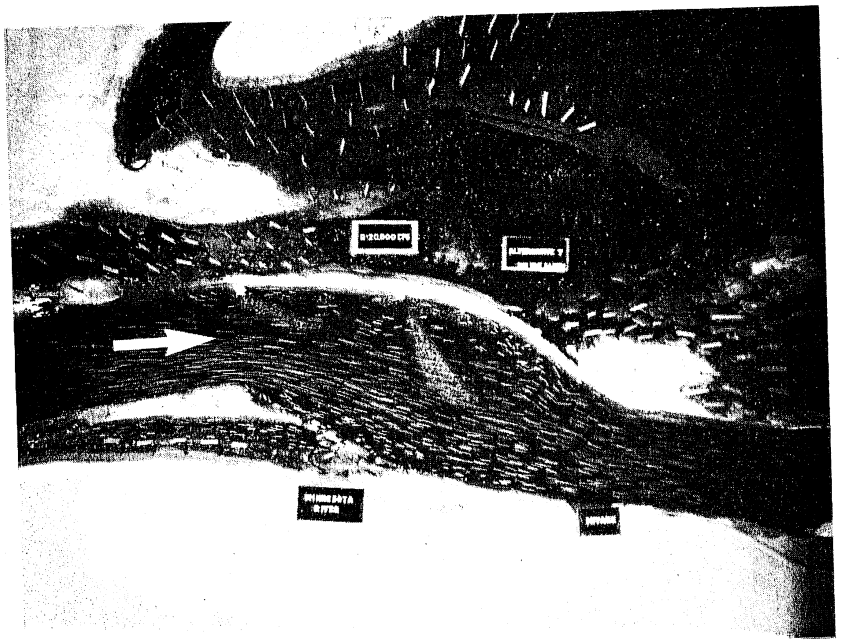

Fig. 63b. Flow streamlines at Q = 20,000 cfs for Alternative 7.

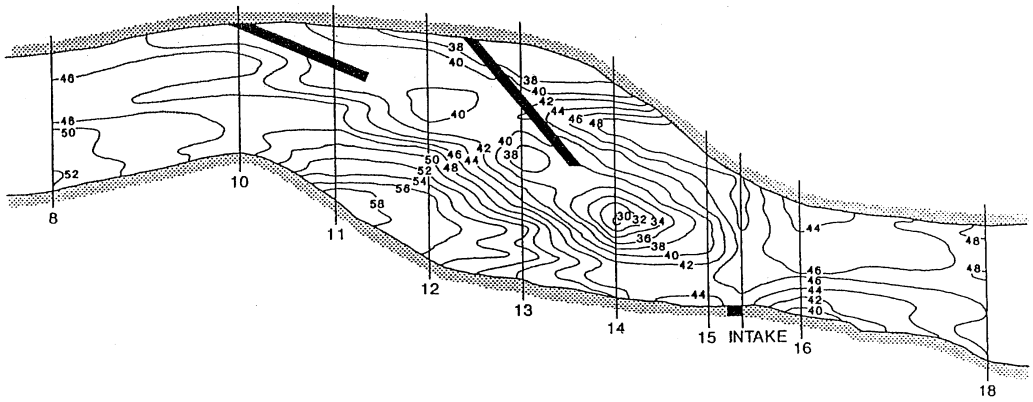

Fig. 64. Bed contours for Alternative 7; Q = 20,000 cfs.

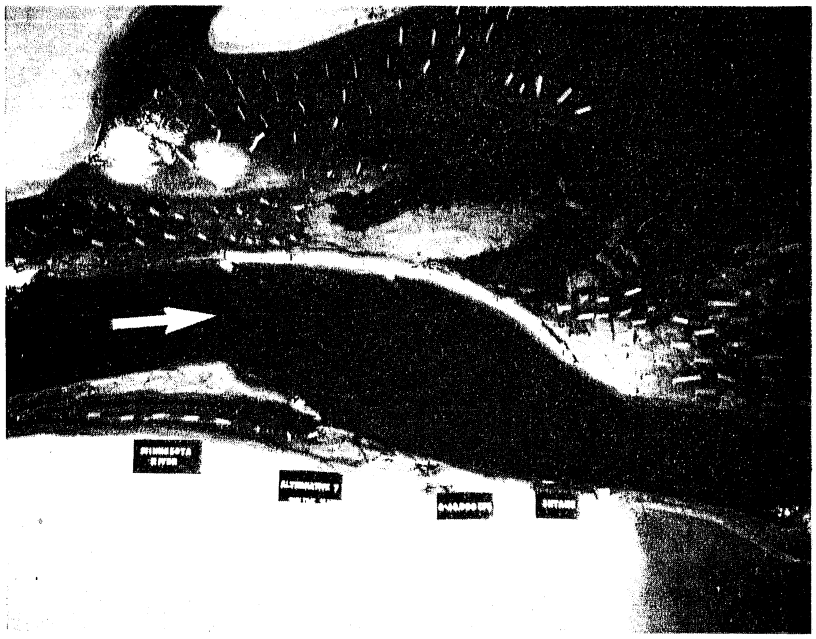

Fig. 65a. Bed configuration at Q = 40,000 cfs for Alternative 7.

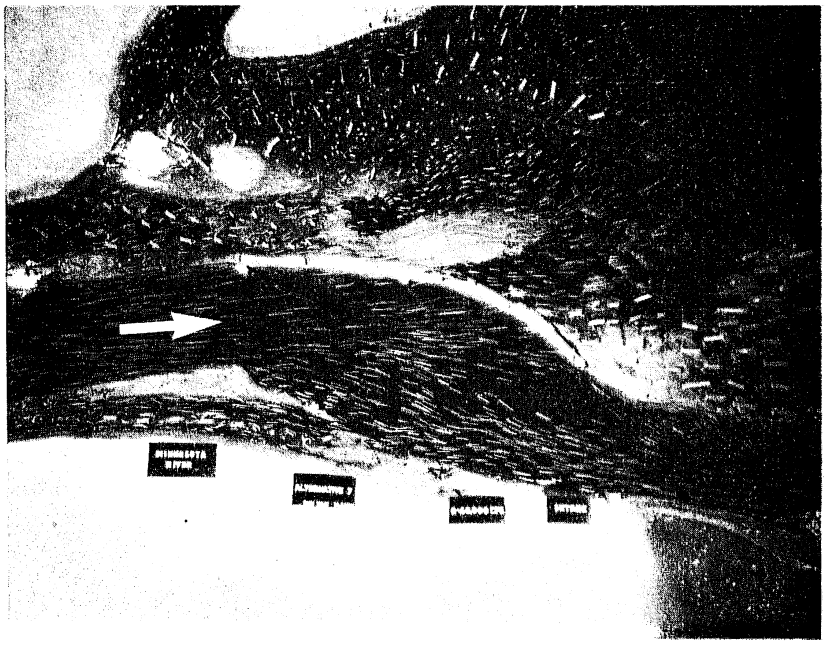

Fig. 65b. Streamline patterns at Q = 40,000 cfs for Alternative 7.

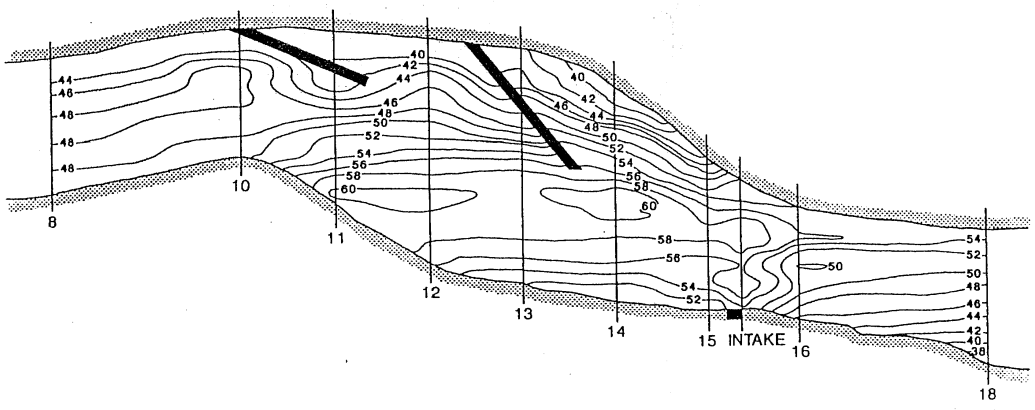

Fig. 66. Bed contours for Alternative 7; Q = 40,000 cfs.

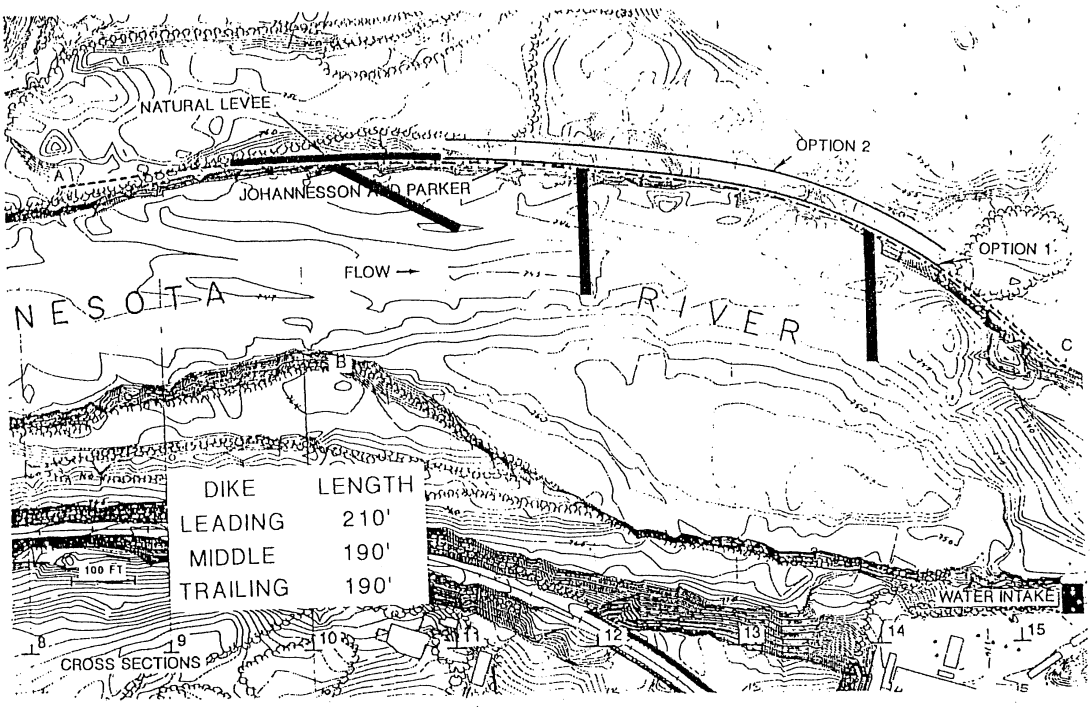

Fig. 67. Schematic diagram illustrating placement of spur dikes for Alternative 8. Bed topography is that of Figure 18.

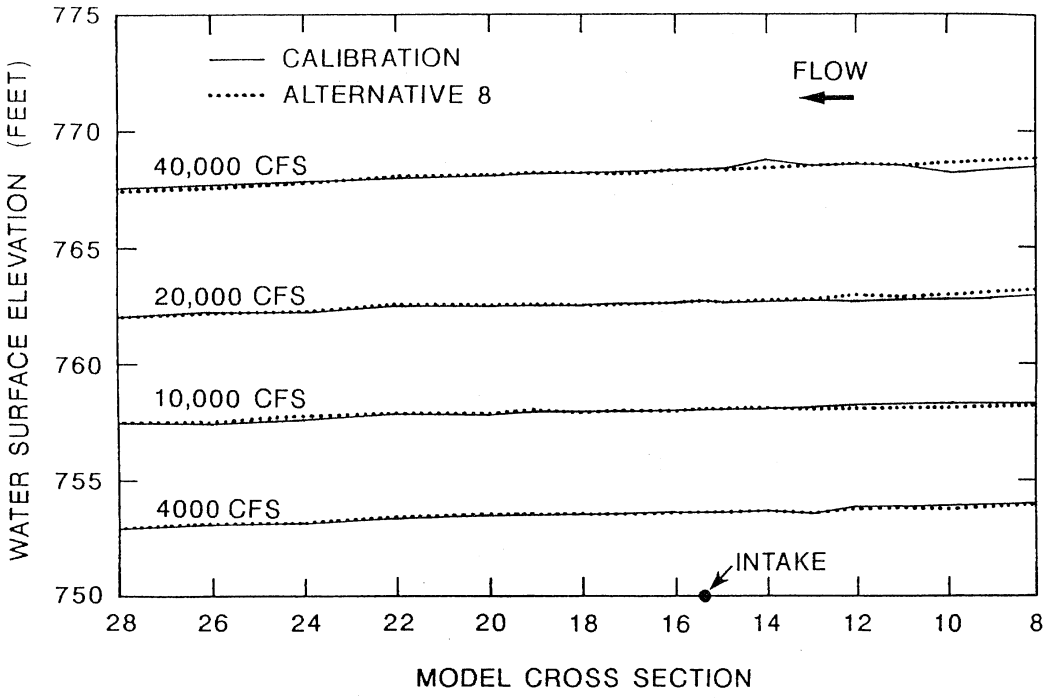

Fig. 68. Water surface profiles in the calibration run and for Alternative 8.

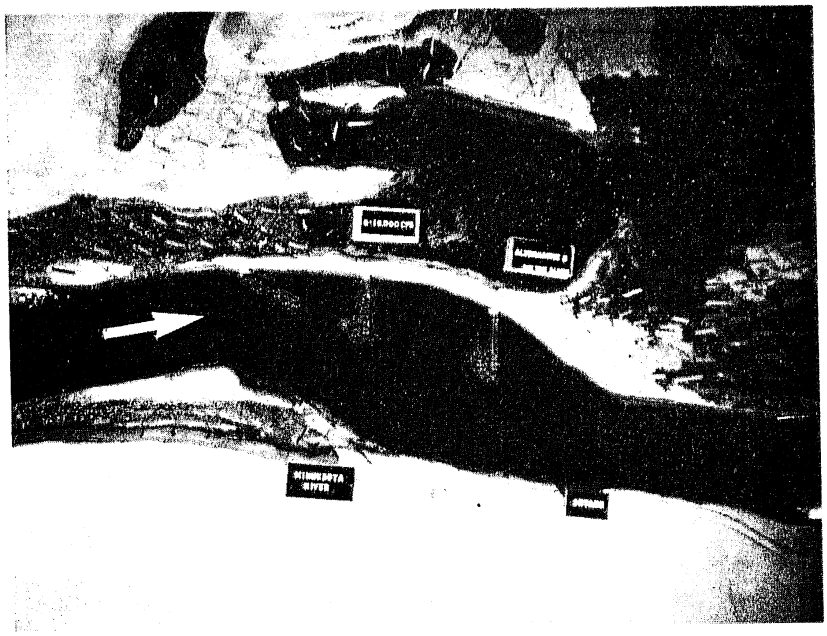

Fig. 69a. Bed configuration at Q = 10,000 cfs for Alternative 8.

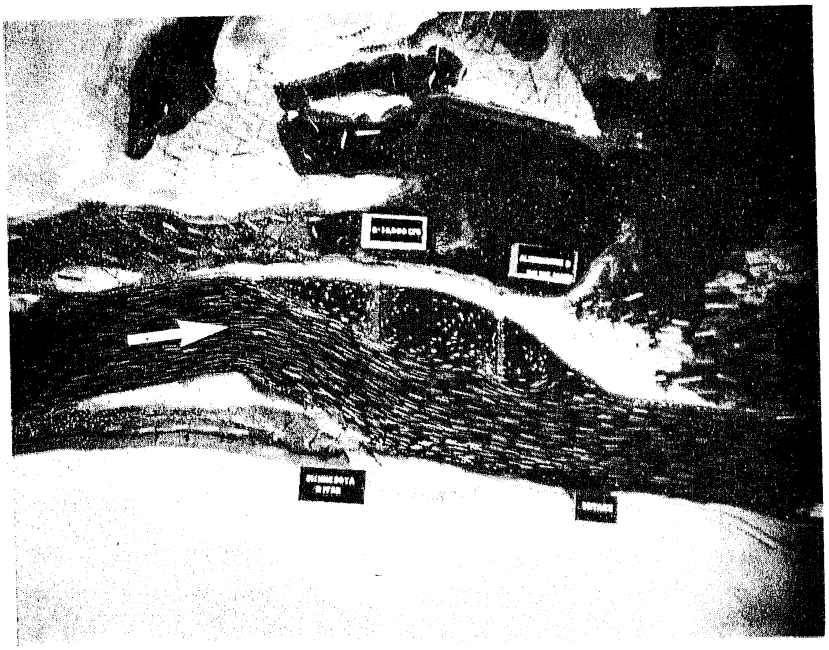

Fig. 69b. Streamline patterns at Q = 10,000 cfs for Alternative 8.

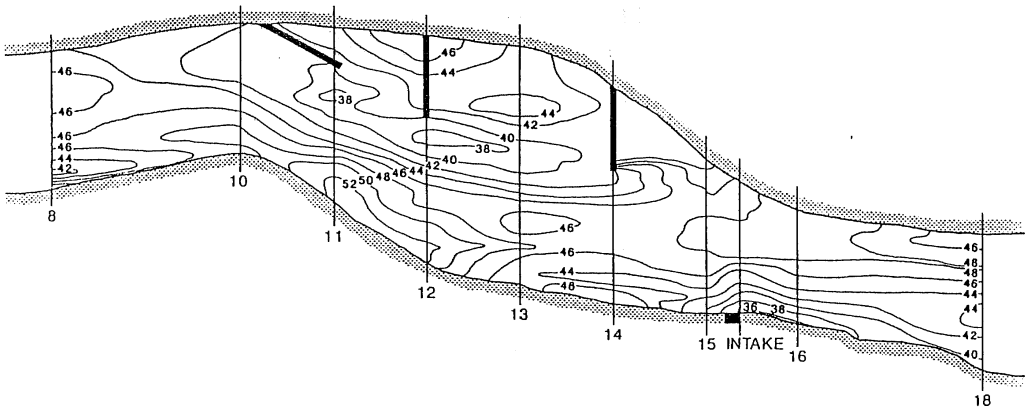

Fig. 70. Bed contours for Alternative 8; Q = 10,000 cfs.

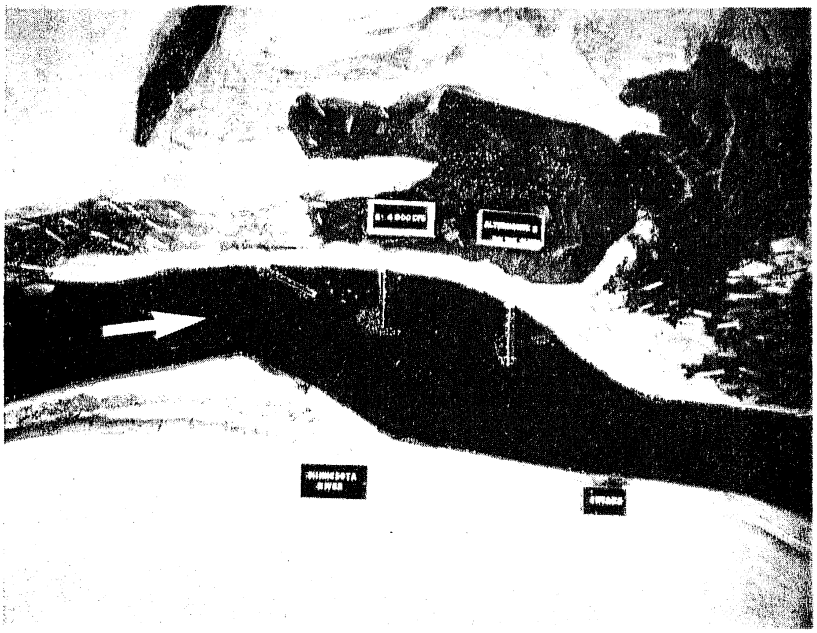

Fig. 71a. Bed configuration at Q = 4,000 cfs for Alternative 8.

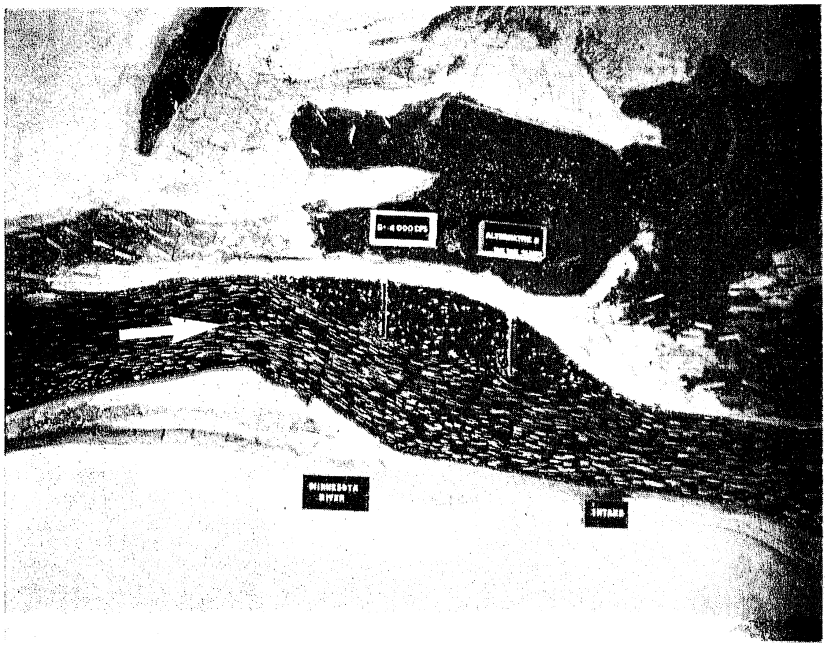

Fig. 71b. Streamline patterns at Q = 4,000 cfs for Alternative 8.

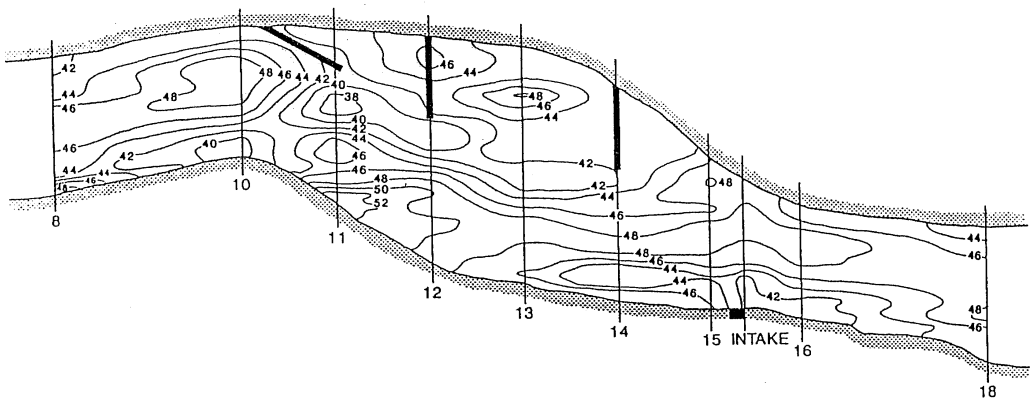

Fig. 72. Bed contours for Alternative 8; Q = 4,000 cfs.

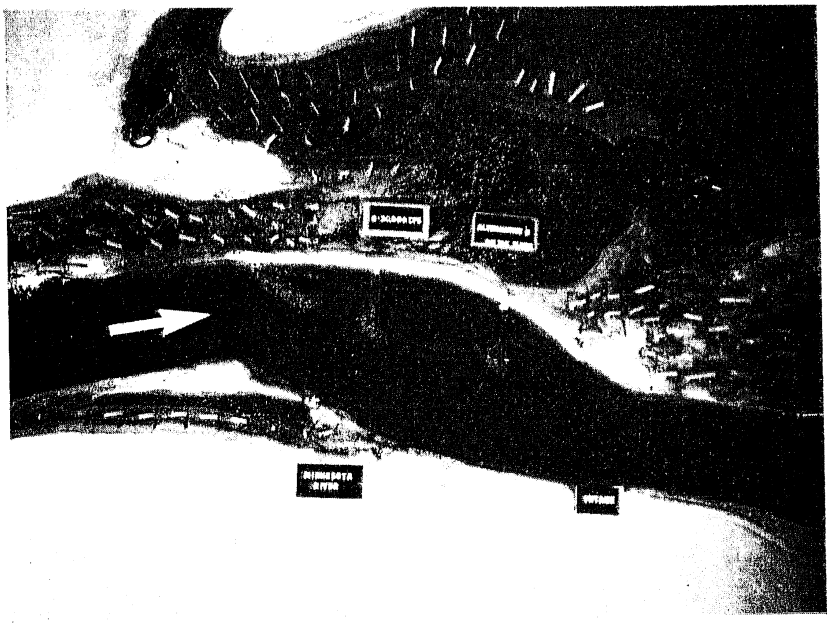

Fig. 73a. Bed configuration at Q = 20,000 cfs for Alternative 8.

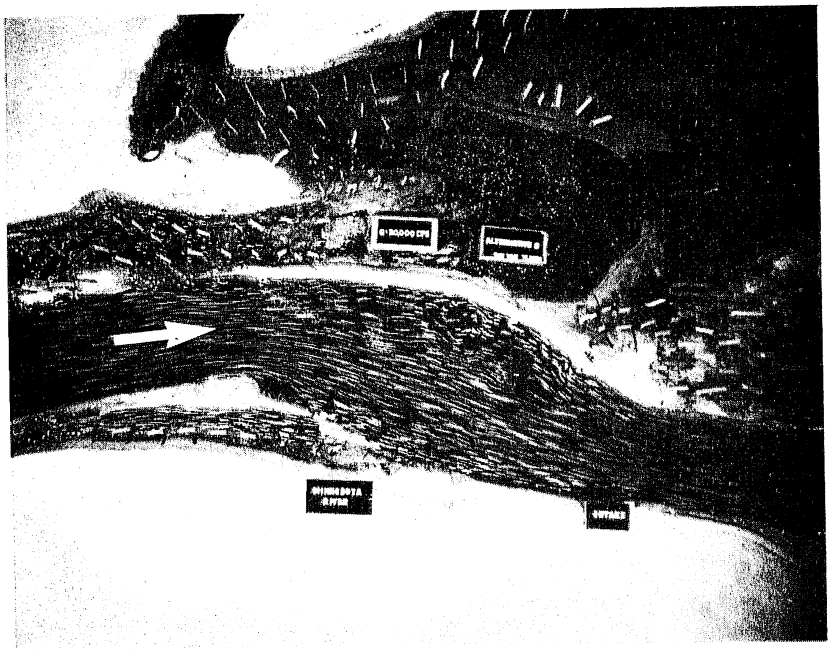

Fig. 73b. Streamline patterns at Q = 20,000 cfs for Alternative 8.

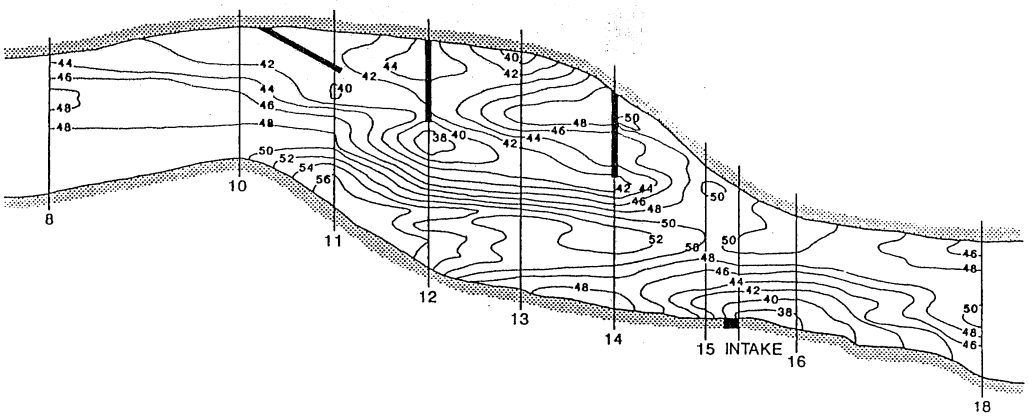

Fig. 74. Bed contours for Alternative 8; Q = 20,000 cfs

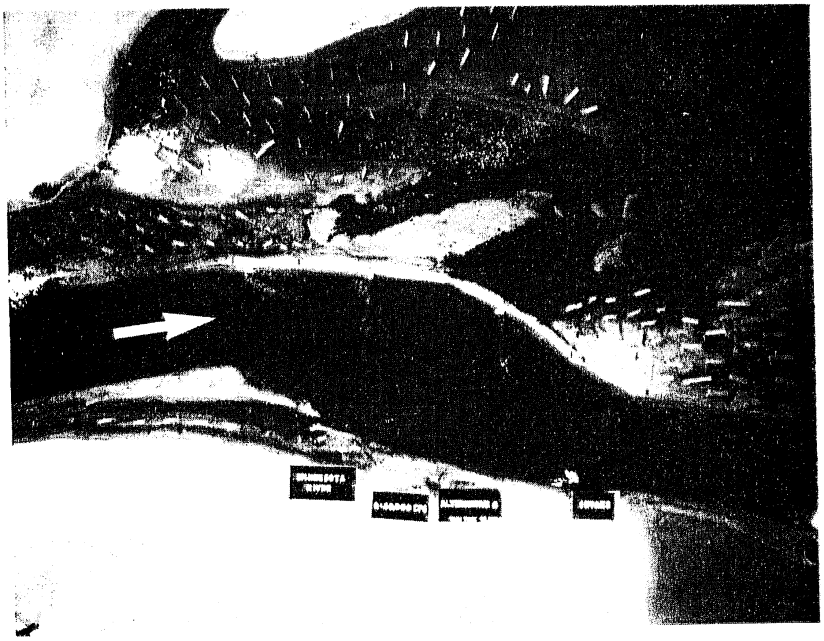

Fig. 75a. Bed configuration at Q = 40,000 cfs for Alternative 8.

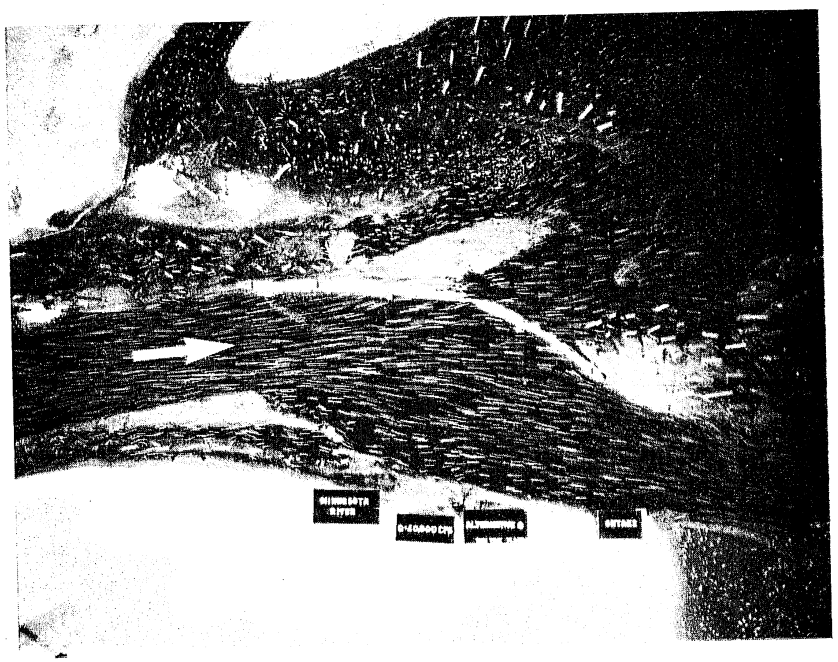

Fig. 75b. Streamline patterns at Q = 40,000 cfs for Alternative 8.

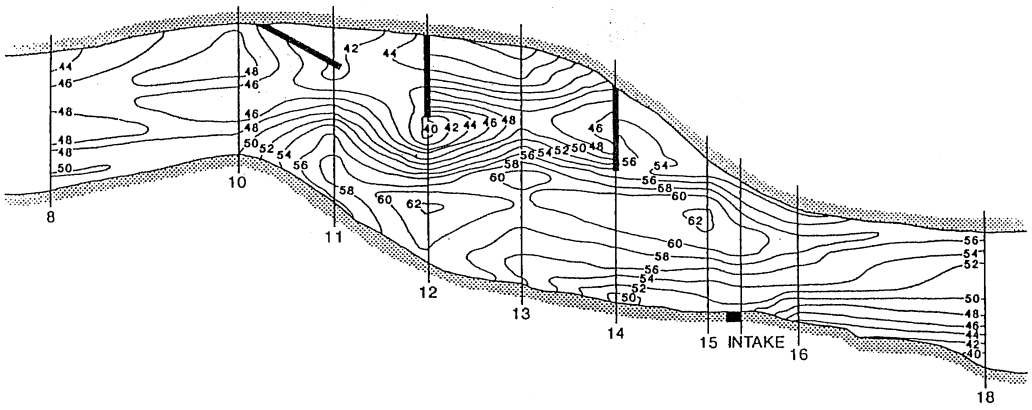

Fig. 76. Bed contours for Alternative 8; Q = 40,000 cfs.